Investigation of biofilm development by antibiotic resistant urinary tract infection pathogens and evaluation of antimicrobial activity of Manuka honey on *Escherichia coli* CTX-M-15 biofilms

Sinan Baho

Thesis submitted to De Montfort University in partial fulfilment of the requirements for the degree of Doctor of Philosophy

De Montfort University

December 2019

Acknowledgements

I would like to pay my sincere gratitude to my supervisor, Dr Shivanthi Samarasinghe, for her guidance, kindness, support, and patience through my PhD journey.

I wish to show my special regards to my second supervisor, Dr Katie Laird, for her useful comments to accomplish this work.

A special thanks to Abdul Razaaq, Richard Smith, Karen, and Karina, for being helpful and generous during my lab work.

I am very grateful to Dr Amos Abioye, for assisting me to get admission to study in this department.

I wish to express my deepest regards to Dr Anfal Motib, and Dr Ahmed Al-Alaq, for their unlimited support during my distress.

I am indebted to Mr Roger, for his honest prays that paved my way towards my target.

Gloria Gracia, my gratitude to you for your positive vibes and moral support cannot be expressed by words, deep thanks from the heart.

Kelly Senti, thank you for mentoring and guiding me on some computer applications that helped me do part of this work.

Father, Brother, and Sister, your support was invaluable and highly appreciated.

Mother, rest in peace with blessings.

I would like to recognize the invaluable assistance that you all provided during my study.

Publications and presentations

1) **Baho S.**, Hoosen H., Samarasinghe S., Walsh S., Lobo-Bedmar MC., del Águila C., Fenoy S., Izquierdo F., Magnet A., Peña-Fernández A. Presence of antibiotic-resistant bacteria in faecal samples collected in urban parks in Leicester, UK. 52nd European Congress of the European Societies of Toxicology. Seville, Spain, 4-7 September 2016. Toxicology Letters 2016; 258S: S183.
2) **Baho, S.**, Reid, R., and Samarasinghe, S. (2018). Adaptability to Various Growth Conditions of Biofilm Associated Extended-Spectrum-Beta-Lactamases Producing Bacteria. Journal of Infectious Diseases and Diagnosis, 3(1), 1-9
3) **Baho, S.**, and Samarasinghe, S. (2018). Multiple Sequence Alignment of NDM-1 DNA Sequence of Different Carbapenemase Producing Gram-Negatives. GSTF Journal of Nursing and Health Care (JNHC), 92-94.
4) Samarasinghe, S., **Baho, S.**, & Czapnik, P. (2019). Preliminary Analysis of the Anti-biofilm Efficacy of Manuka Honey on Extended Spectrum B-lactamase Producing Escherichia Coli Tem-3 and Klebsiella Pneumoniae Shv18, Associated with Urinary Tract Infections.
5) **Sinan Baho** and Shivanthi Samarasinghe. 2017. LuxS sequence alignment of different Gram-Negative bacteria, is it conserved?. Faculty of Health and Life Sciences, School of Allied Health Sciences, De Montfort University, Leicester, UK. asm microbe. New Orleans, USA, 1-5 June 2017.
6) **Sinan Baho** and Shivanthi Samarasinghe. 2017. Analysis of the biofilm formation ability of the antibiotic resistant *Escherichia coli* and *Klebsiella pneumoniae* strains.

Faculty of Health and Life Sciences, School of Allied Health Sciences, De Montfort University, Leicester, UK. Royal Society of Biology, Postgraduate Poster Competition, University of Lincoln.

Abstract

Background

Antibiotic resistance is one of the major healthcare issues worldwide. Over time, bacteria are becoming more resistant, making antibiotics less effective, and this in turn will lead to an increase in the morbidity rate, the mortality rate, and the healthcare system expenses as well. The rise of antibiotic resistance is reaching critical levels as new mechanisms of resistance are emerging and spreading globally, limiting the available effective treatment options. In addition, biofilms are another significant health care issue: they act as a protective cover for infectious microbes. They are also hard to remove: they require a much higher dose of antibiotics than planktonic organisms. When treating biofilm-associated infections, it is important to understand the biology of biofilm development and biofilm-related gene expression. To understand the role of biofilm in pathogenesis, biofilm formation and gene expression in *Escherichia coli* CTX-M-15 were investigated in this study. The antivirulence efficacy of Manuka honey as an alternative treatment was analysed for this strain.

Method

Biofilm formation was measured using the Tissue Culture plate method at different times: after 6, 12, 24 and 48 hours of incubation. Assuming that times correlated with the stages of biofilm development, initial attachment occurred at 6 hours, microcolonies formed at 12 hours, biofilm maturation occurred at 24 hours and biofilm dispersion occurred at 48 hours. Biofilms were quantified in both static and shaking incubators and under three different

growth media: nutrient-poor (AB broth), nutrient-rich (Luria-Bertani broth) and general (nutrient broth). A quantitative Polymerase Chain Reaction was used to determine the biofilm-related gene expression at the *in vitro* biofilm development stages. It was also used to determine the antivirulence effect of Manuka honey on select biofilm-related gene expressions.

Results

The tested strains showed a variable biofilm formation ability when using different media under static and shaking conditions. Antibiotic-resistant strains were high biofilm formers. Regardless of the incubation conditions and growth media used, *E. coli* CTX-M-15 formed varying amounts of biofilm which did not correlate with the stages of biofilm development. Similarly, the same pattern of biofilm-related gene expression was observed, with a large variation in the growth condition tested.

Manuka honey showed potent antibacterial activity: the minimum inhibitory concentration was 6 %, the minimum biocidal concentration was 8 %, and the minimum biofilm elimination concentration was 5 %. The results of the qPCR showed that Manuka honey downregulated the expression of biofilm related genes.

Conclusion

These findings suggested that, for both *E. coli* CTX-M-15 biofilm formation and biofilm-related gene expression, the profiles were not affected by the growth conditions tested in this study. This confirms the successful role of biofilm formation in pathogenesis by adapting to different environmental conditions. The findings suggest that this plays a significant role in the increased prevalence in biofilm-associated infections in third-generation cephalosporin-resistant *E. coli* CTX-M-15.

Lastly, Manuka honey had powerful antibacterial and antibiofilm abilities and can be considered a reliable alternative therapy.

Contents

Table of Figures

Table of Tables

List of Abbreviations

AI: autoinducer

CAZ: ceftazidime

CDC: The Centre for Disease Control

CFU: colony forming units

CLAV: clavulanic acid

CPD: cefpodoxime

CTX: cefotaxime

CTX-M: Cefotaxime

CV: clavulanic acid

DNA: Deoxyribonucleic acid

DPD: 4,5-dihydroxy-2,3-pentanedione

EDTA: Ethylenediaminetetraacetic acid

EUCAST: European Committee on Antimicrobial Susceptibility Testing

ESBL: Extended-spectrum β-lactamase

HSL: homoserine lactones

IMP: Imipenem

KPC: *K. pneumoniae* carbapenemase

LB: Luria-Bertani broth

MBC: Minimum bactericidal concentration

MBEC: Minimum biofilm elimination concentration

MBL: Metallo-β-lactamase

MDR: Multidrug resistance

MRSA: Methicillin-resistant *S. aureus*

MHA: Mueller-Hinton agar

MIC: Minimum bactericidal concentration

NAG: N-acetylglucosamine

NAM: N-acetylmuramic acid

NB: Nutrient broth

NDM: New Delhi metallo-ß-lactamase

OD: Optical density

OXA: Oxacillinase

PBP: Penicillin-binding proteins

PBS: Phosphate buffered saline

PCR: Polymerase Chain Reaction

PHE: Public Health England

QS: Quorum sensing

RNA: Ribonucleic acid

qPCR: quantitative reverse transcription PCR

SHV: Sulfhydryl variable

TAE: Tris-acetate-Ethylenediaminetetraacetic acid

TCP: Tissue Culture Plate

TE buffer: Tris-EDTA buffer

TEM: Temoneira

UMF: Unique Manuka Factor

UTI: Urinary tract infection

WHO: World Health Organization

Chapter 1:

Introduction

1.1 General Introduction

Many researches have dealt with the prevalence of antibiotic resistance worldwide and have proposed temporary solutions, such as reducing the use of the currently effective antibiotics, ensuring cleanliness and preventing infection by vaccination; however, these solutions simply aim to slow down the progression of the problem but not to solve this global issue. In 2018, the World Health Organization (WHO) reported that resistance development is 'critical' in the carbapenem-resistant and extended-spectrum β-lactamase (ESBL) producing *Enterobacteriaceae*, which consists of pathogens associated with common infections, such as urinary tract infection; WHO categorised these pathogens as priority 1 pathogens that need global action to reduce the antibiotic resistance burden (World Health Organization, 2017). Conversely, inadequate research has focused on the characteristics that might contribute to antibiotic resistance; these characteristics include biofilm formation ability, which plays a vital role in the development of antibiotic resistance, in the transfer of the resistance genes among microcolonies within a biofilm layer, and in creating a highly efficient protective cover against the penetration of effective antibiotics (Li et al., 2018; Mah and O'Toole, 2001). In this work, several antibiotic-resistant strains were characterized. One of the characteristics that might contribute to antibiotic resistance is the ability of these pathogens to form biofilms. Therefore, this work investigated the biofilm formation ability of the pathogens in the phenotypic and genotypic contexts. The working hypothesis was that the selected strains are high biofilm formers.

1.2 Urinary Tract Infection (UTI)

UTI is a collective term referring to any type of infection in the urinary tract (i.e. ureters, bladder, kidneys and urethra). The urinary tract is divided into two parts: the upper tract (ureters and kidney) and the lower tract (urethra and bladder) (Tan and Chlebicki, 2016). UTIs may be stratified as community-associated UTIs and healthcare-associated UTIs. Depending on the site of infection within the urinary tract, the infection is classified as cystitis, pyelonephritis or urosepsis. The exact epidemiological overview of UTIs remains lacking due to various limitations: firstly, due to the limited number of coordinated surveillance studies, and secondly, due to the inherent problems in the conduct of studies and in the definitions used in the available studies (Tandogdu and Wagenlehner, 2016). The members of *Enterobacteriaceae* are the most common cause of those infections, causing more than 70 % of UTI cases (Vranic et al., 2017). Among the members of this family, the Gram-negative *Escherichia coli* and *Klebsiella pneumoniae* are the most common causes of UTI worldwide. Data collected from many countries worldwide showed that *E. coli* causes 70–95 % of the upper and lower UTI cases (Obiogbolu et al., 2009; Behzadi and Behzadi, 2008; Ayhan et al., 1988; Ebie et al., 2001; Garofalo et al., 2007). Another microorganism that can cause UTI is *Staphylococcus saprophyticus*, which is involved in other UTI cases (Hooton and Stamm, 1997). Patients with diabetes, urinary catheters, hospitalization history or spinal cord injuries might also contract UTI caused by *Proteus mirabilis, Enterococcus faecalis, Pseudomonas aeruginosa, Serratia marcescens* and group B streptococci (Ronald, 2002). *E. coli* causes approximately 80 % of the infections in the bladder (lower part of the urinary tract; this condition is termed cystitis). By contrast, *K. pneumoniae* causes up to 5 %

of community-acquired UTIs and is usually more common in diabetic patients and in nosocomial setting. Although *K. pneumoniae* commonly causes infection in the urinary tract, it is mostly identified as the cause of pneumoniae in compromised hosts (Rosen et al., 2008; Reid, 2018).

UTI is among the most common types of infection. In 2013, approximately 92 million people worldwide were infected with UTI (Vos et al., 2015). Moreover, it is a significant cause of mortality among old aged people; in England and Wales, 4835 deaths due to UTI were reported in 2012 (Oxford, 2014). Moreover, UTI is more common in women than in men. In the UK, approximately half of all women are infected at least once in their life, whereas only 1 in 2000 men will have such infections every year (University Hospital Southampton NHS Foundation Trust, 2019). According to WHO (2018a), the annual healthcare expenditure due to UTI reaches over $1 billion, and office visits reaches as high as 8.3 million.

Because of the extensive use of antibiotics in UTI treatment, along with other factors, such as urinary catheterization, nursing home stay and hospitalisation history, antibiotic resistance in *Enterobacteriaceae*, mainly in *E. coli* and *K. pneumoniae*, has emerged and has significantly increased worldwide. Therefore, it is important to identify factors causing this resistance and its spread worldwide to minimize its risk and to reserve the usage of the current effective antibiotic among UTI patients (Mazzariol et al., 2017; Tenney et al., 2018). Biofilm formation plays a significant role in UTIs. It is responsible for recurrent infections and relapses in patients. Biofilms in UTIs usually form on catheters, and this phenomenon accounts for a high percentage of all nosocomial infections; also, biofilms are the most common cause of Gram-negative bacteria-associated bacteraemia in patients staying in

hospitals. For this reason, efficient prevention and control measures are urgently needed. Research on biofilms might lead to a deeper understanding and better knowledge on the disease process and will lead to the development of new treatment prevention options (Delcaru et al., 2016). As UTI is caused by bacteria, antibiotics are used to treat this infection. They can be prescribed by a doctor, and the type of antibiotic to be used depends on the species of the infectious bacteria. Nitrofurantoin is usually used as the first line of treatment (Antibiotic Research UK, 2019).

1.3 Antibiotics

Antibiotics are medications used to prevent and treat bacterial infections. They are natural metabolites produced by bacteria, fungi, plants and animals, and they are either bactericidal or bacteriostatic to microorganisms. Antibiotics display several mechanisms of actions, including:

1) inhibition of bacterial cell wall synthesis (e.g. β-lactam antibiotics, such as penicillins, carbapenems, monobactams, and cephalosporins) (Fig 1.1).
2) inhibition of protein synthesis (e.g. aminoglycosides, macrolides and tetracyclines)
3) inhibition of DNA synthesis (e.g. quinolones and metronidazole)
4) inhibition of RNA synthesis (e.g. rifamycins)
5) membrane structure disruption (e.g. polymyxins)
6) inhibition of metabolic pathways (e.g. trimethoprim and sulfamethoxazole) (Zaman et al., 2017; Reid, 2018; Aminov, 2010).

1.4 ß-Lactam Antibiotics

ß-lactams are widely used antibiotics and are the most effective drugs against bacterial infections. They are one of the three largest classes of antibiotics; ß-lactams include penicillin, cephalosporins, carbapenems and monobactams (Fig 1.1), which play a vital role in maintaining human health (Kotra and Mobashery, 1998; Fisher et al., 2005). These antibiotics are called ß-lactams due to the existence of a ß-lactam ring in their structures, and this ring represents their central activity (Worthington & Melander, 2013). The mechanism of action of ß-lactams involves the disruption of the cell wall synthesis by preventing the formation of the cross-links by the enzymes called penicillin-binding proteins (PBP); this action is achieved by mimicking the natural D-Ala-D-Ala (Fig 1.2) substrate of the PBP, thereby preventing cross-link formation between adjacent glycan chains (Fig 1.3) (Tipper and Strominger, 1965).

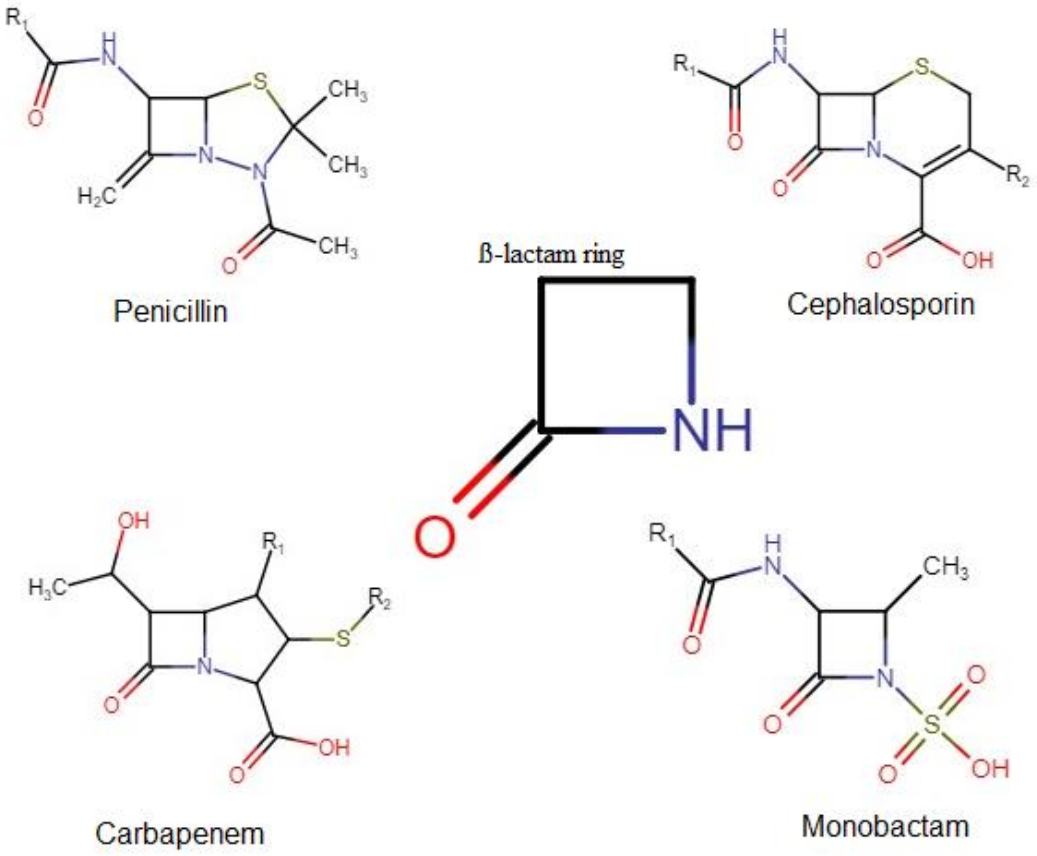

Fig 1.1 ß-lactam antibiotic structure. All ß-lactam antibiotics contain a ß-lactam ring, which is their core structure (as shown in the middle of the figure). The structure of the ß-lactam ring is similar to that of the terminal D-Ala-D-Ala peptide substrate, which is the penicillin-binding protein (PBP) that forms covalent bonds between different peptidoglycan chains during cell growth. The ß-lactam ring and associated side groups becomes tightly bound to the active site of PBP, which in turn inhibits its activity, preventing cell wall synthesis. Figures are adapted from Clarkson (2015). Chemical structures were drawn using chem-space.com.

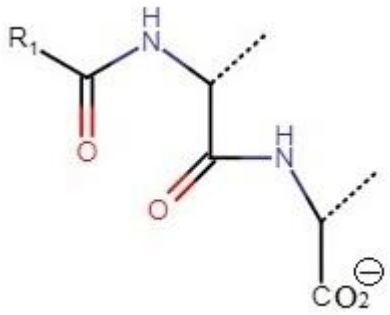

Fig 1.2 The chemical structure of acyl D-Ala-D-Ala, which displays certain similarity with the structure of ß-lactam ring. The figure is adapted from Clarkson (2015). The chemical structure was drawn using chem-space.com.

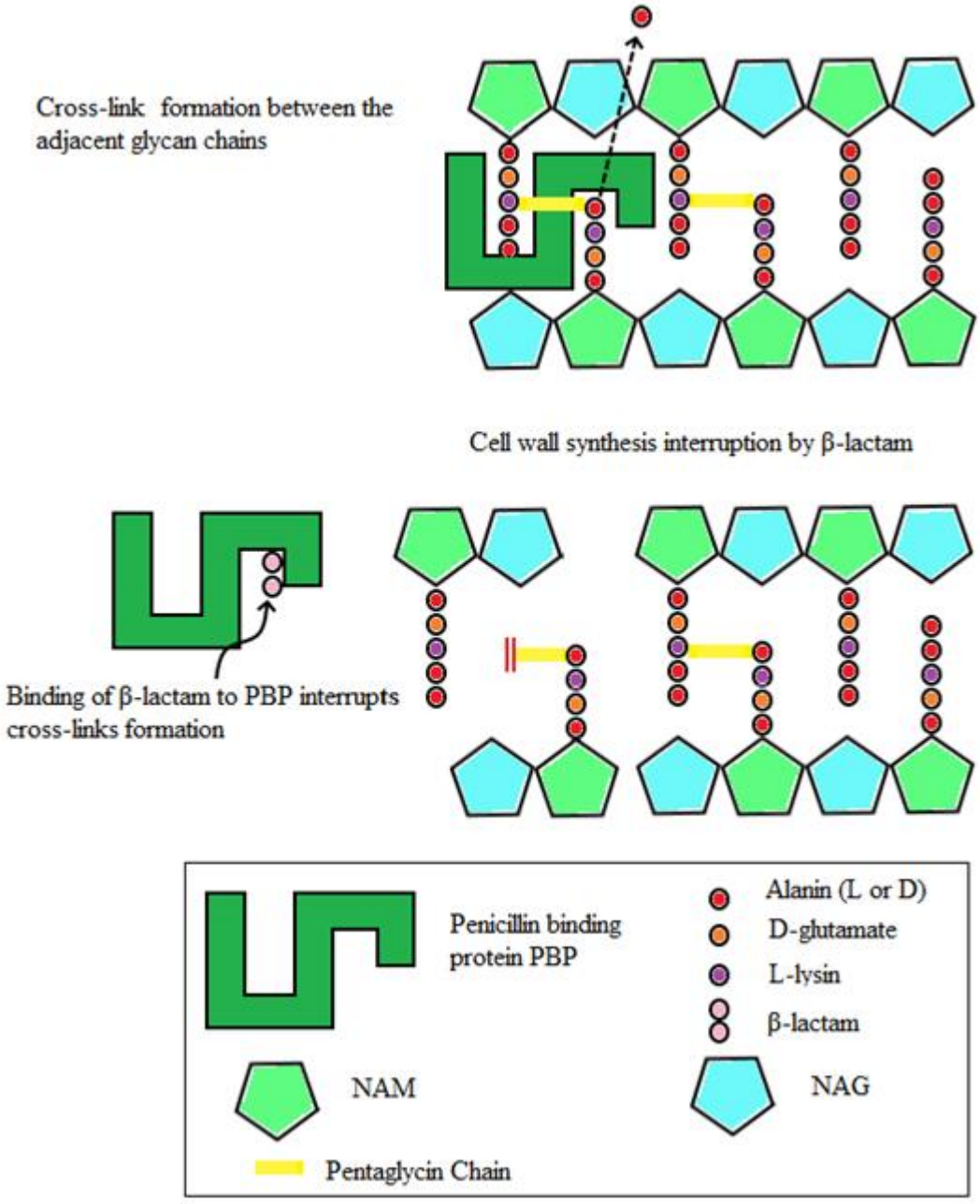

Fig 1.3 Mechanism of action of ß-lactam antibiotics. Through a catalytic reaction, penicillin-binding protein (PBP) forms pentaglycine chains between the adjacent glycan chains, resulting in the removal of a terminal D-alanine residue from one of the peptidoglycan precursors (indicated by a black arrow). Due to the structural resemblance of the ß-lactam ring to the D-Ala-D-Ala substrate for the PBP, ß-lactam ring binds tightly to the PBP. This binding prevents the formation of pentaglycine chains, resulting in the formation of cell wall that is

vulnerable to osmotic forces, possibly leading to cell rupture. NAG: N-acetylglucosamine, NAM: N-acetylmuramic acid. Figure is adapted from Clarkson (2015).

1.5 Antibiotic Resistance

Antibiotic resistance is characterized by the change in bacterial response towards antibiotics, rendering these antibiotics ineffective. It occurs naturally, but it can be accelerated by antibiotic overuse, antibiotic misuse, and the lack of proper healthcare and new drug development industries in countries with poor economy and strict regulatory requirements (WHO, 2018b; Ventola, 2015).

Resistance may occur through one of four mechanisms: (i) the ability to synthesize enzymes, such as β-lactamases, chloramphenicol acetyltransferases and aminoglycoside-modifying enzymes, which inactivate antibiotics (Fig 1.4); (ii) presence of efflux pumps in the cytoplasmic membrane; these pumps eliminate the antibiotic from the cell and prevent its binding to the target site; (iii) regulation of the number of porins, thereby limiting the access of antibiotics; and (iv) natural variation or acquired changes in the target sites of antimicrobials due to spontaneous mutation, affecting antibiotic binding (Kapoor et al., 2017).

Antimicrobial resistance may be due to natural evolution; in such a case, it does not relate to any class of antibiotics. For example, the complexity of the Gram-negative outer layer leads to a more difficult penetration of various types of antimicrobials. This phenomenon is called ‘intrinsic resistance’. Another type of resistance, which can be more dangerous to humans,

is ‘acquired resistance’ wherein bacteria can develop resistance by acquiring specific resistance determinants via transformation, transduction or conjugation. This type of resistance may develop either between the same species or between different species. Moreover, acquired resistance, combined with mutation and selection via antibiotic pressure, enables the bacteria to rapidly adapt to the newly introduced antibiotic. (Kapoor et al., 2017; Reid, 2018)

Antibiotic resistance represents a significant healthcare problem. The loss of the antibiotics’ effectiveness will weaken their ability to fight infectious diseases and to prevent the hospitalisation of patients as a result of the complications of chemotherapy, organ transplantation surgery and renal dialysis; in these patients, treatment of secondary infections is critical. Healthcare providers are compelled to use more toxic doses of antibiotics, and this approach is costly and becomes less effective when all options have been exhausted, that is, when the first- and second-line antibiotic treatments are rendered ineffective by antibiotic resistance or when they become unavailable (Centres for Disease Control and Prevention, 2013). Increased incidence of antibiotic resistance in many pathogens was reported in many places worldwide (Byarugaba, 2005). This increased resistance was attributed to the changing microbial characteristics, to selective pressure and to technological and societal changes that enhanced the development and spread of antibiotic-resistant microorganisms. Despite being a natural biological phenomenon, antimicrobial resistance developed due to the adaptation of infectious agents to the excessive use of antimicrobials and disinfectants for domestic or agricultural purposes (Walsh, 2000).

A breakthrough in the early 1980s involved the introduction of third-generation cephalosporin into the clinical practice. This breakthrough was the forerunner of the battle against the β-lactam-resistant strains. These cephalosporins were developed as a result of the increased resistance against β-lactam antibiotics, such as the ampicillin-hydrolysing β-lactamases TEM-1 and SHV-1 in *E. coli* and *K. pneumoniae* and then diffused into new strains, such as *Haemophilus influenzae* and *Neisseria gonorrhoeae* (Paterson and Bonomo, 2005). In 1983, a plasmid-encoded β-lactamase capable of hydrolysing extended-spectrum cephalosporins was first reported (Knothe et al., 1983). A mutation in a single nucleotide occurred in the gene encoding the β-lactamase compared with the gene encoding SHV-1. Other β-lactamases closely related to TEM-2 and TEM-1 were eventually discovered. These β-lactamases conferred resistance to the extended-spectrum cephalosporins (Brun-Buisson et al., 1987; Sirot et al., 1987). These new β-lactamases were named as extended-spectrum β-lactamases (ESBLs). These ESBLs are fast-growing groups that can hydrolyse the third-generation cephalosporins and aztreonam, but they are inhibited by clavulanic acid. These ESBLs formed through mutations in $bla_{\text{TEM-1}}$, $bla_{\text{TEM-2}}$ or $bla_{\text{SHV-1}}$ that modify the configuration of the amino acid around the β-lactamase active site. This modification increased the susceptibility of β-lactam to hydrolysis caused by ESBLs. ESBLs are encoded by plasmids that frequently carry genes for resistance to other drugs, such as aminoglycosides. Thus, very limited options of antibiotics are available for treating ESBL-producing microbes. Examples of ESBLs include CTX-M, SHV, TEM and OXA (Paterson and Bonomo, 2005).

Carbapenems are the best choice to cure the different types of infections caused by ESBL-producing microbes. However, many isolates have been recently reported to be carbapenem-resistant and what makes them distinct from other ß-lactams is the presence of carbapenems, along with the ß-lactam ring, in their molecular structure which confers them an additional stability against most β-lactamases, including ESBLs (Meletis, 2016). Carbapenem resistance is attributed to the production of β-lactamases that can inactivate carbapenems and other β-Lactam antibiotics; hence, they are called carbapenemases (Walsh, 2010; Poirel et al., 2007). These enzymes hydrolyse all or almost all β-lactams. They are encoded by genes that are transferred horizontally by transposons or plasmids; those transferable elements sometimes carry a gene code for other resistance determinants (Meletis, 2016). In terms of worldwide distribution and carbapenem hydrolysis, the most efficient carbapenemases are the IMP, NDM, KPC and OXA-48 types (Poirel et al., 2012).

According to a recent study (Xue et al., 2016), antibiotic resistance is affected by what is termed ‘quorum sensing’ (QS) through the autoinducer-2 (AI-2). AI-2 upregulates the expression of the TEM-type enzyme in *E. coli* in a LsrR-dependent manner.

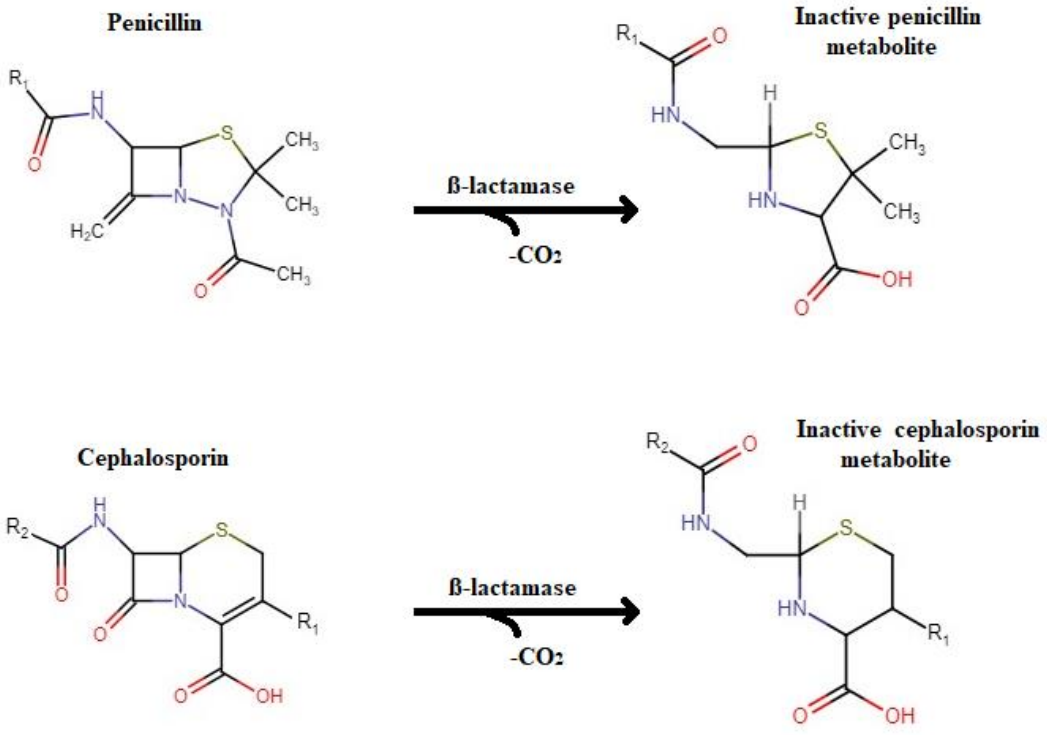

Fig 1.4 Mechanism of action of ß-lactamase. ß-lactamase hydrolyses the core structures of both penicillin and cephalosporin, which share a common four-atom ß-lactam ring. Hydrolysis of ß-lactam antibiotics prevents them from inhibiting bacterial cell wall synthesis. The figure was adapted from Clarkson (2015). The chemical structures were drawn using chem-space.com.

1.5.1 ESBL

ESBLs are ß-lactamases that confer its host a resistance against penicillins, cephalosporins (first, second and third generations) and aztreonam (except for carbapenems or cephamycins) through their hydrolysis, and ESBLs are inhibited by ß-lactamase inhibitors (e.g. clavulanic acid). Moreover, they are usually plasmid-encoded (Bush et al., 1995).

Among the ESBLs, the SHV-type (sulfhydryl variable) usually exists in clinical isolates more than any other types (Jacoby, 1997). SHV refers to sulfhydryl variable, as it was previously thought that the inhibition of its activity by *p*-chloromercuribenzoate was substrate-related and that it was variable according to the substrate used for the test (Sykes and Bush, 1982). As a result of amino acid changes that altered the conformation around the active site, the hydrolysing activity of SHV enzymes evolved from being narrow to being extended-spectrum to include monobactams and carbapenems. Those ESBLs are usually encoded by plasmids that generally carry genes conferring resistance to other drugs, and they have become widespread in several members of *Enterobacteriaceae* worldwide (Liakopoulos et al., 2016). Thus far, 198 allelic variants of SHV have developed resistance to third-generation cephalosporin, and SHV-38 is a unique variant due to its expanded-spectrum that covers carbapenems (Poirel et al., 2003; Tzouvelekis and Bonomo, 1999). PCR-based methods and nucleotide sequence analysis remains the gold standard for the identification of extended-spectrum β-lactamase SHV variants as these methods demonstrate a high sensitivity to variable gene expression levels. Meanwhile, standard microbiological procedures might take several days to perform (Bedenic et al., 2001; Bedenic et al., 2007; Singh et al., 2012; Stürenburg et al., 2003)

The TEM-type (Temoneira) of ESBLs were derived from TEM-1 and TEM-2, although both are not ESBLs (Datta and Kontomichalou, 1965; Buisson et al., 1987). The majority of TEM are encoded by Gram-negative bacteria, and 90 % of ampicillin resistance in Gram-negative bacteria is due to the TEM-encoding genes (Rice et al., 1990). Those ESBLs are usually plasmid-mediated and resulted from mutations in the classic TEM genes (TEM-1 and TEM-

2) via a single or multiple amino acid substitutions around the active site. The first TEM (TEM-1) was isolated from *E. coli* in Greece in 1965 from a patient named Temoneira, and it was found to hydrolyse penicillin and the first-generation cephalosporins, such as cephaloridine. TEM-2 is similar to TEM-1 in its hydrolytic profile, but each one has different isoelectric point; therefore, they are not considered ESBLs (Steward et al., 2000; Zhao and Hu, 2013). The *K. pneumoniae* strain that was isolated in 1987 was found to carry a plasmid-mediated β-lactamase termed CTX-1 because of its greater activity against cefotaxime. This enzyme later was renamed as TEM-3, and it was different from TEM-2 by double amino acid replacements (Alsterlund et al., 2009).

CTX-M (cefotaxime) ß-lactamases are the widest disseminated enzymes. They were initially reported in the mid-1980s, and their occurrence has increased dramatically since 1995 (Bonnet, 2004). It was discovered in 1986 in Japan and was denoted as a non-TEM, non-SHV ESBL in *E. coli* strain resistant to cefotaxime (Matsumoto et al., 1988). Later, in 1989, a clinical cefotaxime-resistant *E. coli* strain was reported in Germany; this strain produces a non-TEM, non-SHV ESBL, which was denoted as CTX-M-1, indicating its hydrolytic activity against cefotaxime (Bauernfeind et al., 1990). Meanwhile, a rapid spread of a *Salmonella* strain carrying resistance to cefotaxime began in South America (Bauernfeind et al., 1992). CTX-M ß-lactamases are abundantly found in enterobacterial species worldwide. Besides being most active against cefotaxime in general, they exhibit little activity against ceftazidime. Based on their amino acid identities, they are grouped into five clusters, as follows: 1) CTX-M-1 cluster, which includes CTX-M-1, -3, -10, -11, -12 and -15; 2) CTX-M-2 cluster, which includes CTX-M-2, -4, -5, -6, -7, -20 and TOHO-1; 3) CTX-M-8 cluster,

which includes CTX-M-8; 4) CTX-M-25 cluster, which includes CTX-M-25 and -26; and 5) CTX-M-9 cluster, which includes CTX-M-9, -13, -14, -16, -17, -19 and TOHO-2. The possible ancestors of the CTX-M-2 and CTX-M-8 clusters are the chromosomal ß-lactamases of *Kluyvera ascorbate* and *K. georgiana*, respectively (Boyd et al., 2004; Poirel et al., 2002).

The ß-lactamase CTX-M-15 was firstly characterized by strains isolated from hospitalised patients in New Delhi. Those strains were *E. coli*, *K. pneumoniae* and *Enterobacter aerogenes* (Karim et al., 2001). CTX-M-15 differs from CTX-M-3 by a single amino acid change, that is, Asp240Gly (according to Ambler numbering), and both CTX-Ms are inhibited by clavulanic acid and tazobactam. However, unlike CTX-M-3, CTX-M-15 displays a catalytic activity towards ceftazidime, and this finding may be a result of the Asp240Gly substitution (Ambler et al., 1991; Poirel et al., 2002). CTX-M-14 and CTX-M-15 are the most important CTX-Ms within the CTX-M family as they are ubiquitous worldwide; the CTX-M-15 type is the most prominent type in the UK. The significance of this family is their multidrug resistance (MDR) ability, and many studies analysed their prevalence. However, insufficient studies dealt with their characteristics and their relationship with MDR (Cantón et al., 2012; Reid, 2018).

1.5.2 Carbapenemases

Carbapenemases is the most versatile ß-lactamases family, and its broad spectrum is incomparable with that of other lactam-hydrolysing enzymes. A significant number of those enzymes recognize almost all hydrolysable lactams, even though they are known as carbapenemases. Moreover, many of them display flexibility against inhibition by all commercially available ß-lactamase inhibitors (Livermore and Woodford, 2006; Queenan and Bush, 2007). The first reported carbapenemases were isolated from Gram-positive bacilli. Compared with other ß-lactamases that were recognized during that period, carbapenemases were inhibited by EDTA. Therefore, they were recognized as metalloenzymes. Experiments showed that all metallocarbapenemases contain at least one zinc atom in their active site, which facilitates the hydrolysis of a bicyclic ß-lactam ring (Frère et al., 2005). Another set of carbapenemases rose in the mid- to late 1980s. Those enzymes' activities were not inhibited by EDTA. Subsequent studies showed that these enzymes utilize serine at their active sites. Besides, the lactamase inhibitors clavulanic acid and tazobactam can inactivate them (Rasmussen et al., 1996; Queenan and Bush, 2007).

Carbapenemases can be divided into three classes: class A, B and D. Class A consists of the serine carbapenemases, for example the *K. pneumoniae* carbapenemase (KPC); class B contains the metallo-β-lactamases (MBLs), for example NDM (New Delhi metallo-ß-lactamase) and IMP (Imipenem); and class D consists of the oxacillinase (OXA) carbapenemases, for example OXA-48 and OXA-23 (Queenan and Bush, 2007; Miriagou et al., 2010).

Detection of carbapenemases is critical for proper treatment. Different tests for phenotypic detection have been introduced, including the modified Hodge test, the inhibition tests for carbapenemase activity, and the detection of carbapenem hydrolysis (Miriagou et al., 2010). However, a test for accurate confirmation and identification of carbapenemases remains unavailable. This is because carbapenemase-producing bacteria, especially the members of *Enterobacteriaceae*, evoke a variety of carbapenem MIC distributions, which are sometimes under the breakpoint, or they have independent carbapenem mechanisms (e.g. active efflux pumping, porin alternations result in reduced permeability, and hyperproduction of class C β-lactamases or ESBLs) which run with or without carbapenemase activity. Furthermore, types within each class of carbapenemases (e.g. IMP and NDM) in MBL cannot be identified with phenotypic assays. Accordingly, a molecular confirmation is recommended for suspected carbapenemase-producing strains (Miriagou et al., 2010; Notake et al., 2013).

OXA β-lactamases are always plasmid-mediated and are nearly rarely found; yet, those β-lactamases were among the earliest β-lactamases that were detected. Usually, their mode of action is restricted to penicillins. However, some β-lactamases could act on cephalosporins. Since the 1980s, *Acinetobacter baumannii* isolates exhibiting carbapenem resistance and carrying plasmid-encoded β-lactamases have emerged; these β-lactamases were categorized as OXA enzymes due to being similar in sequence with earlier OXA β-lactamases, and they were denoted as OXA-23, OXA-40 and OXA-58. Later, it was discovered that all *A. baumannii* strains carry OXA β-lactamase in their chromosomes (OXA-51-like); when the genetic environment promotes its expression, many of them would confer resistance against carbapenems. Similarly, species of *Acinetobacter* that are closely related to *A. baumannii*

have their own chromosomally encoded OXA β-lactamases; many of these enzymes might have been transferred to *A. baumannii* and later formed the basis of transferable carbapenem resistance. In some occasions, OXA-48 β-lactamases have transferred to *Enterobacteriaceae* and have become a significant cause of carbapenem resistance. The evolution of OXA enzymes, which confer carbapenem resistance to *A. baumannii*, has lowered the potency of the carbapenems and has transformed these β-lactamases from a minor obstacle into a significant issue (Evans and Amyes, 2014).

Another OXA type was identified in Istanbul in 2001; it was isolated from a MDR *K. pneumoniae* and it demonstrated carbapenem resistance; it was named OXA-48 (Poirel et al., 2004). This enzyme, along with its variants, are currently broadly spread in *K. pneumoniae* along with other *Enterobacteriaceae*, also it was recently found in *A. baumannii* during a time that it was considered a major concern (Goncalves et al., 2013). Within the active site of OXA-48 and OXA-13, small changes are observed in the amino acid residues and in the β5-β6 loop of OXA-48, and such changes might be responsible for the enzyme's ability to hydrolyse carbapenems, adding a hydrophilic environment to harbour water molecules that are required for hydrolysis. The carbapenem hydrolysis mechanism of OXA-48 differs from that of other carbapenem-hydrolysing oxacillinases. Besides, the active-site cleft of OXA-48 contains a hydrophobic region larger than that of OXA-13 to facilitate diacylation by bringing the antibiotic into proximity with a water molecule. Those features indicate that OXA-48 has developed the ability to hydrolyse carbapenems by adapting a new evolutionary path compared with other OXA-type carbapenemases common in *Acinetobacter* species. The crystal structure of OXA-48 shows that it has a different carbapenem hydrolysis mechanism

compared with other carbapenem-hydrolysing oxacillinases (OXA-40 and OXA-23) in that in the active site of OXA-48 has no hydrophobic bridge. This characteristic suggests that there are other features responsible for its carbapenem hydrolysis ability (Docquier et al., 2009; Evans and Amyes, 2014).

IMP-type carbapenemases are the most prevalent MBL in Japan. It was recognized there in 1991 in *Serratia marcescens* as IMP-1. Later, the IMP genes were detected in Canada and Brazil after being reported in Europe in 1997; subsequently, it slowly spread to the Far East, to the USA and to Australia. The IMP-type Carbapenemases were investigated extensively in *Pseudomonas* and *Acinetobacter* species, as well as in *Enterobacteriaceae* family. Up to 18 IMP-type variants have been identified (Queenan and Bush, 2007; Bush and Fisher, 2011). IMP-1, IMP-2 and IMP-3 display a potent activity against β-lactam antibiotics, excluding monobactams. The activity of IMP-1 against carbenicillin is higher than that against ampicillin, whereas the activities of both IMP-2 and IMP-3 against the above drugs are similar (Watanabe et al., 1991; Livermore and Woodford, 2000).

NDM-1 was mainly described in *E. coli* and *K. pneumoniae*, also in *Pseudomonas* and *Acinetobacter* but with less extent. It confers resistance to all β-lactam antibiotics, except aztreonam, and it is a novel MBL. However, some strains that carry $bla_{\text{NDM-1}}$ are aztreonam-resistant, probably through a different resistance mechanism. This gene is carried on a plasmid that harbours multiple resistance determinants; therefore, it confers extensive drug resistance, allowing a few or no therapeutic choices (Fomda et al., 2014; Yong et al., 2009; Castanheira et al., 2011). The first NDM-1 was reported in 2009 when a Swedish patient (from Indian origion) who travelled from Sweden to New Delhi,

India had contracted UTI through an infection with carbapenem-resistant *K. pneumoniae* that was resistant to all tested antibiotics, excluding colistin (Yong et al., 2009). NDMs are the most relevant enzymes within the MBL family and have been described to have high dissemination tendencies, i.e. tremendous ability to spread. A few variants of NDM, such as NDM-4, NDM-5 and NDM-7, hydrolyse carbapenem more efficiently. The interactions of NDMs with other resistance determinants represent a serious threat for therapy (Sahuquillo-Arce et al., 2015; Rolain et al., 2010). A multinational team published in *The Lancet* in its August 2010 issue a report on the spread and emergence of 180 cases of patients harbouring the NDM-1-carrying strain. Also, 37 cases from the UK and 143 from India and Pakistan were reported, suggesting a widespread dissemination of the carbapenemase (Kumarasamy et al., 2010). Moreover, the highest occurrence of carbapenemase gene was observed in many African countries, including Kenya, Morocco and South Africa (Poirel et al., 2011; Codjoe and Donkor, 2018). The identification of NDM-1 gene in *E. coli* and in *K. pneumoniae* suggests the possibility of *in vivo* conjugation (Yong et al., 2009).

The most relevant among class A carbapenemases (plasmid-encoded) are KPCs. Not only do they hydrolyse nearly all β-lactams, but they are also inserted into mobile genetic elements carrying antimicrobial resistance genes other than β-lactams (Yigit et al., 2001; Sahuquillo-Arce et al., 2015). Twenty types of KPCs have been described. They differ by 1–3 amino acid substitutions and show different hydrolysis profiles (Walther-Rasmussen and Høiby, 2007). KPCs efficiently hydrolyse cephaloridine, benzylpenicillin, cefalotin, amoxicillin, piperacillin and nitrocefin. They can also hydrolyse aztreonam, meropenem, imipenem and cefotaxime but at an activity that is lower by 10-fold to the penicillins and early

cephalosporins. Notably, KPCs show weak hydrolysing activity on cefoxitin and ceftazidime (Queenan and Bush, 2007). *bla*$_{KPC}$ was first identified in *K. pneumoniae* in the USA and it eventually spread worldwide in other *Enterobacteriaceae* and non-fermenting Gram-negative bacteria. The dissemination of *bla*$_{KPC}$ became an endemic issue in Colombia, Puerto Rico, Italy, Greece, Israel, in the east coast of the USA and in the east coast of China; regional or local outbreaks were reported worldwide afterwards. The inter-general spread and high adaptability of KPCs were demonstrated during the first KPC-3 outbreak in Canada between 2009 and 2010, wherein five *Enterobacteriaceae* species were involved (Leung et al., 2012; Munoz-Price et al., 2010; Sahuquillo-Arce et al., 2015). In the KPC group, KPC-3 was the most recent enzyme to be reported. It is closely related to the formers KPC-1 and KPC-2, to which it differs in two and one amino acid, respectively. It was isolated from *K. pneumoniae*, *E. coli* and *Enterobacter cloacae*. KPC-3 hydrolyses carbapenems, cephalosporins, penicillins and even sulbactam. Cephalothin is the best substrate for KPC-3 (Bratu et al., 2005; Alba et al., 2005).

Another virulence factor that has a significant role in antibiotic resistance is the ability of bacteria to form biofilm. Bacterial community within a biofilm can resist the antimicrobial effects and display a high survival rate even when they are antimicrobial-sensitive as there are several mechanisms supporting the multi-factorial antibiotic resistance. Moreover, gene exchange, especially the resistance genes, might happen within the biofilm, which in turn might add another role for biofilms in the development of antimicrobial resistance (Stewart and Costerton, 2001; Singh et al., 2017). Thus, this study combines the antibiotic-resistance criteria with biofilm formation ability for the analysis of specific antibiotic-resistant isolates.

1.6 Microbial Biofilm

Biofilm is defined as a microbial community irreversibly attached to a biological or synthetic surface and lodged in a matrix formed of extracellular polysaccharide, proteins, and extracellular DNA (Soto, 2014; Fattahi et al., 2015; Wolska et al., 2015; Anderson et al., 2004).

Biofilm formation (Fig 1.5) occurs in five steps (Stoodley et al., 2002, Soto, 2014), as follows:

i) planktonic cells reversibly attach to a surface;

ii) irreversible attachment of planktonic cells to a surface mediated by exopolymeric material formation;

iii) formation of biomolecular complex layer and secretion of exopolysaccharides that constitute the outer layer; biofilm maturation starts at this stage;

iv) formation of three-dimensional biofilm structure containing macrocolonies in clusters; within clusters, channels are formed to allow water and nutrient transport and to facilitate elimination of wastes; and

v) after maturation, detachment of biofilm occurs, allowing cells to spread by taking the planktonic form and by reattaching to other surface(s) and form a new biofilm.

Bacteria may exist in two forms during their proliferation and growth: planktonic (as single and independent cells) or ordered ‘sessile’ aggregates (i.e. the biofilm). During their planktonic form, bacterial infections are mainly curable with traditional antibiotics; this kind of infection is termed acute infection. By contrast, the untreatable infection involves biofilm

formation and termed chronic infection, where bacteria mainly have their ultimate resistance to antibiotics and to other traditional antimicrobial agents (Bjarnsholt, 2013).

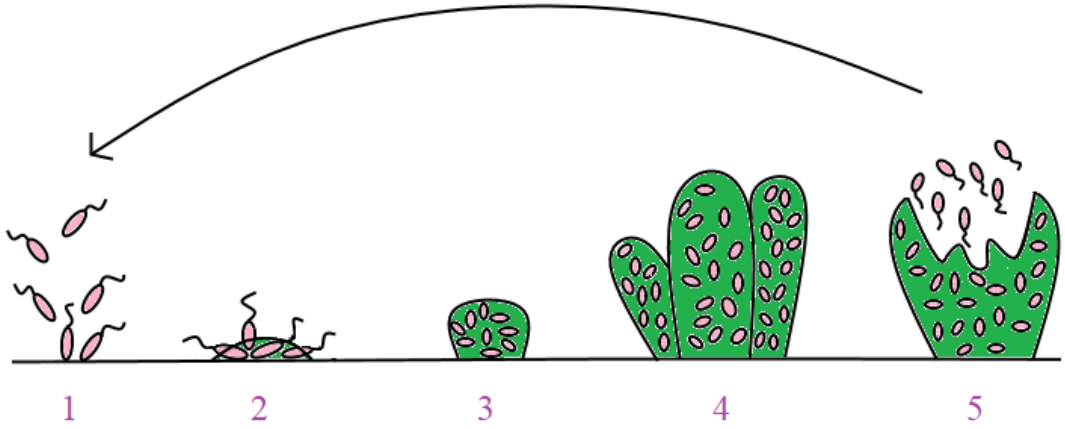

Fig 1.5 Step in biofilm formation: the process starts when planktonic cells aggregate and reversibly attach to a surface (1); the cells start to form exopolymeric materials and attach irreversibly (2); the biofilm starts to mature by forming a complex layer of biomolecules and through the secretion of exopolysaccharides (3); the mature biofilm with a three-dimensional structure contains macrocolonies clusters interspersed by channels for nutrient and waste transfer (4); after maturation, the biofilm cells detach and spread (5).

Atshan et al. (2013) studied the biofilm formation steps in *Staphylococcus aureus* by using a scanning electron microscopy at four time points of growth (i.e. 6, 12, 24, and 48 h); they noticed that mesh-like structures started to appear after 12 h of growth, and the structures became denser at 24 and 48 h with fibrous materials.

Sessile cells differ from planktonic cells physiologically and phenotypically, and their increased resistance to antimicrobial agents is one of their important characteristics (Donlan and Costerton, 2002, Mah and O'Toole, 2001, Stewart and Costerton, 2001). Biofilm formation represents a significant challenge due to its hidden role in the failure of antimicrobial therapy, and nearly 65–80 % of all infections are presumably related to biofilm (Costerton et al., 1999; Parsek and Singh, 2003; Hall-Stoodley et al., 2004).

The physiology of microcolonies and biofilm structure confer inheritable resistance to antimicrobial agents. There are three possible mechanisms to which resistance can be attributed: (i) biofilm matrix can delay the penetration of the antimicrobial agent; (ii) microcolonies slow down their growth rate; and (iii) some physiological changes related to the biofilm mode of growth, such as nutrient limitations and toxic metabolite accumulation, which induce stress response genes and eventually promote the formation of high-density biofilms, improve cell viability (Donlan and Costerton, 2002).

Biofilms can colonize biotic and abiotic surfaces and can exert useful or harmful impacts to human health, to the environment and to the industry (Costerton et al., 1987). The biofilm structure, namely, its polymeric matrix and adhesive surface, provides cells with high water concentration and nutrition and is an ideal avenue for signalling pathway, enzyme and metabolite interaction and exchange of genetic materials(Davey and O'Toole G, 2000). Biofilm-associated cells are characterized by increased resistance to the host immune system, to detergents and to antibiotics; they can also adapt to environmental changes and adverse environmental conditions, such as low pH, desiccation, limited nutrient supply and predation. Moreover, a biofilm can provide cells with conditions characterized by high osmolarity, high

cell density and low oxygen supply (Lewandowski et al., 1991; Vieira et al., 2004; Prigent-Combaret et al., 1999; Stewart and Franklin, 2008; Rinaudi and Giordano, 2010). Astronauts may suffer from compromised immune systems that drive them to be easy victims of bacterial infections. This is because bacteria are not only able to survive in space but also can proliferate and become virulent. The International Space Station has been demonstrated to be contaminated with bacterial biofilms and slime (Nickerson et al., 2004, Kim et al., 2013).

Regarding the industrial aspects, biofilm can have some hazardous impacts; for instance, biofilms act as heat exchangers, and biofouling becomes a major problem when marine ship cages and ship hulls come into contact with water (Braithwaite and McEvoy, 2005; Coetser and Cloete, 2005; Flemming, 2002). Moreover, formation of biofilm in drinking water tanks directly affects human health. In this case, biofilms might block these systems as well as serve as a health risk to consumers by providing a shelter for pathogenic bacteria, such as *E. coli* and *Legionella pneumophila* (Flemming, 2002; Juhna et al., 2007). However, there are considerably useful applications of microbial biofilms, including fermentation (Kunduru and Pometto, 1996), bioremediation (Singh et al., 2006), production of biofuel (Wang and Chen, 2009), electricity generation using microbial fuel cells (Rabaey et al., 2007), fine chemical production (Li et al., 2006) and wastewater treatment (Nicolella et al., 2000).

Biofilm complexity is made even more complicated by their being genetically heterogeneous (Stewart and Franklin, 2008). Biofilm could be stratified (in its natural community) which is caused by the migration of its resident microorganisms towards the areas with optimal conditions to gain light, secondary metabolites, nutrients, oxygen and signalling compounds (Becraft et al., 2011; Kim et al., 2014; Ramsing et al., 2000). There are three general factors

that contribute to biofilm heterogeneity: (i) Physiological heterogeneity, wherein bacteria adapt to the environmental conditions. For instance, oxygen and nutrients diffuse from the source into the biofilm and become available to the bacteria for utilization. Such a diffusion will cause the development of a chemical concentration gradient, which in turn might interact with the gradients for waste products and signalling compounds, Resulting in formation of a variety of unique microenvironments in the same biofilm structure, ultimately resulting in a growth condition that differs completely from that for planktonic bacteria. The bacteria in turn respond to the changing conditions and thus the physiology of the individual cells may differ from that of the nearby cells (Rani et al., 2007; Rasmussen and Lewandowski, 1998; Werner et al., 2004). (ii) Genetic variability, wherein mutation might occur in a clonal population of cells. This phenomenon might cause cellular differentiation (Boles et al., 2004; Hansen et al., 2007). (iii) Stochastic gene expression, wherein the same genes are expressed at different levels among groups of cells, though these cells are exposed to the same environmental conditions. This phenomenon leads to the development of subpopulation of cells within the same community, and these cells differ from the mother cells in a way that the persister cells display a better antibiotic resistance than the other members of the same community (Baty et al., 2000a, Baty et al., 2000b, Vlamakis et al., 2008, Gelens et al., 2013).

Investigation on biofilms is usually performed in the natural environment and in laboratory-scale bioreactors designed to simulate a natural biofilm. Bioreactors are operated in two ways: under static conditions or under continuous flow conditions. In the first case, bacteria in a biofilm may be subjected to growth phases (lag phase, log phase and stationary phase), the same as in growing planktonic cultures *in vitro*. For continuous cultures, the process is

usually done under ‘wash-out’ conditions wherein the residence time of the bacterial cell is shorter than its doubling time. Residence time is defined as the ‘time for one reactor sized volume of liquid to flow through the reactor’. In this approach, all planktonic cells are washed out from the reactor, and only the bacteria that adhered to the surface are kept within the reactor. In this kind of bioreactors, usually the biofilm surfaces are either a coupon that could be easily removed from the reactor for later analysis or the walls of the reactor could be directly imaged (Franklin et al., 2015; Coenye and Nelis, 2010; BioSurface Technologies Corp, 2016).

1.6.1 Biofilm and UTIs

In UTI, biofilm formation involves many processes following infection. The main cause of biofilm formation is catheterization, which induces a robust immune response leading to the accumulation of fibrinogen on the catheter; the fibrinogen in turn creates an ideal environment to attach the uropathogens that express fibrinogen-binding proteins. Neutrophil infiltration will be induced by this infection. After the initial attachment of bacteria onto the fibrinogen-coated catheter, the bacteria multiply, forming biofilms and subsequently promoting epithelial damage; the kidneys will be seeded by infection wherein toxin production will induce tissue damage. The infectious microorganisms that cause complicated UTIs can also progress to bacteraemia by crossing the tubular epithelial cell barrier if they are left untreated (Flores-Mireles et al., 2015).

1.6.2 Biofilm analysis

Static biofilms (Fig 1.6) have been used in some biofilm studies. The simplest method to facilitate growth of and to screen biofilm was developed by O'Toole and co-workers (1998). In this method, bacterial strains are incubated in a microtiter plates' wells. After incubation, the cells are washed out, and the remaining cells associated with the wells are stained with a colorimetric indicator (e.g. crystal violet); the amount of crystal violet taken up by the cells is assayed to estimate the biofilm amount. This method can be used to compare the amount of biofilm produced by the wild-type strains and the mutant strains to study the effect of gene deletion or mutation on biofilm formation and on bacterial adhesion onto the surfaces (O'Toole and Kolter, 1998a, O'Toole and Kolter, 1998b). Another method that involves the use of microtiter plates and which is a modification of the method above involves the use of the Calgary Device. In this method, the biofilm that grows on the pegs that were immersed in the wells of the microtiter plates is assayed rather than the organisms growing on the wells. This method minimizes the interference of planktonic cells that might remain at the bottom of the wells following washing but are not biofilm bacteria; in this way, only the peg-adherent bacteria are assayed (Ceri et al., 1999). Biofilms may be cultivated under static conditions either on coupons placed in the wells of microtiter plates or as pellicles at the air–water interface. Some organisms prefer to grow under static conditions and form thick biofilms, whereas they do not form intrinsic biofilms when grown under continuous flow. This technique might reflect the preference of some organisms under static conditions where they are found in their natural habitat (Branda et al., 2001; Chimileski et al., 2014).

Colony biofilm might be used as another type of static biofilm. In this approach, biofilms are cultivated on filters placed on agar Petri plates' surface. The filters are subsequently transferred into a new fresh medium at regular intervals, and the biofilms are given a semi-continuous supply of fresh nutrients. The greatest benefit of this method is that biofilms are easy to grow using cheap laboratory techniques. This method is usually used in cryoembedding and in thin sectioning experiments given that the biofilm generated using this method is thick (Huang et al., 1996). The disadvantage of this method is that since there is no wash-out process, planktonic cells might interfere with the biofilm assay (Franklin et al., 2015).

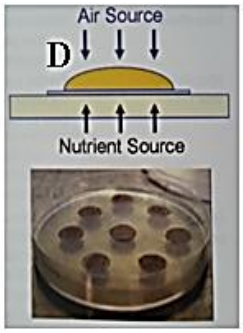

Fig 1.6 Methods for growing biofilm under static conditions

A) Microtiter plate: cells are incubated in wells (Basak et al., 2013).

B) Calgary device: biofilm grows on pegs immersed in the wells of the microtiter plates (Emery Pharma, 2014). **C)** Static/Coupon: biofilm is cultured on a coupon of glass (Chimileski et al., 2014). **D)** Colony biofilm: biofilms are cultivated on filters placed on the agar petri plates' surface (Franklin et al., 2015).

In simulating natural biofilms, continuous flow reactors (Fig 1.7) have been developed for advanced biofilm studies. The reactors used for continuous flow include the Centre for

Disease Control (CDC) biofilm reactor (Goeres et al., 2005), the drip-flow reactor (Goeres et al., 2009) and the reactors designed for confocal laser scanning microscopy (CLSM) imaging (Lawrence et al., 1991; Nivens et al., 2001; Stapper et al., 2004). The CDC biofilm reactor is a perfectly large-scale reactor that supplies ports for medium inlet and outlet. The chamber contains rods carrying removable coupons made of glass, metals or hydroxyapatite. In this bioreactor, the biofilm is formed on the surface of the coupons and then removed aseptically over time. This technique is used for direct imaging of the sample using CSLM, for determining colony-forming units and direct bacterial cell counts, and for omics studies. The biofilm formed by this method is usually thick and mimics natural biofilms; these characteristics are achieved by running the CDC biofilm reactors under wash-out conditions with fluid shear. However, one disadvantage of this method is that the reactors need a large medium tank, making it a low-throughput technique (Goeres et al., 2005). The drip-flow reactor is similar to a continuous flow reactor. In this case, the medium is dripped onto the coupon surface and then allowed to flow over the coupon. In the drip-flow reactor, the resulting biofilms are often thick. Also, the reactor creates an excellent mimic for some natural biofilms in that the fluid flows across the surface with an air interface. In this technique, the biofilms usually show some heterogeneity across the slide from the initial site of the medium input to the outlet. This method allows the conduct of studies related to cryoembedding and thin sectioning (Goeres et al., 2009; Lenz et al., 2008; Xu et al., 2001). The imaging flow cells system is another form of a continuous flow reactor. The flow cells usually contain a window, which is made of a glass coverslip that permits viewing of the biofilm under a microscope. These biofilms can be imaged using CSLM that reveals the three-dimensional architecture of the biofilms. A modification of this technique is the

capillary flow cell biofilm wherein the biofilms are cultured in small square capillary tubes. In this technique, the biofilms that form on the walls of the capillary tubes can be directly imaged. A challenge for this approach is the formation of clog inside the small tubes. Therefore, this technique is suitable only for short-term experiments (Lawrence et al., 1991; Nivens et al., 2001; Stapper et al., 2004; Dunsmore et al., 2002; Rani et al., 2005; Xi et al., 2006).

Fig 1.7 Methods for growing biofilm under continuous flow **A)** The CDC reactor: the biofilm is formed on the surface of the coupons and then removed aseptically over time (ECOMETAL, 2011). **B)** Drip-flow reactor: the medium is dripped onto the coupon surface and then allowed to flow over the coupon (Standardization, 2008). **C)** Imaging flow cells: biofilms can be imaged using CSLM that reveals the three-dimensional architecture of the biofilms (Franklin et al., 2015).

1.6.3 Genes involved in biofilm formation in *E. coli*

In addition to environmental factors, such as pH, temperature, ionic force of the medium and surface nature, genetic signals control every step in the process of biofilm development and maturation (Roux et al., 2010). Niba and co-workers (2007) have identified many genes involved in biofilm formation in *E. coli* k-12 strain.

crr codes for a protein product, Crr, which is involved in glucose transport, along with another protein (PtsG) by forming an enzyme complex known as the enzyme II complex. The PtsG/Crr picks up the exogenous glucose and releases its phosphate ester into the cell cytoplasm in preparation for metabolism by glycolysis (Curtis and Epstein, 1975; Weigel et al., 1982).

Genes that codes for curli are distributed in two operons: *csgBA* and *csgDEFG* (Fig 1.8). The *csgBA* operon encodes the subunits of curli proteins that form fibres at the cell surface; these fibres are called fimbriae, which are involved in adhesion and cell–cell attachment (UniProtKB, 2019f). CsgA is the major subunit protein of the fibre, whereas CsgB is the nucleator protein homologous in sequence to CsgA. Both are encoded by the *csgBA* operon. CsgA is secreted outside of the cell and then CsgB nucleates it into a fibre. When CsgB is absent, the curli are not assembled and CsgA is secreted in an unpolymerized form from the cell. CsgG is an outer membrane protein and it is needed for the secretion of the two curli structural subunits (i.e. CsgA and CsgB). CsgE and CsgF are periplasmic proteins that interact with CsgG in the outer membrane. CsgE, CsgF and CsgG promote the secretion and assembly of CsgA into a fibre. CsgD is a positive transcriptional regulator of the *csgBA* operon (Hammar et al., 1995; Barnhart and Chapman, 2006).

*fli*S codes for the flagellar protein FliS, which is the flagellin-specific chaperone that binds flagellin (the major protein of the filament) and facilitates its export. It also plays a significant role in motility (Galeva et al., 2014; Juhas et al., 2014).

fliL is another flagellar protein located in an operon, along with other genes that code for export apparatus and motor/switch proteins for flagellar development. An *E. coli* carrying a deletion mutation in *fliL* will generate a cell defective in swarming motility but not in swimming motility. The lack of *fliL* will lead to a single flagellar motor that rotates at reduced speeds and switches directions less frequently. It also plays an essential role in torque generation, particularly at high viscous loads (Partridge et al., 2015; Attmannspacher et al., 2008).

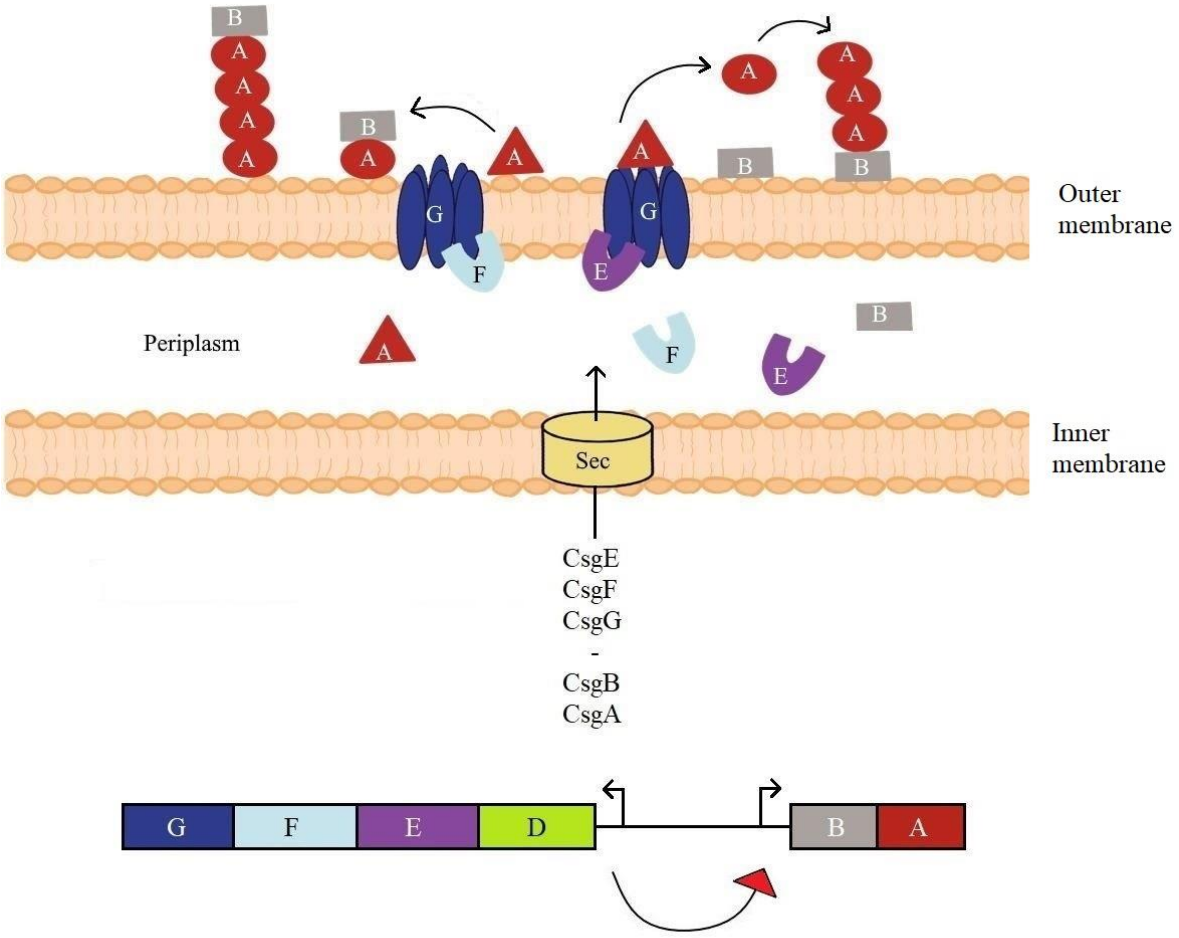

Fig 1.8 A schematic diagram illustrating the two curli gene operons; *csgBA* and *csgDEFG*. CsgD positively regulates the *csgBA* operon. The outer membrane protein (CsgG) is required for the secretion of the two curli structural subunits CsgA and CsgB. CsgE and CsgF will interact with CsgG and are needed for efficient curli assembly. CsgB nucleates CsgA into a fiber when the latter secreted outside of the cell. The diagram is adapted from Barnhart and Chapman (2006).

tolB gene is a part of the *tol-pal* gene cluster that codes for seven genes, which are organized in an operon with an internal promoter. The proteins encoded by the *tol-pal* gene cluster participate in supporting the integrity of the cell envelope, but their precise task in the cluster

remains ambiguous. Mutation in this gene cluster results in a leaky membrane, in defective cell division and in defective sensitivity to detergents and antibiotics. tolB is one of the transcripts derived from the gene product of this operon, and it is a periplasmic protein (Lazzaroni et al, 1999; Llamas et al, 2000; Sturgis, 2001).

The protein product of *yie*O is proposed to function as a multidrug transmembrane transporter, although insufficient studies confirm the exact function of this gene (Kvist et al., 2008).

*mdo*H is involved in the biosynthesis of a protein called osmoregulated periplasmic glucan (OPG). OPG is required in the pathway which is part of glycan metabolism for OPG biosynthesis (UniProtKB, 2019a). On gene expression work on the plant pathogen *Xylella fastidiosa* during biofilm formation, De Souza et al. (2004) found that this gene is upregulated during biofilm maturation.

fimA is the major subunit of the *E. coli* type 1 fimbriae (pili). It plays a function in cell adhesion and pilus organization. Moreover, it has a role in single-species biofilm formation via attachment to abiotic surfaces (UniProtKB, 2019g; Roux et al., 2010).

rfaH affects the expression of different operons that encode extracytoplasmic components in *E. coli*. It enhances the expression of different factors that play a significant role in virulence. Inactivation of *rfaH* significantly decreases the virulence of uropathogenic *E. coli*. *rfaH* represses biofilm formation by reducing the antigen 43 (Ag43) level. Ag43 mediated auto aggregation and biofilm formation and it is encoded by *flu*, wherein *rfaH* has been shown to indirectly downregulate the expression of *flu* (UniProtKB, 2019g; Beloin et al., 2006).

Accordingly, the expression of the above genes regulates biofilm formation and contributes to microorganisms' ability within the biofilm to resist the antimicrobials via a variety of mechanisms; such as coordination with other genes that function in decreasing antimicrobials diffusion into the biofilm matrix, production of exopolysaccharides that confer chlorine resistance, and reduction of microbial growth rate (Watnick and Kolter, 2000).

Moreover, the regulatory effects of the QS mechanism coordinate the heterogeneous architecture of biofilm and regulate the synthesis of degradative enzymes and facilitate the new mode of growth of microcolonies within the biofilm (Hassett et al., 1999). Many genes studied in this work, such as *motB, crl,* and *nl*pC, which contribute to biofilm formation are regulated by QS mechanisms (DeLisa et al., 2001).

1.7 Quorum sensing

QS is defined as the regulation of gene expression according to microbial cell density population fluctuation (Miller and Bassler, 2001). It enables bacteria to communicate, integrate, sense, respond to changes in their environment, and it coordinate these responses within the cell population using chemical molecules termed as autoinducers (Fuqua et al., 2001). A QS system regulates many Gram-positive and Gram-negative bacterial physiological activities, such as virulence, sporulation, competence, symbiosis, antibiotic production, conjugation, motility, light production, bioluminescence and biofilm formation (Miller and Bassler, 2001; Kaper and Sperandio, 2005; Visick and McFall-Ngai, 2000; Whitehead et al., 2001). During bacterial growth, the extracellular signals (i.e. the

autoinducer (AI) molecules) are produced and detected by the same bacterial groups or by other microorganisms to determine the cell population density. AIs have been classified into two main types: AI-1 and AI-2. AI-1 molecules are acyl homoserine lactones (HSLs). They are assumed to play as intra-species signals. By contrast, AI-2 is a DPD-derived molecule (DPD is 4,5-dihydroxy-2,3-pentanedione) and functions in inter-species communication. Synthesis of AI-1 depends on LuxI-like synthases and on the combination between LuxR-like transcriptional regulator protein with its cognate HSL. This combination (LuxR–HSL complex) then stimulates the target gene transcription and expression of the related physiological functions. AI-2 is synthesized by LuxS-like synthases and recognized by LuxP and LuxQ; a phosphorylation-relay cascades then transmits the signal and activates the target gene transcription and the consequent physiological behaviour of many Gram-positive and Gram-negative bacteria (Miller and Bassler, 2001; Withers et al., 2001; Camilli and Bassler, 2006; Xavier and Bassler, 2003).

1.7.1 AI-2 and related QS circuit

AI-2 is a common inter-species signal that enables one species to identify other species' cell population densities. It is a furanosyl borate diester and relies upon LuxS-like synthases for its synthesis. In the AI-2 QS circuit, AI-2 is recognized by LuxP and LuxQ proteins; a phosphorylation cascade then starts, in which a signal is transmitted, and transcription of the target gene is activated (Xavier and Bassler, 2003). Peptide signalling molecules are utilized instead of HSLs as QS signals in Gram-positive bacteria; the signals are transported via a mechanism involving a two-component system. Examples of activities controlled by such

kind of QS are virulence factors and genetic competence (Kleerebezem et al., 1997; Bassler and Losick, 2006; Sturme et al., 2002).

QS regulated by AI-2 is widely spread among many Gram-negative and Gram-positive bacteria (Xavier and Bassler, 2003). The bioluminescence of *Vibrio harveyi* was the first cell function reported to be controlled by AI-2 (Greenberg et al., 1979; Pereira et al., 2013). Biofilm formation in *Streptococcus mutans* and *Salmonella typhi* and the virulence factor expression in *Vibrio cholera* have also been reported to be mediated by AI-2. (Merritt et al., 2003; Pratt and Kolter, 1998; Zhu et al., 2002). In addition, AI-2 was reported to control Type III secretion in enterohaemorrhagic *E. coli* (Sperandio et al., 1999), transcriptional virulence gene expression in *Clostridium difficile* (Lee and Song, 2005), *Clostridium perfringens* alpha, kappa and theta toxins (Ohtani et al., 2002), prodigiosin, secreted haemolysin and biosynthesis of carbapenem antibiotics in *Serratia marcescens*(Coulthurst et al., 2004). For some bacterial species, a *luxS* mutation leads to an altered structure or decreased biofilm volume in comparison with the correlated wild-type strains, such as in *S. typhi* (Prouty et al., 2002), *S. mutans* (Merritt et al., 2003) and *K. pneumoniae* (Balestrino et al., 2005). In *E. coli*, the role of AI-2 differs among various strains; for instance, it regulates motility in K12 strains (Herzberg et al., 2006; Wood et al., 2006), whereas it plays a metabolic role in O157:H7 (Clarke and Sperandio, 2006, Walters and Sperandio, 2006). However, it was found that AI-2 in *K. pneumonia* plays a role in the early stages of biofilm formation (Balestrino et al., 2005).

In *E. coli*, synthesis of AI-2 depends on the quantity of carbohydrate in the medium and is subjected to the growth phase. Production and secretion of AI-2 by cells occur during the

exponential growth phase, whereas AI-2 is no longer produced in the stationary phase (Surette and Bassler, 1998; Cappuyns et al., 2009). It was reported that AI-2 signal was not produced in the absence of glucose (Surette and Bassler, 1998; Surette et al., 1999). Moreover, DeLisa et al. (2001) reported that AI-2 production was stimulated by the addition of glucose, iron and NaCl in the nonpathogenic *E. coli* strains. Also, in LB medium, AI-2 was produced with or without the addition of glucose. This finding indicates that glucose is non-essential for AI-2 synthesis, although it can increase its production. Niu et al. (2013) reported that LuxS might affect *E. coli* biofilm production and other phenotypes in two ways: through production of AI-2 signal and through AI-2-independent modification of intracellular metabolite levels.

The loss of AI-2 at the stationary phase is due to its uptake by *E. coli* as it is imported through an ATP-binding cassette (ABC) transporter, which is called the *luxS*-regulated (Lsr) transporter. *lsr* operon (*lsrACDBFG*) is regulated by cyclic AMP/cyclic AMP receptor protein, and the transporter proteins are a part of this operon. The genes *lsrK* and *lsrR* are located upstream of *lsr*, and both belong to the same operon, *lsrRK*, which is positively regulated by cyclic AMP receptor protein and negatively regulated by LsrR. AI-2 is phosphorylated to an activated molecule by the cytoplasmic kinase LsrK, which in turn thought to bind and derepress the *lsr* repressor LsrR (Li et al., 2007; Wang et al., 2005). The mechanism of action of this AI-2 QS circuit is illustrated in Fig (1.9)

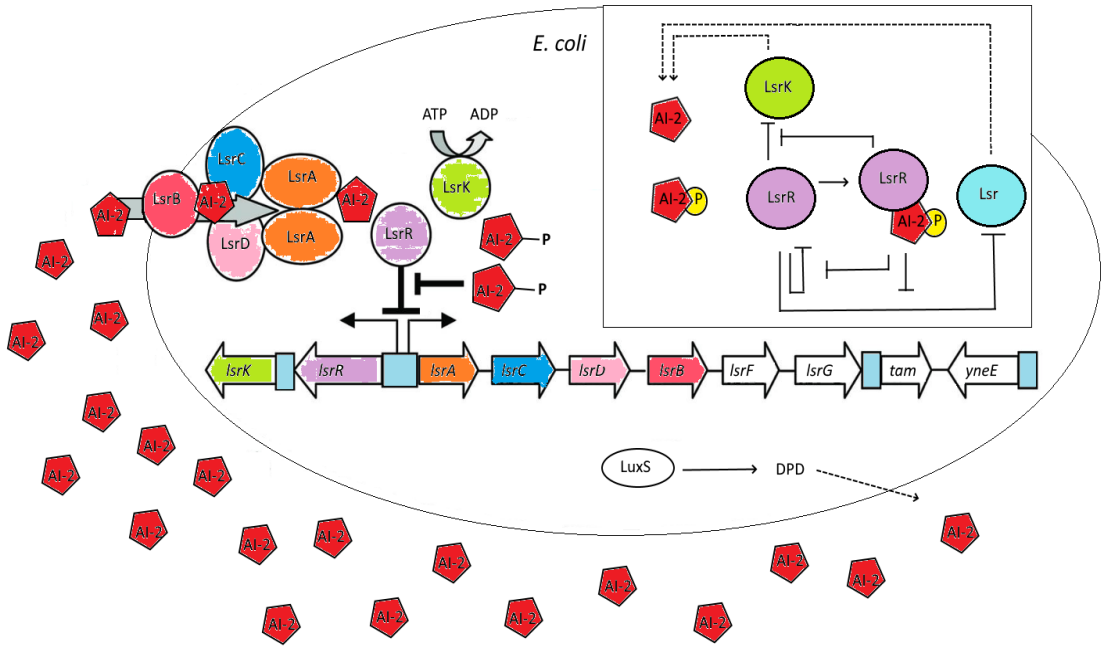

Fig 1.9 The LsrR/phospho-AI-2 circuit during AI-2 uptake in *E. coli*. LsrR supresses an *lsr* operon, *lsrRK* operon, along with other genes. LsrACDB imports AI-2 into the cell, which in turn will be processed as phospho-AI-2 via the kinase LsrK. Studies showed that phospho-AI-2 binds LsrR and relieves its repression of the *lsr* transporter genes and thus triggers their expression, which in turn triggers additional AI-2 uptake (Li et al., 2007).

Studies showed that *E. coli* has an AI-2-mediated QS system that might regulate its virulence factors, DNA processing, cell division, flagellar development, motility and biofilm formation (Sperandio et al., 2002). In *E. coli*, AI-2 controls the expression of some genes that plays different functions (DeLisa et al., 2001). *mot*B expression, which is controlled by AI-2, is a transmembrane protein that functions in transmembrane proton conduction. Along with the products of *mot*A, both genes' products comprise the stator element of the flagellar motor

complex that is required for the rotation of the flagellar motor, which is operated by H^+ ion gradient across the cytoplasmic membrane (Zhou et al., 1998; UniProtKB, 2019e; Sowa et al., 2014).

The protein product of *crl* binds to the sigma-S subunit of RNA polymerase, increases the activity of RpoS by direct interaction with the RpoS holoenzyme, and activates the expression of sigma-S-regulated genes, such as the csgBA operon, which encodes the subunits of curli proteins that form fibres at the cell surface; these fibres are called fimbriae that are involved in adhesion and cell–cell attachment (Cavaliere and Norel, 2016; Arnqvist et al., 1992; Pratt and Silhavy, 1998). *nlp*C is a lipoprotein hydrolase that plays a function in membrane biogenesis and is involved in biofilm formation (Petersen, 2018). AI-2 synthesis will upregulate both *mot*B and *crl* but will downregulate *nlp*C (DeLisa et al., 2001).

Due to the continuous development of antibiotic resistance despite the introduction of new antibiotics, along with the issue on biofilm formation, the need to search for an alternative therapy is indispensable to maintain the human life for the next generations. In this study, the antibacterial and antibiofilm ability of Manuka honey was analysed; Manuka honey is a suggested alternative medicine to treat the antibiotic-resistant pathogens as well as a means to address the problem on biofilm formation.

1.8 Gene Expression Analysis using Quantitative PCR (qPCR)

Gene expression analysis (also called mRNA analysis) is a frequently used approach in qPCR technique. As a first step, researchers usually convert RNA into cDNA (reverse transcription)

and then use the cDNA as a template for the detection and quantification of gene expression product in a qPCR machine (Thermo Fisher Scientific, 2019). Gene expression is a process by which the information from the gene is used to synthesize a functional gene product, such as proteins. Yet, for non-protein coding genes, such as rRNA genes, the product is a housekeeping RNA (Taft et al., 2010; Livak and Schmittgen, 2001).

qPCR is a powerful and sensitive technique for gene analysis used for the detection, quantification and typing of different microbial products in the clinical field, in food safety and in veterinary diagnostics, such as quantitative gene expression analysis, pathogen detection and genotyping (Kralik and Ricchi, 2017; Thermo Fisher Scientific, 2019). After each cycle in the qPCR, fluorescence is measured, and the intensity of the fluorescent signal indicates the momentary amount of amplified DNA in real time. In the first cycles, the amount of DNA is usually too low to be detected. The specific point at which the fluorescence intensity increases above the detectable level, which proportionally corresponds to the initial number of template DNA molecules in the sample, is termed as the quantification cycle or Cq (Kubista et al., 2006; Kralik and Ricchi, 2017).

In the qPCR, the analysis of the amount of gene transcript can either be absolute quantification or relative quantification (Tyburski et al., 2008). In absolute quantification, the copy number of the template is quantified based on a standard curve prepared from serial dilutions of known concentration of the solution of the test sequence. In relative quantification, the curve is used mainly for calculating the efficiency of the reaction, and the result is calculated relative to a calibrator. Generally, a transcript number is given in relation to the quantity of what is termed the reference genes. This normalization can correct the

differences between the compared samples. In performing relative quantification in qPCR, reference genes should be prepared; these genes can be defined as an internal reaction control whose sequences are different from that of the target. For a gene to be nominated as a reference, it should meet some significant criteria; most importantly, its expression level should be unaffected by any experimental factors. Moreover, the gene should display minimal variability in its expression in tissues and under different physiological states of the organism (Chervoneva et al., 2010; Kozera and Rapacz, 2013).

1.9 Manuka Honey and its Antibacterial Activity

Manuka honey is a monofloral honey that is synthesized from the nectar of flowers of Manuka tree (*Leptospermum scoparium*) by the honeybee *Apis mellifera* (Alvarez-Suarez et al., 2014). Rating of Manuka honey is usually performed using a classification system known as the Unique Manuka Factor (UMF). A UMF value is directly related to methylglyoxal (MGO) content (Mavric et al., 2008; Johnston et al., 2018).

Honey has generally been used as a traditional remedy to treat infections since the ancient times. The antibacterial activity of honey varies depending on the honey type and the source. The inhibitory ability of honey has been attributed to its multiple components, mostly to the presence of hydrogen peroxide (H_2O_2) (Mavric et al., 2008). Other factors that contribute to honey activity are the osmotic effects caused by high sugar concentration, the low pH values due to presence of several organic acids, the antimicrobial peptide bee defensin-1, the MGO, the polyphenols, and other compounds that have not yet been fully elucidated (McLoone et al., 2016; Olaitan et al., 2007; Mavric et al., 2008).

Manuka honey has considerably attracted the researcher's attention due to its biological properties, mainly its antimicrobial and antioxidant abilities (Alvarez-Suarez et al., 2014). Manuka honey consists of carbohydrates, fatty acids, proteins, minerals and phenolic and flavonoid compounds. These compounds might also be found in other types of honey. However, some unique characteristics can be found in Manuka honey, the remarkably high level of MGO is an example, which is formed from dihydroxyacetone to which the antibacterial activity of this honey is attributed. Many recent studies demonstrated the antibacterial activity of honey in terms of minimum inhibitory concentration (MIC), which is the minimum concentration of honey required to inhibit microbial growth (Mavric et al., 2008; Johnston et al., 2018). However, many studies attribute the antimicrobial activity of Manuka honey to its unique level of MGO (Adams et al., 2008; Mavric et al., 2008). Lu et al. tested the antibacterial activity of three types of honey: Manuka (M), Kanuka (K) and Manuka–Kanuka (MK) that have originated from different floral sources. They found that each honey displayed a different antibacterial activity and which was not related to the MGO or H_2O_2 concentrations. For example, MK1 had the lowest MGO level but showed the highest antibacterial activity against *S. aureus*, *B. subtilis* and *E. coli* when exposed to catalase (to remove H_2O_2). MK2 showed a dramatic inhibitory drop down to 16 % against *B. subtilis* when exposed to catalase. MK3 exhibited a partial inhibition against *P. aeruginosa* but only without exposure to catalase. The researchers concluded that MGO and H_2O_2 did not merely participated in bacterial growth inhibition (Lu et al., 2013; Lu et al., 2014), and the activity might be related to different phenols or other compounds (Paramasivan et al., 2014; Kwakman et al., 2001).

Researches on Manuka honey have investigated its antibacterial activity against several human pathogens, even the antibiotic-resistant ones. Manuka honey showed antibacterial activity against *E. coli*, *Salmonella typhimurium, E. aerogenes, S. aureus,* methicillin-resistant *S. aureus* (MRSA), vancomycin-resistant *Enterococci* (VRE) and β-*haemolytic streptococci* (Visavadia et al., 2008; Mandal and Mandal, 2011).

The effect of different types of Manuka honey as antibiofilm have been studied. At low concentrations, Manuka honey may prevent biofilm formation, which was proposed to be induced by a stress-response as would an antibiotic. The activity of Manuka against biofilm was observed in many forms: (i) reduction of biofilm formation due to the MGO and sugar contents of the honey and (ii) reduction of biofilm mass by killing bacterial cells inside the biofilm matrix. In addition, the release of planktonic cells from the biofilm matrix did not show any resistance to the tested honey samples (Lu et al., 2014). Another study confirmed that no bacterial resistance has developed after Manuka treatment. This finding might be attributed to the honey components' complexity that work either individually or synergistically to prevent resistance against honey (Cooper et al., 2010). The safety of Manuka honey with UMF 20+ for consumption has been evaluated in healthy individuals; results showed that it has no significant allergic effect, no detrimental effect against advanced glycation end products that are involved in many conditions (e.g. diabetes, renal disease, heart disease and neurodegenerative disease) and it does not alter the homeostasis in gut microbiota. Thus, its safety for healthy individuals is confirmed (Wallace et al., 2010).

This study will shed light on the ability of selected antibiotic-resistant Gram-negative bacteria to form biofilm in different media at specific time points, demonstrating the

expression of some genes related to biofilm formation at those selected time points and suggesting an alternative therapy, which is supported by data on gene expression, to overcome the current two major global issues: antibiotic resistance and biofilm formation.

1.10 Research Gaps

The purpose of this study is to augment the knowledge gap due to the unavailability of studies dealing with the characteristics of biofilm formation at different time-points, due to the unavailability of studies dealing with genetic characteristics during biofilm formation involving the *E. coli* CTX-M-15 strain in different media, and due to the unknown correlation of these characteristics with the increased prevalence of and increased ability for antibiotic resistance. Moreover, no study has analysed the effect of Manuka honey on the selected genes of this strain.

1.11 Overall Aims and Objectives

1) To determine the biofilm formation ability.
2) To analyse the expression of genes that are related to biofilm formation.
3) To determine the antibacterial effect of Manuka honey on the biofilm-related gene expression.

Chapter 2:

Biofilm formation by antibiotic-resistant bacteria associated with urinary tract infections

2.1 Introduction

Biofilm formation includes many steps, beginning with planktonic cell attachment to a living or nonliving surface. This attachment is followed by micro-colony formation, giving rise to three-dimensional structures that, after maturation, can detach from the surface (Jamal et al., 2018). There are limited researches on phenotypic and genotypic characteristics of antibiotic-resistant UTI pathogens, and most work has concentrated on the prevalence of antibiotic-resistant UTI pathogens and prevention of antibiotic misuse (Weber et al., 1999; Erb et al., 2007; Cai et al., 2015). This work investigates the phenotypic characteristics of selected antibiotic-resistant isolates of *E. coli* (CTX-M-15, TEM-3 and IMP-type) and *K. pneumoniae* (OXA-48, SHV-18, NDM-1 and KPC-3) with respect to their ability to form biofilms, and compares their characteristics to those of non-resistant strains (*E. coli* 12241 and *K. pneumoniae* 9633). Most UTIs are associated with biofilm formation, and the study of this ability is of high importance because the microorganisms in the biofilms are hard to treat with the current traditional antimicrobials (Niveditha et al., 2012; Soto et al., 2006; Soto et al., 2007). Besides, many studies showed a relation between antibiotic resistance and biofilm formation (Cho et al., 2018; Cepas et al., 2019).

2.1.1 Aims and Objectives

Aim

The aim of this research is to investigate the phenotypic characteristics of the selected antibiotic-resistant isolates *E. coli* (CTX-M-15, TEM-3 and IMP-type) and *K. pneumoniae* (OXA-48, SHV-18, NDM-1 and KPC-3) for their ability to form biofilms, compare their characteristics with the non-resistant strains (*E. coli* 12241 and *K. pneumoniae* 9633), and try to find through those characteristics why those strains are antibiotic-resistant.

Objectives

- to confirm the species and the type of antibiotic-resistance of the selected strains
- to determine the biofilm densities of the growing cells in the different media at the four time-points via measuring the absorbency at 570 nm.

2.2 Materials and methods

2.2.1 Buffers, solutions and reagents

Table 2.1 The reagents and solutions used in this study and their preparations.

Reagent/Solution	**Preparation**
Crystal violet for gram staining	For 100 mL, 0.5 g crystal violet (Acros Organics), 25 mL methylated spirit (Fisher Scientific), 75 mL distilled water
Iodine solution for gram staining	For 500 mL, 5 g iodine (Fisher Scientific), 10 g KI (Fisher Scientific), 500 mL distilled water
Safranine	For 100 mL, 0.5 g safranine (Fisher Scientific), 100 mL distilled water
Crystal violet for biofilm staining	For 100 mL, 2 g crystal violet (Acros Organics), 25 mL methylated spirit (Fisher Scientific), 75 mL distilled water
Phosphate buffered saline (PBS)	For 100 mL, 1 tablet of PBS (Thermo Fisher Scientific) was dissolved in 100 mL distilled water at a pH of 7.3-7.5 followed by autoclave at 121°C for 15 min
Agarose gel electrophoresis	For 1 % agarose, 1 g of UltraPure™ Agarose (Thermo Fisher Scientific, Catalogue number: 16500500) was dissolved in 100 mL of SYBR® Safe DNA gel stain in 1X TAE buffer (Thermo Fisher Scientific, Catalogue number: S33112)
GeneRuler 50 bp DNA Ladder	Ready-to-use (Thermo Fisher Scientific, Catalogue number: SM0373)

2.2.2 Growth media

Table 2.2 The different types of growth media used in this study and their preparations.

Media	**Preparation**
Nutrient agar (Oxoid)	28 g in 1000 mL distilled water, autoclaved at 121°C for 15 min
Mueller-Hinton agar (Mast group)	36 g in 1000 mL distilled water, autoclaved at 121°C for 15 min
Nutrient broth (Oxoid)	13 g in 1000 mL distilled water, autoclaved at 121°C for 15 min
Luria-Bertani (Invitrogen)	20 g in 1000 mL distilled water, autoclaved at 121°C for 15 min
AB medium	**A (5X)**: 2 g $(NH_4)_2SO_4$ (Sigma-Aldrich), 6 g Na_2HPO_4 (Fisher Scientific), 3 g KH_2PO_4 (Sigma-Aldrich), 3 g NaCl (Fisher Scientific), dissolved in 200 mL H_2O and autoclaved **B (1X)**: 1 mL sterile 0.1 M $CaCl_2$ (Sigma-Aldrich), 1 mL sterile 1 M $MgCl_2$ (Sigma-Aldrich), 1 mL sterile 0.003 M $FeCl_3$ (Sigma-Aldrich), 797 mL sterile H_2O. All B salt solutions were autoclaved separately, then added to the H_2O for a final volume of 800 mL. 200 mL of A was added to 800 mL of B for a final volume of 1 L. Sterile 0.2 % glucose (Fisher Scientific) as a carbon source, and 10 µg/mL sterile thiamine (Fisher Scientific) were added to the final 1000 mL volume of AB medium.

2.2.3 Bacterial strains and growth conditions

All bacterial strains used in this study were obtained from Public Health England (PHE). Nutrient agar was used to culture the bacterial strains (Table 2.2) in a static incubator at 37℃. Bacterial colonies were obtained from the overnight growths, placed into Protect bead tubes (Microorganism Preservation System) according to the manufacturer's instructions, and stored at -80°C until use. All strains listed in Table 2.3 were antibiotic-resistant except *K. pneumoniae* 9633 and *E. coli* 12241, with non-resistant strains used for comparison.

Table 2.3 The bacterial strains used in this study, along with their characteristics. Strains were ordered directly from NCTC and later confirmed in this study.

Organism	Strain name	Characteristics	Reference
K. pneumoniae	NCTC 13442	Sequence type 353 with OXA-48	(Dimou et al., 2012)
K. pneumoniae	NCTC 13368	SHV-18 (ATCC 700603)	(Culture collections, 2013a)
K. pneumoniae	NCTC 13443	New Delhi Metallo-β-lactamase (NDM-1)	(Culture collections, 2013a)
K. pneumoniae	NCTC 13438	Member of the International ST258 clone that produces KPC-3 carbapenemase	(Woodford et al., 2008)
K. pneumoniae	NCTC 9633	(ATCC 13883) Type strain / P. R. Edwards, CDC Atlanta in 1955 / Capsular serotype 3	(Culture collections, 2013c)
E. coli	NCTC 13353	Strain EO 487. CTX-M-15 ESBL producer. Control strain for group 1 $bla_{\text{CTX-M}}$ multiplex PCR assays	(Woodford et al., 2004)
E. coli	NCTC 13351	TEM-3 ESBL. Transconjugant of strain isolated in 1985 in Clermont-Ferrand	(Sirot et al., 1987)
E. coli	NCTC 13476	IMP-type (unsequenced)	(Collections, 2013a)
E. coli	NCTC 12241	Clinical isolate/control organism for sensitivity testing of bacteria to different antibiotics	(Collections, 2013b)

2.2.4 Gram staining

Gram staining was performed to confirm that the tested strains were Gram-negatives (Willey, 2005).

2.2.4.1 Making and fixing samples

Slides were labelled on the frosted panel, and a small drop of distilled water was placed on the transparent area of the slide. A smear of culture was picked using a sterilized loop (flamed and cooled) and mixed to emulsify the bacteria, then spread to create a thin smear and dried by gently passing over a flame.

2.2.4.2 Staining with Gram stain

Crystal violet was added to the fixed smear for 30 seconds and then washed with distilled water and drained. Slides were then covered with iodine solution for 60 seconds and again washed with distilled water. The smear was subsequently decolorized by dipping in 95 % alcohol for 30 seconds and washed with distilled water. Finally, safranin was added as a counterstain for 60 seconds and washed with distilled water. Slides were allowed to dry before examination under a light microscope.

2.2.5 API 20E test

API 20E is an Enterobacteriaceae and other Gram-negative non-fastidious rods standardized identification system that utilizes 21 miniaturized biochemical tests and a database. The test consists of 20 microtubes containing dehydrated substrates. API 20E testing was performed according to the manufacturer's instructions. Briefly, microtubes were inoculated with the tested bacteria in suspension and then incubated at 37°C for 18 to 24 h. Color changes occur during incubation due to bacterial metabolism. These changes can be observed directly or after the addition of specific reagents provided in the kit. Reaction results are read according to the reading table, and identified by matching to the Analytical Profile Index or using included identification software (API 20E, 2010).

Strains were cultured on nutrient agar plates and incubated overnight at 37°C in a static incubator. One colony was picked from each plate and inoculated into 10 mL of sterilized distilled water with shaking to ensure mixing. Using a sterile Pasteur pipette, each compartment of the API 20E strip was filled to the limit established by the manufacturer. Certain compartments contained oil to provide anaerobic conditions. Finally, strips were placed onto wetted trays, covered with lids, and incubated at 37°C for 24 h. After incubation, results were documented and interpreted using https://apiweb.biomerieux.com. Interpretation of the results is facilitated by a seven-digit number representing the Profile Recognition Number. The Profile Register Index associates the species with the given number (Janin and Pierre, 1976).

An oxidase test was performed independently as part of the detection process. Several colonies from a single culture grown on a nutrient agar plate were wiped onto the paper zone

of the diagnostic strip containing N, N-dimethyl-p-phenylenediamine. Results were read and recorded after one min. A dark blue or black spot indicated a positive result; no color change indicated a negative result (Collins et al., 2004).

2.2.6 Antibiotic sensitivity testing using double-disk diffusion

Double-disk diffusion tests were performed according to the manufacturer's instructions (Mast group), and the two sets used in this assay were D67C and D70C. The presence of ESBL or Carbapenemases was confirmed by comparing the zone sizes between the antibiotic and antibiotic plus inhibitor.

The European Committee on Antimicrobial Susceptibility Testing (EUCAST) standardized disc susceptibility testing method was utilized for the preparation of the inoculums to generate semi-confluent growth of bacterial colonies after overnight incubation (Fig 2.1) (BSAC, 2015). Subsequently, these inoculums were compared to the 0.5 McFarland standard.

The 0.5 McFarland standard was made by mixing 0.5 mL of 0.048 M $BaCl_2$ with 99.5 mL of 0.18 M H_2SO_4 and stir constantly. Absorbance was measured at 625 nm. Absorbance ranges were adjusted via dilution to fall between 0.08 and 0.13. Standards were equally delivered into screw-cap tubes of the same volume and size as those used for broth cultures, stored away from light at room temperature.

After incubation, strains that were grown on nutrient broth were streaked onto Mueller-Hinton agar (MHA) and incubated with the related disks sets at 37°C for 18 to 20 h. two

types of disks were used in this study; D67C and D70C. D67C and D70C were used to detect the presence of ESBLs and Carbapenemases, respectively. ESBLs were defined as positive when a zone of diameter difference at least 5 mm for D67C disks (Fig 2.2). For D70C disks, a zone of diameter difference of at least 4 mm was used with disk C, and at least 5 mm with disk B, compared to disk A (Fig 2.3). Tests for each strain were done in triplicate and results are represented as the mean of three replicates of the zone of inhibition diameter.

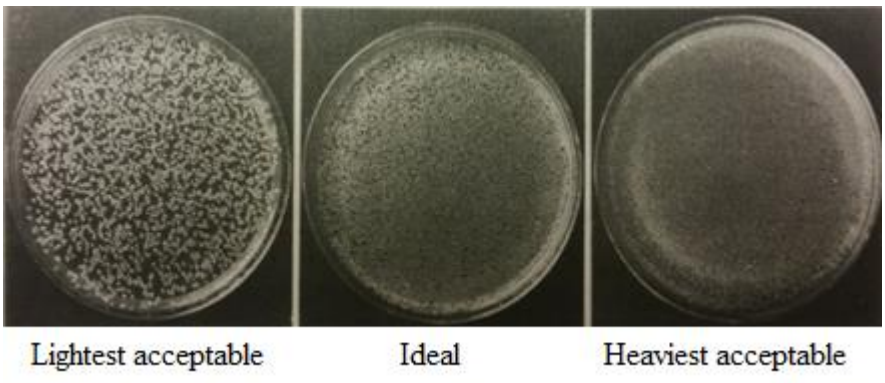

Fig 2.1 Acceptable range of inoculums density for Gram-negative rod bacteria (BSAC, 2015).

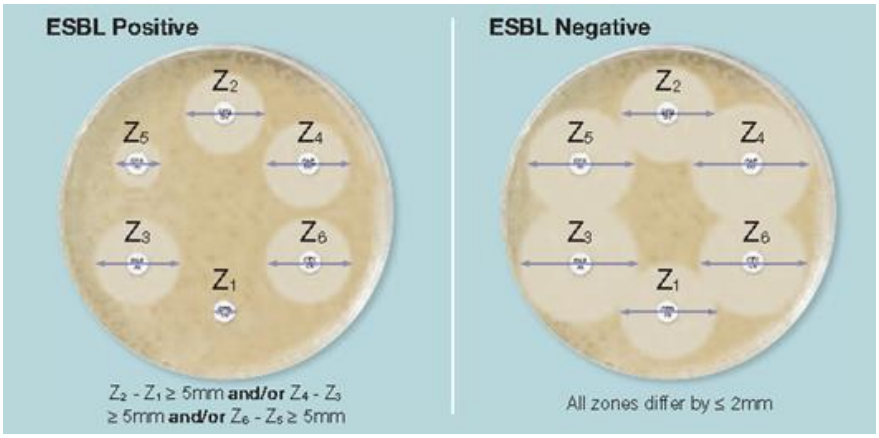

Fig 2.2 D67C (CAZ30, ceftazidime 30 µg; CAZ30/CLAV10, Ceftazidime 30 µg + Clavulanic acid 10 µg; CTX30, Cefotaxime 30µg; CTX30/CLAV10, Cefotaxime 30µg + Clavulanic acid 10µg; CPD10, Cefpodoxime 30µg, CPD10/CLAV1, Cefpodoxime 30µg + Clavulanic acid 10µg) confirmation of production of ESBL in *Enterobacteriaceae* that has no chromosomal de-repressed or inducible *ampC*. ESBL Positive if Z_2-$Z_1 \geq 5$mm and/or Z_4-$Z_3 \geq 5$mm and/or Z_6-$Z_5 \geq 5$mm. CAZ, ceftazidime; CLAV, clavulanic acid; CTX, cefotaxime; CPD, cefpodoxime (Mast, 2015).

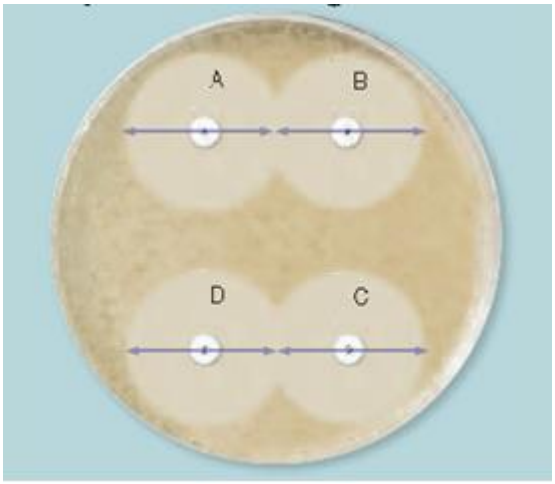

Fig 2.3 D70C cartridge A, carbapenem 10 µg discs; cartridge B, carbapenem 10 µg + MBL (Metallo-β-lactamase) inhibitor discs; cartridge C, carbapenem 10 µg KPC inhibitor discs; cartridge D, carbapenem 10 µg + AmpC inhibitor discs. Detection of production of carbapenemase enzyme in Enterobacteriaceae: If disc B shows a zone difference ≥ 5 mm more than disc A, the organism has MβL activity. If disc C shows a zone difference ≥ 4 mm more than disc A, the organism has KPC activity. If discs C and D show zone differences of ≥ 4 mm and ≥ 5 mm, respectively, compared to disc A, the organism has AmpC activity coupled with porin loss (Mast, 2015).

2.2.7 Genotypic confirmation of antibiotic-resistant gene using PCR

Polymerase chain reactions were conducted with a thermal cycler (Garrec et al., 2011). A suitable set of primers were designed to target the resistance gene specific to the given strain (Table 2.4) using gene sequences obtained from the NCBI website (https://www.ncbi.nlm.nih.gov/, National Center for Biotechnology Information, Bethesda, USA). Gene sequences were copied and pasted into the primer request tool on the IDT website (https://eu.idtdna.com/, Integrated DNA Technologies). Three fresh colonies were picked from each strain after overnight growth on agar medium. Colonies were inoculated

into 50 µl of sterilized distilled water in an Eppendorf tube, boiled for 10 min in a dry bath, and centrifuged for 1 min. One µl of the supernatant was used as a template for the PCR reaction. PCR amplification was performed in a 50 µl volume for each sample in accordance with the GoTaq® DNA polymerase manufacturer instructions (Table 2.5), and the PCR conditions were adjusted as described in Table 2.6.

Table 2.4 Primers used in this study. Primers were designed using the OligoAnalyzer 3.1 (Integrated DNA Technologies Inc, Illinois, USA). Primers were then checked for specificity by the BLAST software (National Center for Biotechnology Information, Bethesda, USA). All PCR products were run on a 1 % agarose gel for 90 mins at 60 Volts. A GeneRuler 50 bp DNA Ladder was used for comparison.

Primer	**Sequence (5′-3′)**	**Target**	**Amplicon size (bp)**	**Reference**
OXA-48F	CGGAATGCCTGCGGTAGCA	*bla*$_{\text{OXA-48}}$	713	This study
OXA-48R	TGATGGCTTGGCGCAGC			
KPC-3F	GCGGAACCATTCGCTAAAC	*bla*$_{\text{KPC-3}}$	864	This study
KPC-3R	GACAGTGGTTGGTAATCCATGC			
NDM-1F	AATGGAACTGGCGACCAAC	*bla*$_{\text{NDM-1}}$	322	This study
NDM-1R	TCGACAACGCATTGGCATAA			
IMP-6F	GCAGCATTGCTACCGCAG	*bla*$_{\text{IMP-type}}$	657	This study
IMP-6R	CCGCCTGCTCTAATGTAAGT			
CTX-M-1-F	AAAAATCACTGCGCCAGTTC	*bla*$_{\text{CTX-M-15}}$	415	(Al-Mayahie, 2013)
CTX-M-1-R	AGCTTATTCATCGCCACGTT			
SHV-18F	CTCAAGGATGTATTGTGGTTATGC	*bla*$_{\text{SHV-18}}$	912	This study
SHV-18R	CGAGCCGGATAACGCGCGCG			
TEM-1F	GTAAAAGATCCTGAAGATCAG	*bla*$_{\text{TEM-3}}$	768	This study
TEM-1R	CCAATGCTTAATCAGTGAGG			

Table 2.5 The reagents used in PCR amplification reaction and their volumes.

Component	Final volume
5X Green GoTaq® Flexi Buffer	10 µl
$MgCl_2$	5 µl
PCR Nucleotide Mix	1 µl
Upstream primer	0.5 µl
Downstream primer	0.5 µl
GoTaq® Flexi DNA Polymerase	0.25 µl
Template DNA	1 µl
Nuclease-Free Water up to	50 µl

Table 2.6 Cycling parameters for PCR reaction.

Step	Time/cycles	Temperature
Initial activation step	2 min	98°C
Denaturation	10 s	98°C
Annealing	1 min	50°C
Extension	30 sec/kb	72°C
Final extension	5 min	72°C
Number of cycles	40 cycles	
End of PCR cycling	Indefinite	4°C

2.2.7.1 Agarose gel electrophoresis

PCR products were run on 1 % agarose gel. 1 g of agarose was dissolved into 100 mL of 1X TAE buffer containing SYBR® Safe dye, heated in a microwave, and poured into a casting tray. A well comb was fixed and allowed to cool and solidify. The comb was removed, and the unit was enclosed in a gel box. TAE buffer was poured into the gel box to cover the upper area of the gel. Samples were prepared, and 5 µl of each were loaded into the gel wells. The first and last wells were inoculated with 5 µl of DNA ladder for sizing. All units were covered, and the voltage was adjusted to 5 V/cm for 90 mins. Fragments were visualized using a Gel Doc^{TM} EZ System gel imaging instrument.

2.2.7.2 Sequencing for genotypic confirmation

PCR products (50 µl) along with 100 µl of their DNA primer pairs **were sent to** Macrogen Europe to confirm the DNA sequences of the genes from each antibiotic-resistant strain. Sequencing results data were delivered online, and the DNA sequences were checked for compatibility using the NCBI BLAST tool (Nucleotide BLAST).

2.2.8 Biofilm formation assay (tissue culture plate assay)

A tissue culture plate (TCP) assay was conducted according to the protocols set out by Fattahi et al., (2015), Lee et al., (2011), and Beehan et al. (2015), with modifications. Six-well tissue culture plates (TCP, Techno Plastic Products) were used in this assay. Three types of growth media were provided, namely LB broth, AB medium, and NB.

A loopful of bacterial colonies were inoculated into 5 mL of LB and NB and incubated overnight at 37°C with either static incubation or shaking at 70 rpm. After incubation, cultures were diluted to an OD_{600} of 0.01 in 5 mL in each well. Colonies grown in LB were inoculated into TCP containing LB and AB, while those grown in NB were inoculated into TCP containing NB. Each strain was cultured in triplicate for each biological replicate. All inoculated TCPs were incubated at 37°C in a static incubator (for cultures previously incubated in stasis) or shaker incubator at 70 rpm (for cultures previously incubated with shaking) and evaluated at 6, 12, 24, or 48 h. After incubation, the broth was removed, and wells were washed three times using sterile PBS. Bacteria in wells were fixed with 5 mL of 99 % methanol for 15 min. The methanol was discarded, and wells were dried in an inverted position for 30 min at room temperature. 5 mL of 2 % crystal violet were used to stain each well and for 5 min at room temperature, after which excess stain was rinsed with sterilized distilled water. The remaining dye was re-solubilized with 4 mL of 33 % glacial acetic acid and allowed to sit at room temperature for 30 min. Finally, optical densities at 570 nm were measured for each well using a Helios Gamma UV-Vis spectrophotometer and recorded. Mean values of three technical replicates (which represent one biological replicate) were obtained, then the mean value of the three biological replicates was calculated.

2.2.9 Statistical analysis

Since data are normally distributed, results were assessed with one-way ANOVA to evaluate the significance of differences in biofilm formation among the tested strains. Microsoft Excel 365 and Prism 6 version 6.01 were used to perform statistical calculations. For both tests, a

p-value of less than 0.01 was considered statistically significant. Comparisons of biofilm density values were evaluated among the four growth stages. A descriptive study was conducted by classifying all isolates into categories according to their highest OD_{570} values, wherein 0 indicated no adherence, 0.2 indicated weak adherence, 0.2 to 0.4 indicated moderate adherence, and above 0.4 indicated strong adherence. Statistical analysis was performed for three technical replicates of each of three biological replicates.

2.3 Results

2.3.1 Gram staining

Gram staining was performed to verify the strains used in this study. All test strains showed a pink color and were thereby confirmed to be Gram-negative (Fig 2.4).

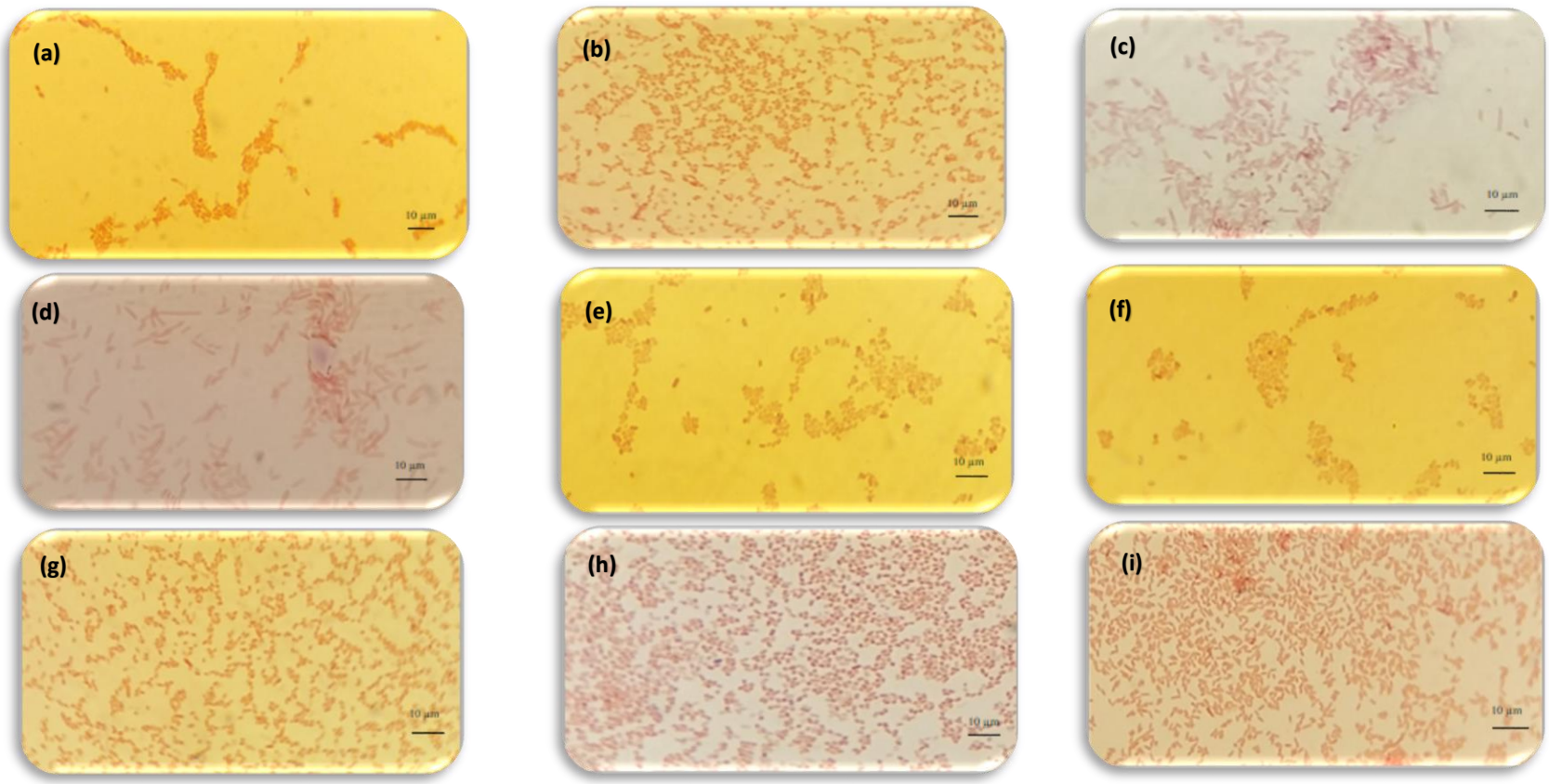

Fig 2.4 Gram-staining of test strains showing all were Gram-negative. **(a)** *E. coli* IMP-type; **(b)** *K. pneumoniae* OXA-48; **(c)** *E. coli* CTX-M-15; **(d)** *E. coli* TEM-3; **(e)** *K. pneumoniae* SHV-18; **(f)** *K. pneumoniae* KPC-3; **(g)** *K. pneumoniae* NDM-1; **(h)** *K. pneumoniae* 9633; **(i)** *E. coli* 12241. Magnification 100.

2.3.2 API 20E

API 20E is a standardized identification system for Enterobacteriaceae and other non-fastidious, Gram-negative rods. Table 2.7 shows the API 20E and oxidase test results, which were interpreted using API identification software. Strains were confirmed based on their Profile Recognition Numbers.

Table 2.7 API 20E biochemical tests results; (+), positive; (-), negative. Abbreviations represent tests for the presence of specific enzymes or fermentation of specific sugars.

Strain	ONPG	ADH	LDC	ODC	CIT	H2S	URE	TDA	IND	VP	GEL	GLU	MAN	INO	SOR	RHA	SAC	MEL	AMY	ARA	OX
K. pneumoniae OXA-48	+	-	+	-	+	-	+	-	-	+	-	+	+	+	+	+	+	+	+	+	-
K. pneumoniae SHV-18	+	-	+	-	+	-	+	-	-	+	-	+	+	+	+	+	+	+	+	+	-
K. pneumoniae NDM-1	+	-	+	-	+	-	+	-	-	+	-	+	+	+	+	+	+	+	+	+	-
K. pneumoniae KPC-3	+	-	+	-	+	-	+	-	-	+	-	+	+	+	+	+	+	+	+	+	-
K. pneumoniae 9633	+	-	+	-	+	-	+	-	-	-	-	+	+	+	+	+	+	+	+	+	-
E. coli IMP-type	+	-	+	+	-	-	-	+	-	-	-	+	+	-	+	+	+	+	-	+	-
E. coli CTX-M-15	+	-	+	+	-	-	-	+	-	-	-	+	+	-	+	+	+	+	-	+	-
E. coli TEM-3	+	-	+	-	-	-	-	+	-	-	-	+	+	-	+	+	-	+	-	+	-
E. coli 12241	+	-	+	-	-	-	-	+	-	-	-	+	+	-	+	+	-	+	-	+	-

Results are shown as percentages representing the probability of being the expected species in the specified test. These values were 97.3 % for *K. pneumoniae* OXA-48, SHV-18, NDM-1, and KPC-3, 94.8 % for *K. pneumoniae* 9633, 98.4 % for *E. coli* IMP-type and CTX-M-15, and 89.7 % for *E. coli* TEM-3 and 12241.

2.3.3 Antibiotic sensitivity tests

The mean values of each test, performed in triplicate, were recorded on a table and interpreted using MAST standard instructions (Tables 2.8 and 2.9). As shown in Table 2.8, *K. pneumoniae* SHV-18, *E. coli* CTX-M-15, and *E. coli* TEM-3 showed a zone of diameter difference of at least 5 mm between the antibiotic and its inhibitor, indicating they were ESBL.

Table 2.8 D67C ESBL set for confirmation of production of ESBL in Enterobacteriaceae that has no chromosomal de-repressed or inducible AmpC. *K. pneumoniae* OXA-48, NDM-1, KPC-3, and *E. coli* IMP-type are a special class of antibiotic-resistant organisms that produce carbapenemase, as shown by negative test results (non-ESBL). (CV: clavulanic acid)

D67C ESBL Set							
strain	CPD	CPD CV	CTX	CTX CV	CAZ	CAZ CV	interpretation
K. pneumoniae OXA-48 (resistant)	17.7	17.7	20.7	20.7	22.3	22.7	Non-ESBL
K. pneumoniae SHV-18	8.3	19.3	15.3	20.3	9.0	21.0	ESBL
K. pneumoniae NDM-1 (resistant)	7.0	7.3	7.3	6.7	6.7	6.7	Non-ESBL
K. pneumoniae KPC-3 (resistant)	6.0	6.0	9.3	10.3	6.3	6.0	Non-ESBL
K. pneumoniae 9633 (non-resistant)	25.0	25.0	28.7	28.7	23.3	22.3	Non-ESBL
E. coli IMP-type (resistant)	6.0	6.0	7.7	7.7	6.0	6.0	Non-ESBL
E. coli CTX-M-15	6.0	17.3	6.0	15.0	11.0	23.7	ESBL
E. coli TEM-3	6.0	21.7	13.0	23.0	10.0	26.7	ESBL
E. coli 12241 (non-resistant)	22.3	23.0	29.3	30.3	27.0	27.0	Non-ESBL

In tests with the D70C carbapenemase detection disk (Table 2.9), *K. pneumoniae* NDM-1 and *E. coli* IMP-type were confirmed as MBLs by showing a zone of diameter difference of greater than 5 mm between disk A and disk B, and *K. pneumoniae* KPC-3 was confirmed as having KPC activity by showing a zone of diameter difference greater than 4 mm between

disk C and disk B. *K. pneumoniae* OXA-48 did not show any carbapenemase activity; however, this assay only detects isolates with MBL, KPC and/or AmpC activity. As such, additional testing for confirmation was required.

Table 2.9 D70C carbapenemase detection disk set for the detection of carbapenemase enzyme production in *Enterobacteriaceae*. This test detects MBL and KPC-type carbapenemase.

D70C Carbapenemase					
strain	**D70A**	**D70B**	**D70C**	**D70D**	**Interpretation**
K. pneumoniae OXA-48 (resistant)	18.7	17.7	17.7	18.7	Molecular testing required
K. pneumoniae SHV-18 (resistant)	26.7	25.7	25.7	26.7	-ve
K. pneumoniae NDM-1	7.0	14.3	7.0	7.3	MBL activity
K. pneumoniae KPC-3	6.0	7.7	13.3	9.0	KPC activity
K. pneumoniae 9633 (non-resistant)	29.3	27.0	27.3	27.7	-ve
E. coli IMP-type	13.0	22.3	14.7	16.0	MBL activity
E. coli CTX-M-15 (resistant)	27.3	26.3	26.7	27.0	-ve
E. coli TEM-3 (resistant)	30.7	29.3	30.3	31.3	-ve
E. coli 12241 (non-resistant)	28.3	27.7	27.3	28.3	-ve

2.3.4 Genotypic confirmation of antibiotic-resistant gene with PCR

Figure 2.5 shows the gel electrophoresis results for the tested strains. The resulting fragments were compared with their expected sizes, and all were roughly the same as expected, indicating that all our test strains were harbouring the antibiotic resistance gene related to their strains. The negative controls (-ve) had no template added (no bacterial DNA).

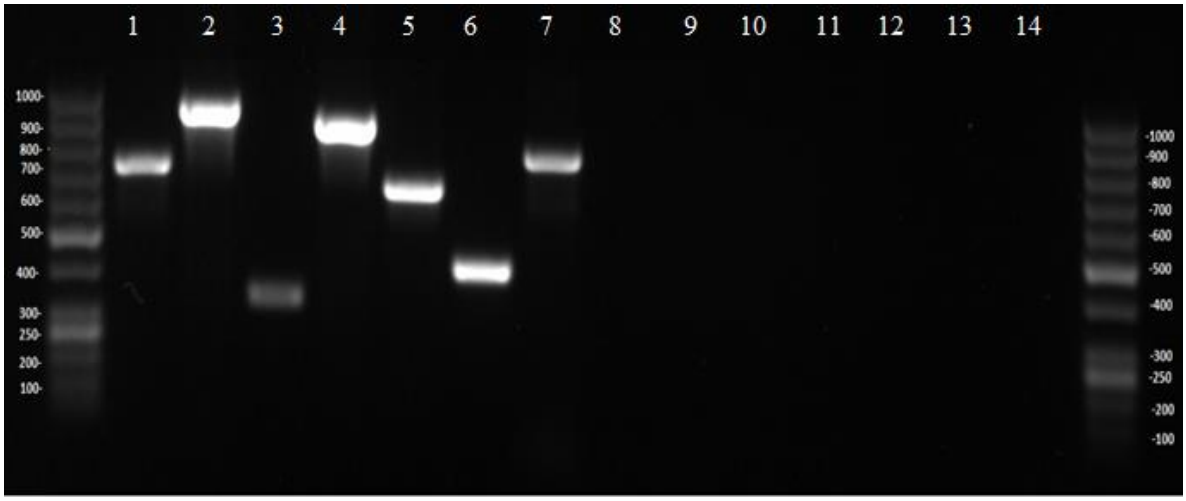

Fig 2.5 PCR products of the seven antibiotic resistance gene primers run on 1 % agarose in TAE buffer. The bands of DNA fragment from the left; 1: 713 bp for the OXA-48, 2: 912 bp for SHV-18, 3: 322 bp for NDM-1, 4: 864 bp for KPC-3, 5: 657 bp for IMP-type, 6: 370 bp for CTX-M- 15, and 7: 768 bp for TEM-3. Control sequences; 8: -ve OXA-48, 9: -ve SHV-18, 10: -ve NDM-1, 11: -ve KPC-3, 12: -ve IMP-type, 13: -ve CTX-M-15, and 14: -ve TEM-3. The gel was run at 5 V/cm.

2.3.5 Genotypic confirmation of antibiotic-resistant gene sequence

PCR products of the antibiotic resistance sequences for each of the tested strains were sent for sequencing for further confirmation that the tested antibiotic-resistant isolates carried the expected antibiotic resistance gene sequence. Results of sequencing data were obtained online, and the NCBI BLAST tool was used to assess their percentage similarities with corresponding sequences. Percentages of similarity for each sequence are shown in Table 2.10.

Table 2.10 Sequence similarity for antibiotic resistance genes.

Strain	% similarity
K. pneumoniae OXA-48	99.26
K. pneumoniae SHV-18	97.70
K. pneumoniae NDM-1	99.13
K. pneumoniae KPC-3	96.51
E. coli IMP-type	98.51
E. coli CTX-M-15	99.72
E. coli TEM-3	99.75

2.3.6 Biofilm formation assay

OD_{570} values which represent biofilm densities were recorded and plotted as bar charts (Fig. 2.6 – 2.11).

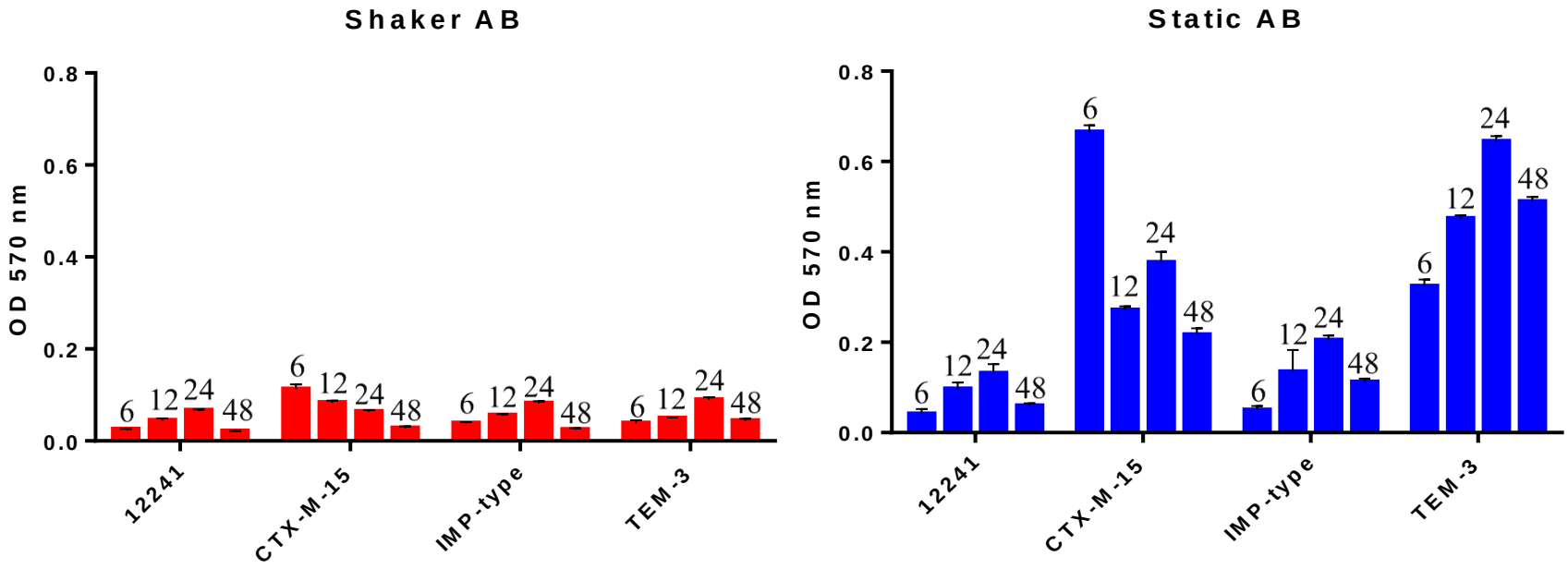

Fig 2.6 Biofilm formation of *E. coli* strains CTX-M-15, IMP-type, TEM-3, and 12241 grown in AB broth with shaking and static incubation at 6, 12, 24, and 48 h. The experiment was done in three biological replicates, and data represent the means of those biological replicates. Error bars represent the standard deviation of the mean.

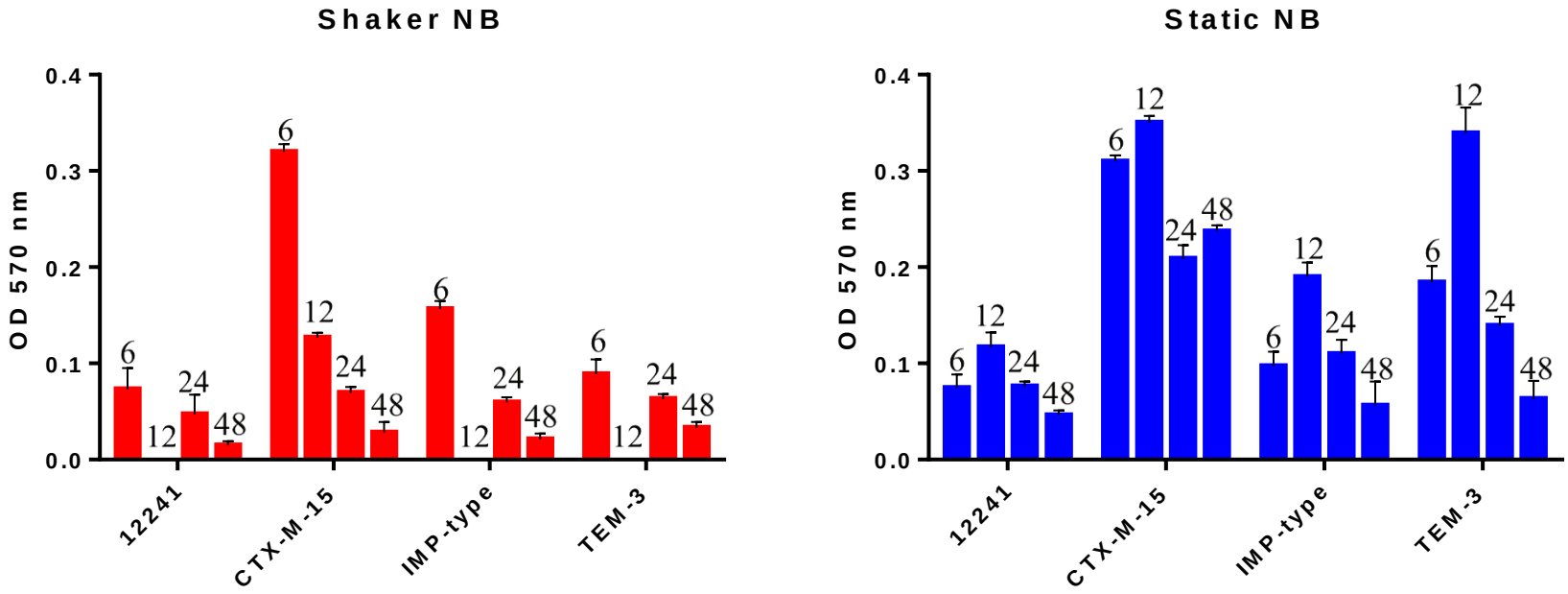

Fig 2.7 Biofilm formation of *E. coli* strains CTX-M-15, IMP-type, TEM-3, and 12241 grown in NB broth with shaking and static incubation at 6, 12, 24, and 48 h. The experiment was done in three biological replicates, and data represent the means of those biological replicates. Error bars represent the standard deviation of the mean.

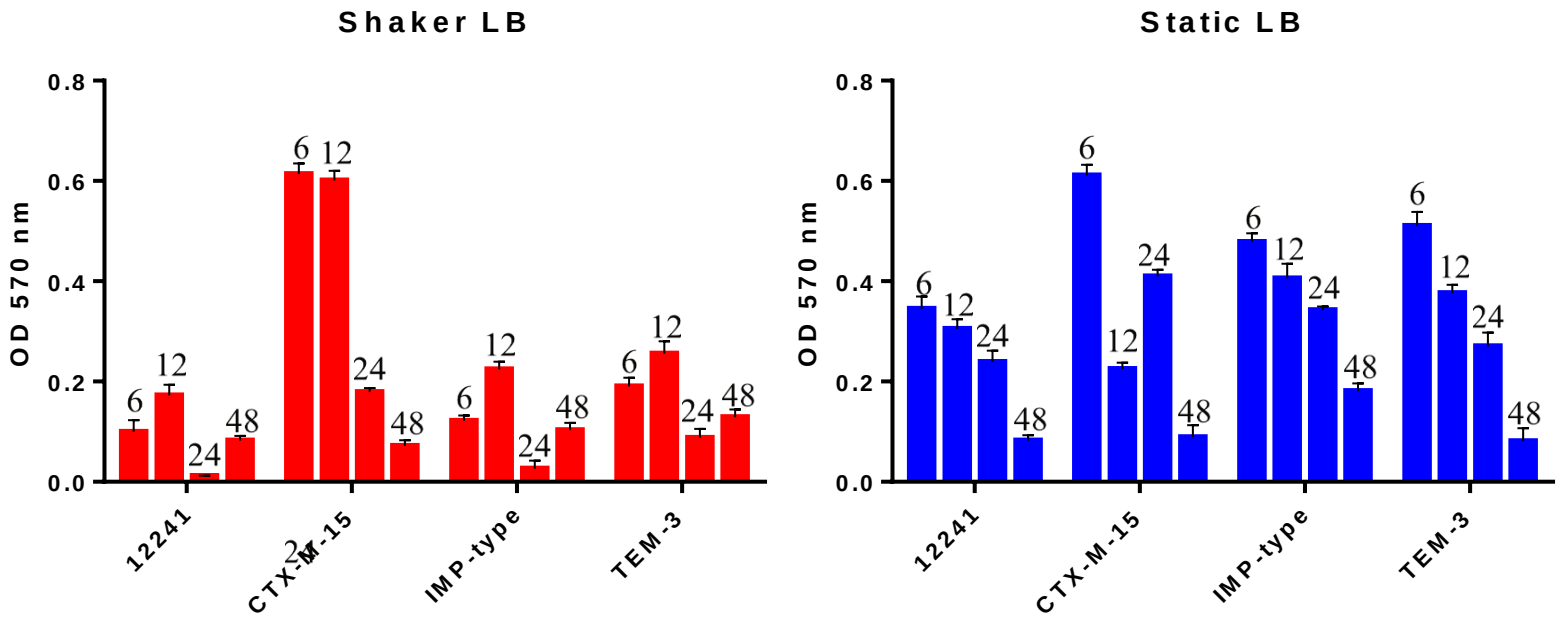

Fig 2.8 Biofilm formation of *E. coli* strains CTX-M-15, IMP-type, TEM-3, and 12241 grown in LB broth with shaking and static incubation at 6, 12, 24, and 48 h. The experiment was done in three biological replicates, and data represent the means of those biological replicates. Error bars represent the standard deviation of the mean.

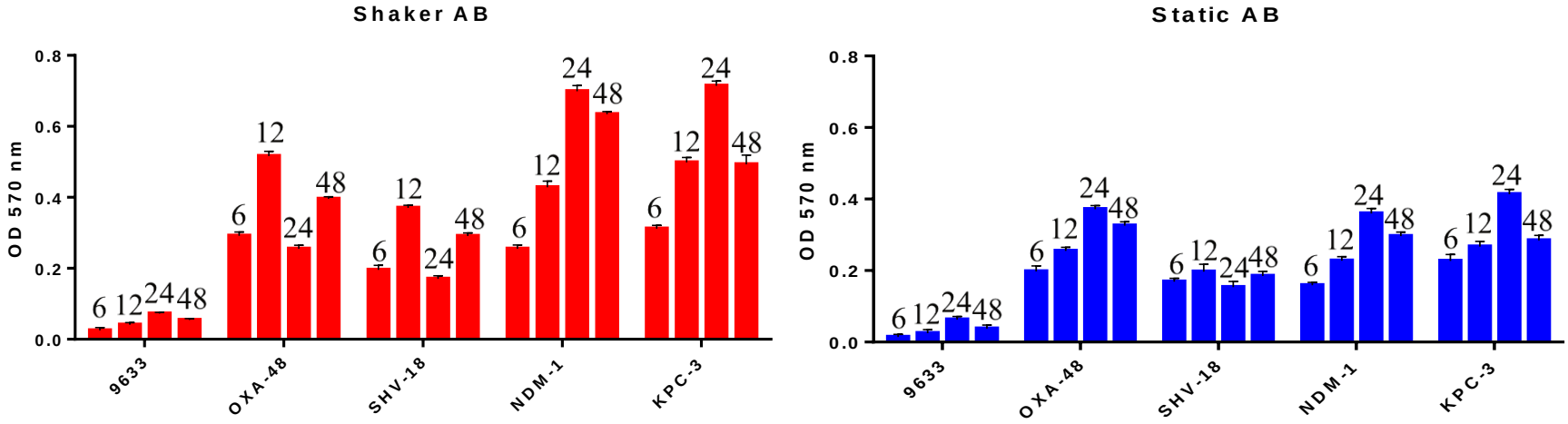

Fig 2.9 Biofilm formation of *K. pneumoniae* strains KPC-3, NDM-1, SHV-18, OXA-48, and 9633 grown in AB broth with shaking and static incubation at 6, 12, 24, and 48 h. The experiment was done in three biological replicates, and data represent the means of those biological replicates. Error bars represent the standard deviation of the mean.

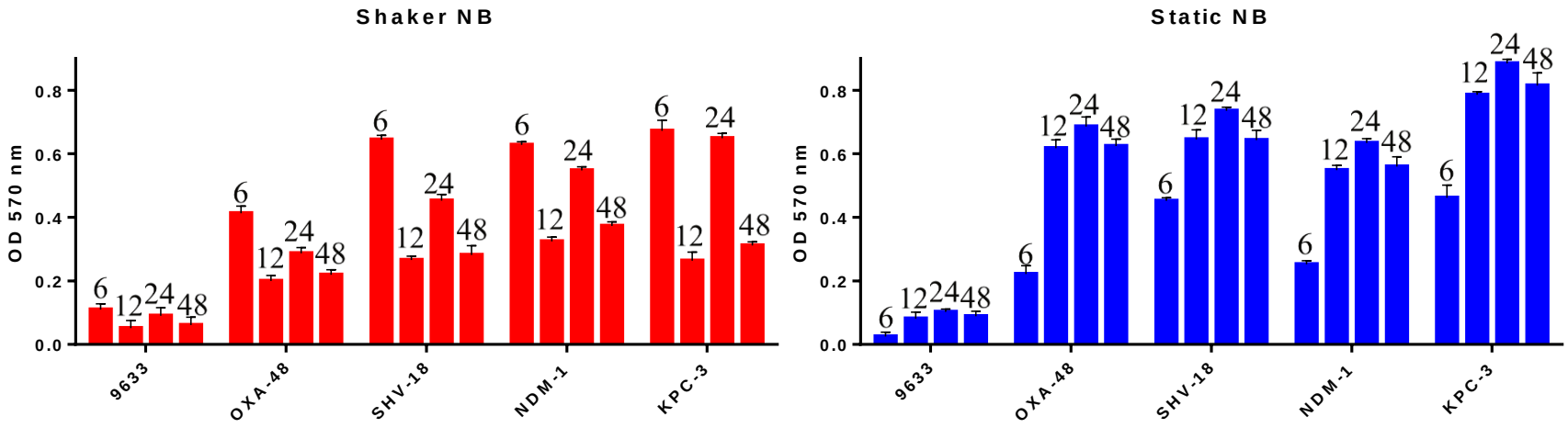

Fig 2.10 Biofilm formation of *K. pneumoniae* strains KPC-3, NDM-1, SHV-18, OXA-48, and 9633 grown in NB broth with shaking and static incubation at 6, 12, 24, and 48 h. The experiment was done in three biological replicates, and data represent the means of those biological replicates. Error bars represent the standard deviation of the mean.

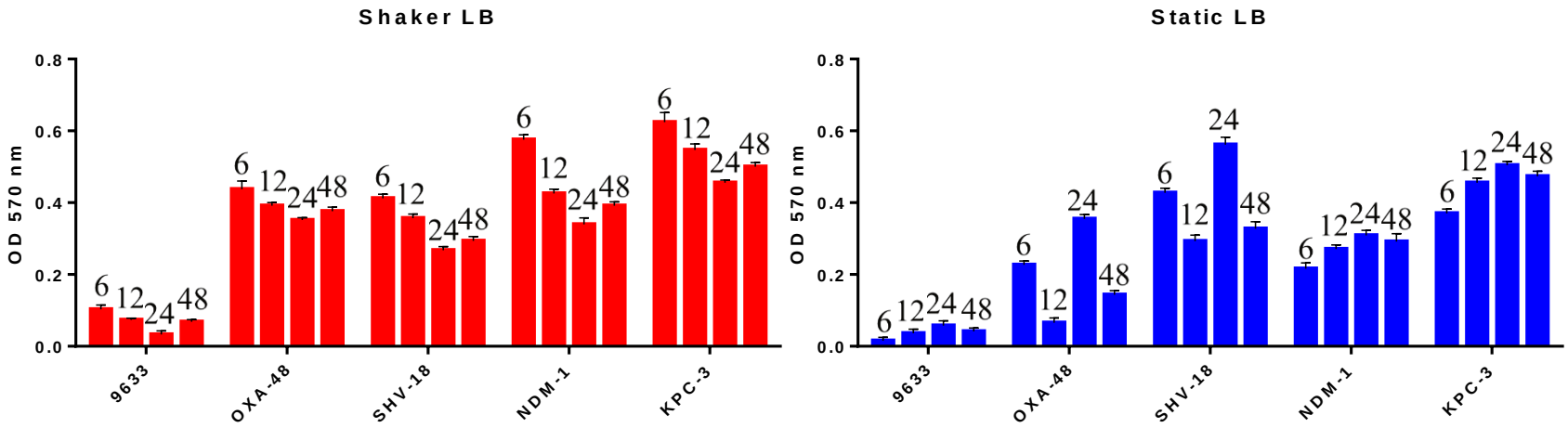

Fig 2.11 Biofilm formation of *K. pneumoniae* strains KPC-3, NDM-1, SHV-18, OXA-48, and 9633 grown in LB broth with shaking and static incubation at 6, 12, 24, and 48 h. The experiment was done in three biological replicates, and data represent the means of those biological replicates. Error bars represent the standard deviation of the mean.

For *E. coli* grown in AB medium (Fig 2.6), the standard patterns of biofilm formation stages in all the tested strains (except *E. coli* CTX-M-15) emulate the selected time-points illustrated in the virtual graph in Fig 2.12 for both static and shaking incubations. Comparing the biofilm density, there was noticeably more biofilm density in static incubation compared with shaking incubation.

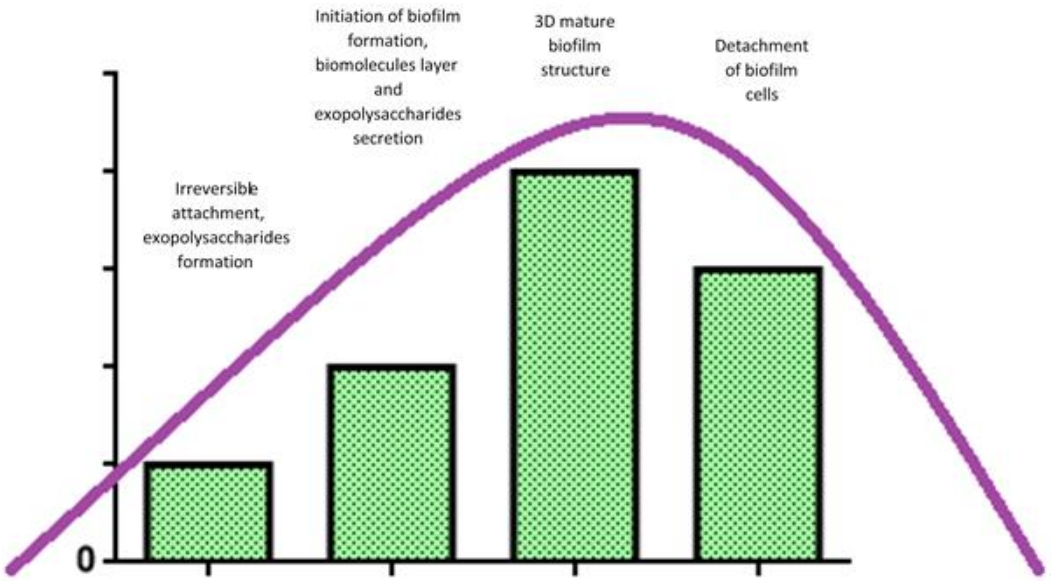

Fig 2.12 Virtual bar chart represents a presumed ideal result for what could be obtained in biofilm measurements if the selected time-points match the sequential biofilm formation stages of the selected tested strains. This bar chart shows the time-points presented by hours (6, 12, 24, and 48) and the description of the events on the specified time-point (Stoodley et al, 2002).

In Fig 2.7, the biofilm formation cycle started early for all *E. coli* strains when grown on NB, as the graph shows a decrease in density after 12 h in static and after 6 h in shaking (except

E. coli CTX-M-15) incubation that could suggest that the attachment stage somehow started early, before the 6 h of incubation.

In LB media (Fig 2.8), the biofilm initiation started early for both static and shaking incubation. There was a different pattern of biofilm formation as shown in both graphs. In shaking incubation, all strains (except *E. coli* CTX-M-15) showed undulating bars. In static incubation, the graph showed bars decreasing in length, which might also indicate an early biofilm formation stage but with higher density than in shaking (except *E. coli* CTX-M-15).

For *K. pneumoniae* strains grown in AB broth (Fig 2.9), both bar charts show a clear biofilm stages emulating the virtual bar chart, regardless of the density values of biofilm compared to both stages, apart from OXA-48 (in shaking incubation) and SHV-18 (in static and shaking incubations), which showed undulating bars that in turn might indicate two biofilm cycles.

In NB (Fig 2.10), all *K. pneumoniae* strains showed undulating bars when grown under shaking conditions, which might also indicate two biofilm cycles. While in static incubation, they showed the standard pattern of biofilm stages, regardless of the biofilm level difference between the resistant strains and the non-resistant control.

For LB broth (Fig 2.11) in shaking incubations, strains showed an early biofilm formation initiation stage as can be seen from the high biofilm level at 6 h, decreasing afterwards. There was an increase in biofilm level at 48 h, which might indicate a second biofilm cycle as there is a 24 h difference between 24 h and 48 h. On the other hand, under static conditions, both NDM-1 and KPC-3 showed the same standard pattern of biofilm stages as the control strains,

while both OXA-48 and SHV-18 showed the undulating bars which might indicate two biofilm cycles as well.

One-way ANOVA was used to detect whether there is any significant difference in biofilm density values measured in OD_{570} among the selected time-points for each strain for all media and for both static and shaking incubations. Results are presented in Appendix II (Tables 2.I through 2.XII).

Tested strains were classified by OD_{570} value in accordance with results from a previous study by Beehan et al. (2015) (section 2.2.9). According to Table 2.11, an OD_{570} value above 0.2 in any test was considered an adherence indication for biofilm formation.

Table 2.11 Mean value for each strain's biofilm at the maturation stage when it reached the maximum value by means of OD_{570} value during the four recorded time-points (6, 12, 24, and 48 h). Green colors represent the weak adherence (OD_{570} value < 0.2), yellow colors represent the moderate adherence (OD_{570} value 0.2 - 0.4), and pink colors represent the strong adherence (OD_{570} value >0.4).

Strain	AB		LB		NB	
	Shaker	Static	Shaker	Static	Shaker	Static
K. pneumoniae OXA-48	0.52	0.37	0.44	0.35	0.41	0.69
K. pneumoniae SHV-18	0.37	0.20	0.41	0.56	0.64	0.74
K. pneumoniae NDM-1	0.70	0.36	0.58	0.31	0.63	0.63
K. pneumoniae KPC-3	0.71	0.41	0.62	0.50	0.67	0.88
K. pneumoniae 9633	0.07	0.37	0.10	0.06	0.11	0.10
E. coli IMP-type	0.08	0.20	0.22	0.48	0.16	0.19
E. coli CTX-M-15	0.11	0.67	0.61	0.61	0.32	0.35
E. coli TEM-3	0.09	0.64	0.26	0.51	0.09	0.34
E. coli 12241	0.06	0.131	0.17	0.345	0.073	0.12

2.4 Discussion

This chapter focuses on the ability of selected antibiotic-resistant strains to form biofilms. These strains comprise the main class of antibiotic-resistant organisms characterized by PHE and have been associated with urinary tract infections (UTIs) (Public Health England, 2018). Strains used in our study are listed by WHO as priority group 1 pathogens, tiered as "critical" in need for research and development of new antibiotics. These pathogens are grouped by species and type of resistance (Tacconelli et al., 2017). The selected strains in this study belong to the family of *Enterobacteriaceae,* which includes *K. pneumoniae* and *E. coli.*

Results revealed that timing of biofilm stages would not be the same for all strains due to phenotypic and genotypic variations among them. This important feature must be considered when selecting the proper treatment for biofilm infections, as antimicrobial tolerance increased proportionally with biofilm maturation (Ciofu et al., 2017). Results also showed the adaptability of these strains to the different experimental conditions, and that might be one of the reasons these strains are highly successful in causing UTIs.

Analyses showed that all antibiotic-resistant *E. coli* strains were high biofilm formers when grown in LB under static incubation. Antibiotic-resistant *K. pneumoniae* strains were, in general, a high biofilm former, particularly in NB and shaker LB. This suggests that those media are preferred by the tested strains. These results suggest that the antimicrobial tolerance will increase under such conditions, as the biofilm thickness controls the antimicrobial penetration (Stewart, 1996). This can lead to an increased tolerance by the microorganisms and the subsequent development of antimicrobial resistance (Levin-Reisman et al., 2017).

Results showed the most significant variation was associated with *E. coli* CTX-M-15, as it conferred the highest biofilm density values in all the growth media (Table 2.11). Besides, *E. coli* CTX-M-15 which did not follow the same pattern for other *E. coli* strains used in this study, as it showed different patterns of biofilm formation stages (Fig 2.6-2.8). These findings could explain why the CTX-M family is the most prevalent type of ESBL in the UK (Lupo et al., 2013), and CTX-M-15 is one of the most prevalent variants among UTIs in the UK (Cantón et al., 2012; Reid, 2018). It is also expected that those findings are related to the increased resistance of these strains demonstrated in previous studies.

The process and parameters involved in biofilm formation remain poorly understood (Rabin et al. 2015). Although extensive research has been carried out on biofilms, limited studies have compared biofilm formation stages produced by antibiotic-resistant *E. coli* and *K. pneumoniae* strains associated with UTIs among different types of growth media, static versus shaking incubation, and different time-points. In this study, all the above were compared.

Gram-staining and API 20E were performed to confirm the species of the tested strains, while double-disk diffusion tests D67C and D70C were performed to confirm whether the tested strains are antibiotic-resistant and the type of resistance. D70C was designed to detect Carbapenemases with Metallo-ß-lactamase and KPC activity and not oxacillinase (OXA) according to the manufacturer. Accordingly, molecular testing was required to detect the presence of the OXA-48 resistant gene, and to further confirm the presence of resistance genes in the other tested strains.

Gel electrophoresis of PCR products for the resistance genes confirmed the type of resistance by matching the expected fragments' sizes with the resultant fragments that appeared on the gel. Moreover, sequencing the resultant fragments added more confirmation. The NCBI BLAST tool results of similarity showed a percentage ranged from 96.51 % to 99.75 % of matches, which represents a high and accepted values of matches.

OD_{570} values representing biofilm densities showed variable quantities of absorbency for each of the tested strain in every time-point of growth, in all the growth media, under static and shaking incubations as shown in Figures 2.6 through 2.11.

It was presumed that the four bars arrangement (that represents the absorbency value corresponding to biofilm densities of the selected four time-points) in the bar chart would look like a bell-shape, as presented in the virtual bar chart above. Those four time-points were selected according to a previous study done by Atshan et al. (2013), who studied the biofilm formation ability of *Staphylococcus aureus* at four time-points of growth (6, 12, 24, and 48 h), which represented the biofilm development stages according to that study.

In general, the majority of the results of this work did not follow the presumed bars sequence in the above bar chart. Instead, there was a variability in each condition depending on the strain type, type of media, and static and shaking incubation (Fig 2.6 through 2.11).

Growth medium composition affects biofilm formation (Hancock et al., 2011; Reisner et al., 2006), and the present study tested the effect of three different media types on biofilm formation, namely nutrient broth (NB), Luria-Bertani (LB), and AB media. The effect of biofilm formation was analysed in the poor nutrient media (AB medium) to mimic nutrient

conditions in the urinary tract, a nutritionally poor, nitrogen-rich environment (Alteri & Mobley, 2015), then compared with the one in the rich LB broth to find out whether nutrition could significantly affect biofilm density between the two media. The effect of aeration and nutrient on the biofilm formation process were also explored by incubating test strains under shaking and static conditions for all tested media and growth stages. Results showed that all of the above influenced biofilm formation timing and density.

This work investigates the biofilm formation ability of the strains mentioned above by comparing their produced biofilms at the four different time-points depending on media and growth conditions (static and shaking). Statistical analyses were conducted to detect significant differences among those four time-points.

In order to confirm that the biofilm density values are significantly different between the time-points for the specific strain, a one-way ANOVA statistical test was applied to calculate whether there is a significant difference in absorbency values, which represent biofilm density values. Data were sorted into tables of comparisons and strains were arranged into columns inside the tables along with the comparisons and their resultant *p* values. A *p* value of less than 0.01 was considered to be significant. One-way ANOVA statistical analysis results showed a significant difference ($p < 0.01$) in biofilm density values among time-points for all the tested strains, except *K. pneumoniae* SHV-18 grown in static AB and *K. pneumoniae* 9633 grown in shaking NB (Tables 2.I through 2.XII of Appendix). This indicates that the selected time-points (6, 12, 24, and 48 h) were ideal to be chosen for illustrating biofilm formation steps, as it showed it in distinctive stages. Moreover, there were considerable and significant variations in biofilm density values among tested strains.

Table 2.11 shows each strain's biofilm at the maturation stage when grown in the different selected media under static and shaking conditions. Thus, it highlights the optimal conditions for each strain to produce the highest biofilm regarding the conditions mentioned above; for instance, *E. coli* TEM-3 produced the highest biofilm density with static incubation in AB medium. Specific strains did, however, exhibit a preference for growth media and stage. For example, *K. pneumoniae* SHV-18 produced the highest biofilm density when grown in NB, but when grown in AB medium, the produced biofilm was significantly lower. A possible explanation for this finding might be the variable nutrient contents of the media; in other words, genetic factors associated with biofilm formation were found to be affected by the nutrient composition of the growth medium (Stepanović et al., 2004; Reisner et al., 2006). In this study, static and shaking incubations were used to investigate the effects of aeration and nutrient distribution on biofilm.

E. coli 12241 and *K. pneumoniae* 9633 were the non-resistant strains considered as a control to compare their biofilm density values and stages with other resistant tested strains. In this study, all tested strains showed the same pattern of biofilm formation as the non-resistant strain (except with *E. coli* CTX-M-15 and in some cases with *K. pneumoniae* OXA-48 and SHV-18) with the difference in biofilm density value. There are not enough studies that could categorically confirm a relationship between the antibiotic resistance and the ability to form high biofilm. Over the past two decades, many studies showed conflicting results. Abidi et al. studied 22 *Pseudomonas aeruginosa* isolates and inferred that biofilm production was significantly higher in MDR isolates (Abidi et al., 2013), while Eyoh et al. did not get similar results with MDR and non-MDR *Staphylococcus aureus* (Eyoh et al., 2014). Gurung et al.,

however, studied 60 isolates and found a positive relationship between biofilm formation and antibiotic resistance while working with 60 isolates of *Acinetobacter baumannii* (Gurung et al., 2013). In this study, the resistant strains always formed a higher biofilm than the non-resistant, and this might be one of the mechanisms that helped them to develop the resistance to escape the antibiotic effect through exposure to low levels of antimicrobials inside the biofilms (Ahmed et al., 2018). The Corehtash group surmised that this might be due to the delayed penetration of antimicrobial agents into the bacterial cell (Corehtash et al., 2015).

Medium composition effects cannot solely increase or decrease antimicrobial tolerance, as one experiment showed that *E. coli* grown in LB medium was susceptible to kanamycin with little effect from glucose added to the medium, while a previous experiment on *Pseudomonas aeruginosa* demonstrated bacterial resistance to ampicillin in LB medium that was attenuated by the addition of glucose to the medium. These findings suggest that media composition can affect microbial physiology and thereby susceptibility to antimicrobials, while antimicrobial tolerance remains a unique characteristic of microbial biofilms (Stewart et al., 2000).

Crystal violet was used to evaluate the density value of biofilm in early stages, bacterial attachment, and exopolysaccharides production. A basic dye, crystal violet attaches to remaining bacteria and exopolysaccharides that persist after washing with distilled water. Though it is a simple technique, the crystal violet assay is considered the gold standard for biofilm evaluation due to its extensive range of usage in the detection of bacterial and fungal biofilms (Crémet et al., 2013). Benefits include a high throughput of isolates, flexible protocol, and low cost (O'Toole, 2011).

Limitations of this study include a lack of microscopic examinations to confirm the presence or formation of exopolysaccharides during the four growth stages. We chose a crystal violet assay as the standard protocol for evaluations of early-stage biofilm formation (Reisner et al., 2006). This study illustrated the effect of certain parameters on the density values of biofilm produced by antibiotic-resistant strains of *E. coli* and *K. pneumoniae*.

In summary, the antibiotic-resistant strains formed higher density of biofilm than the non-resistant ones. The next question addressed by this experiment was whether variations in biofilm formation conditions correlated with expression patterns of genes associated with biofilm formation. Therefore, *E. coli* CTX-M-15 was selected for the next step to investigate the genetic role in biofilm formation during the selected time-points.

Chapter 3:

Analysis of the gene expression during the biofilm formation in *E. coli* CTX-M-15 at different growth conditions

3.1 Introduction

The previous chapter of this work demonstrated the ability of specific antibiotic-resistant strains to form a biofilm, and the results showed that *E. coli* CTX-M-15 demonstrated variations in biofilm formation in different conditions, which highlights that this strain can adapt to many environments. Moreover, it is the most prevalent strain in the UK. For those reasons, *E. coli* CTX-M-15 was selected for the next step of this research.

Work on this chapter focuses on identification of whether the variation in biofilm formation analysis observed among the selected time-points is correlated with the gene expression which is related to biofilm formation. Additionally, gene expression of the selected genes was attempted to be linked with the level of biofilm amount recorded during the four different growth stages of the selected strain grown in LB and AB. According to the Figure 3.1, biofilm amount recorded for the selected time-points formed consecutive rising and dropping levels for both media. Therefore, this chapter attempts to determine the related gene expression with each stage of biofilm time-point.

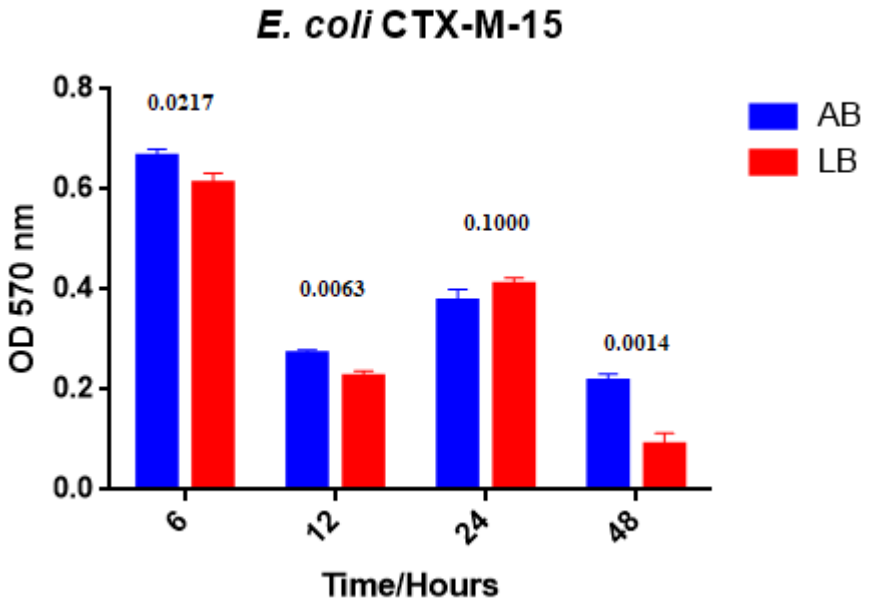

Fig 3.1 Comparison between biofilm amount formed in AB and LB broths during the four selected time-points (6, 12, 24, and 48 h) of growth in *E. coli* CTX-M-15. Numbers above the columns represent the *p* values of the t-test that was calculated to find out whether there is a significant difference between the biofilm formed among the two broths.

For this analysis, genes that are related to biofilm development, QS, and antibiotic resistance were selected.

3.1.1 Aims and Objectives

Aim

The aim of this research was to analyse the expression of genes related to biofilm development, quorum-sensing controlled genes, and antibiotic resistance during various growth stages and in different growth conditions.

Objectives

- to grow the selected *E. coli* CTX-M-15 in AB and LB broth for 6 h, 12 h, 24 h, and 48 h
- to extract the RNA from each of the above time-points for both media
- to measure gene expression level using qPCR technique

3.2 Materials and methods

3.2.1 Bacterial strain and culture conditions

Antibiotic-resistant ESBL *E. coli* CTX-M-15 was used in this study, obtained from National Collection of Type Cultures (NCTC), cultured on nutrient agar plates, and incubated at 37°C for overnight. Prior to perform the assay, a loopful of bacterial colonies was inoculated into 5 ml of LB and incubated for 18 h at 37°C in a static incubator.

3.2.2 RNA isolation from biofilm

The protocol of Atshan et al. (2013) was used with modifications and as follows: in order to measure gene expression of the selected genes in the two media, six-well TCP (Techno Plastic Products) were used in this assay. Two types of growth media were provided, namely LB broth and AB medium. Using a micropipette, the LB overnight static-incubated *E. coli* CTX-M-15 at 37°C were diluted to give a final OD_{600} of 0.01 in 5 ml in each well of the six-wells TCPs that separately contain both media; AB and LB, and incubated at 37°C for 6 h, 12 h, 24 h, and 48 h in a static incubator for each of the above-mentioned media to let the bacteria develop the various amounts of biofilm at each stage and in each medium. After incubation, the broth was carefully drawn from each well using a Pasteur pipette, and the wells were washed three times using a sterile distilled water. In each well of the TCP for each time-point in each medium, the adhered cells were disrupted by rapidly scraping them from the plate surface using a sterile micropipette tip until no visible layer was left, and suspended in cold sterile distilled water. The suspensions of each well were immediately transferred to Corning® 50 mL centrifuge tubes (Sigma Aldrich) and labelled according to the growth

medium and incubation time, and each tube was incubated with two volumes of RNA protect (Qiagen) according to the manufacturer instructions, vortexed for 5 s, and incubated for 5 min at room temperature. The mixture was pelleted by centrifugation at 10000 x g for 10 min, supernatant was decanted, and pellets were stored for a short period at -15°C awaiting RNA extraction (section 3.2.3).

3.2.3 RNA extraction using Qiagen RNeasy Mini Kit

The protocol for "Enzymatic Lysis of Bacteria" (Qiagen) was adhered to as follows: the recommended volume of TE buffer containing lysozyme was added to the pellets in the 50 mL centrifuge tubes from the previous step, mixed by vortexing for 10 seconds, and incubated in a shaker incubator 25°C for 30 min. Buffer RLT was added according to the volume recommended by the manufacturer and vortexed vigorously, followed by addition of the appropriate volume of ethanol 70 %. Total RNA was isolated according to RNeasy mini kit (Qiagen) and as follows: up to 700 µl of each sample was transferred to an RNeasy Mini spin column placed in a 2 ml collection tube which is supported with the kit, labelled, and centrifuged for 15 s at 10000 x g in a refrigerated centrifuge, and the flow-through was discarded. 700µl of buffer RW1 was added to the RNeasy spin column and centrifuged for 15 seconds at 10000 x g, and the flow-through was discarded. The spin column was placed into a new 2 ml collection tube and 500 µl of Buffer RPE was added and centrifuged for 15 s at 10000 x g in a refrigerated centrifuge. Another 500 µl Buffer RPE was added and centrifuged for 2 min at 10000 x g. Finally, the spin column was placed into a new 1.5 ml collection tube and 50 µl RNase-free water was added directly to the spin column membrane

and centrifuged for 1 min at 10000 x g to elute the RNA. Using agarose gel electrophoresis and a NanoDrop™ Lite Spectrophotometer, the RNA quality and quantity were determined. RNase-free DNase set (Qiagen) was used to remove residual DNA after RNA elution. Resulting RNA samples were analysed for contaminating DNA present after enzyme treatment by PCR targeting the 16s rRNA gene; forward primer (5′-CGGACTACGACGCACTTTAT-3′) and reverse primer (5′-CGCAACCCTTATCCTTTGTTG-3′). PCR amplification reaction and conditions were the same as detailed in Table 2.5 and 2.6, with Tm of 55°C. PCR products were run on agarose gel electrophoresis to confirm the complete digestion of the contaminating DNA. Samples that showed bands were re-treated with DNase while samples that showed no bands were immediately converted into cDNA.

3.2.4 Conversion of RNA to complementary DNA (cDNA)

To avoid RNA degradation, purified RNA was converted immediately to cDNA using RevertAid H Minus First Strand cDNA Synthesis Kit (Thermo Scientific, Catalogue number: K1632) according to the manufacturer instructions and as follows: using random hexamer primers, the following ingredients were added for the final volume of 20 µl: Template RNA (after adjusting RNA quantity between 0.1 ng-5 µg), primers (random hexamers) 1 µl, and the total volume was completed to 12 µl nuclease-free water. Then, the following components were added in the following order: 5× reaction buffer 4 µl, RiboLock RNase Inhibitor 1 µl, 10 mM dNTP mix 2 µl, and RevertAid H Minus reverse transcriptase 1 µl. All

components were mixed gently and centrifuged, then incubated at 25°C for 5 min followed by 60 min at 42°C. The reaction was terminated by heating in a dry bath at 70°C for 5 min.

3.2.5 Primers and their specificities for qPCR

Genes' sequences were obtained from the free software (NCBI), and their primers were designed using the free software of Integrated DNA Technologies (IDT). Optimum primer length was 18-22 bp, with a minimum product size of 80 bp and a maximum of 200 bp (Table 3.1). cDNA obtained in 3.2.4 was used as the template for PCR reaction. PCR products were compared according to their fragment sizes with the expected designed fragment size after running on an agarose gel. The presence of primer-dimers and nonspecific amplification was identified through analysis of melting curve data.

Table 3.1 The list of primers that were used in this study.

Genes	Nucleotide sequence of primers (5'-3')	*Type	Annealing temperature	Amplicon size (bp)	Reference
16s rRNA	TAGCGGTGAAATGCGTAGAG CCTCCAAGTCGACATCGTTTA	REF	62	148	This study
bla$_{CTX-M}$	GGAATCTGACGCTGGGTAAA TATCGTTGGTGGTGCCATAG	TRG	63	165	This study
*Lux*S	ATCCCTCTTTCTGGCATCAC AGCTTCACAGTCGATCATACC	TRG	63	143	This study
*mot*B	TGGATAGCGGCAAAGTGTTA CCTGTTCGGCTTGTTTGTTC	TRG	63	98	This study
crr	TGTTCGTCCACTTCGGTATC CAGGGTAGACTTGGCTTTCT	TRG	62	146	This study
*csg*B	CCGCAGCAGGTTATGATTTAG GTCCCAGCTTGACCAATTATG	TRG	62	103	This study
*csg*E	CGCCGTTGAGGTAGAAGTC ACGTCCTGATTGACCGTTATT	TRG	63	180	This study
*csg*F	GCGTGTCAAACATGCAGTAG ACGCTGAGGGTGTTTCAATA	TRG	63	200	This study
*fli*S	AGAGAGCAAAGACGAACTAACC TTTCCAGGCATCGGCAATA	TRG	63	145	This study
*mot*A	AAGCCTTGGAGCACTCTATC CCTTCAGCGTGCCTTTAATC	TRG	62	110	This study
*tol*B	TACGTCAGGTGGCTTCATTC GGTCGGTTCGGTATTGTTACT	TRG	63	176	This study
*yie*O	ACGGTGGCGATGCTTATT GACTCACGGCAAGGGTAAA	TRG	63	82	This study
*mdo*H	TGCTGTTCCATACGGTCTTC CAGCCCACACTAACCCTAAC	TRG	63	147	This study

*REF indicates reference gene, TRG indicates target gene

3.2.6 Primer efficiency

The efficiency of each primer pairs was calculated using serial dilutions of amplicons (diluted 1:100) in triplicate, then the resulting data were used to produce the standard curve for each primer set. A correlation coefficient (R2) of 0.99 or greater was preferred. The amplification efficiency = [10(-1/slope)] – 1. The amplification efficiency of 80-120 % was preferred.

3.2.7 Quantitative real-time PCR

The RT-qPCR analysis was conducted using the Thermo Scientific™ PikoReal™ Real-Time PCR System. Each reaction contained 5 µl of SensiFAST™ SYBR® No-ROX Mix (Bioline), 0.5 µl cDNA, 0.4 µl of forward and reverse primers each, and 3.7 µl of RT-PCR grade water (Thermo Fisher Scientific) in a total volume of 10 µl. Amplification conditions were as follows: 95 °C for 2 min followed by 40 cycles of 5 s at 95 °C, 10 s at 60 °C, and 10 s at 72°C. The melting curve was obtained by melting the amplified template from 60 to 95°C. No-template control and no-reverse transcriptase control were included. For each sample, three technical replicates were used. All primer pairs' amplification efficiency was evaluated using tenfold dilutions of pooled cDNA. Analysis followed MIQE guidelines (Bustin et al., 2009).

3.2.8 No reverse transcriptase

A no-reverse transcriptase control was used in triplicate for each sample (6 h, 12 h, 24 h, and 48 h) by using the eluted pure RNA after the DNase treatment step without conversion into cDNA.

3.2.9 Validation of the reference genes

Four genes (16s rRNA, arcA, gapA, and rpoS) were chosen for potential stability as a reference gene by running qPCR for the four growth stages (6 h, 12 h, 24 h, and 48 h) in triplicate. A change in Cq value among the selected stages of less than 0.5 was accepted (Reid, 2018). Only one gene, 16s rRNA, was determined as a suitable reference gene. Due to time constraints, no more genes were tested for suitability as reference genes. The three genes that had failed as reference genes were then discarded.

3.2.10 Data analysis using the relative standard curve method

6 h of growth was used as the calibration sample to calculate the expression of the selected biofilm forming genes and AI-2 controlled genes at the 12, 24, and 48 h of growth in both AB and LB media. The X-fold change in the level of transcription was calculated using the relative standard curve method. Standard curves were made for both target and reference genes. Data were analysed using equations from Pikoreal software user manual (Thermo Scientific) that were put into the Excel sheet, and calculations for each gene studied were performed.

3.3 Results

3.3.1 RNA integrity and stability

Before starting any work with RNA, it is recommended to ensure the extracted RNA is intact and free from degradation. RNA integrity is a critical prefix step to obtain meaningful data of gene expression, while using low quality RNA could weaken the experimental results, for example, with qPCR expression analysis. Therefore, using intact RNA is a crucial element for the successful qPCR application (Fleige & Pfaffl, 2006). To check RNA integrity, extracted RNA samples were run on agarose gel, and samples that showed intense bands of 16S and 23S rRNA indicated that the RNA in that sample was intact and not degraded.

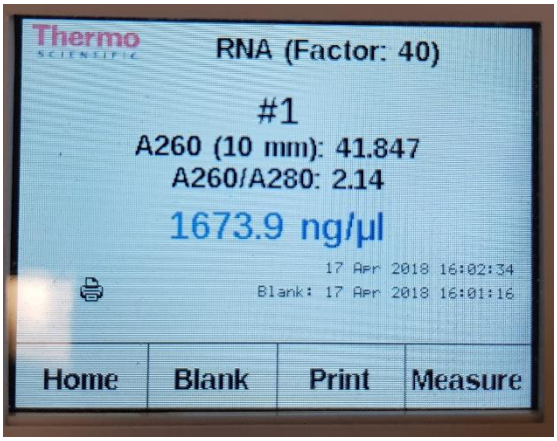

Fig 3.2 The amount of the extracted RNA measured in nanogram per microliter. NanoDrop™ Lite Spectrophotometer used to determine the eluted RNA concentration. Also, the ration A260/A280 indicated that the eluted RNA sample was pure (in other words, >2).

The RNA extracted at different time-points showed a satisfactory quality and quantity (Fig 3.2-3.4). The cDNA synthesis produced large quantities.

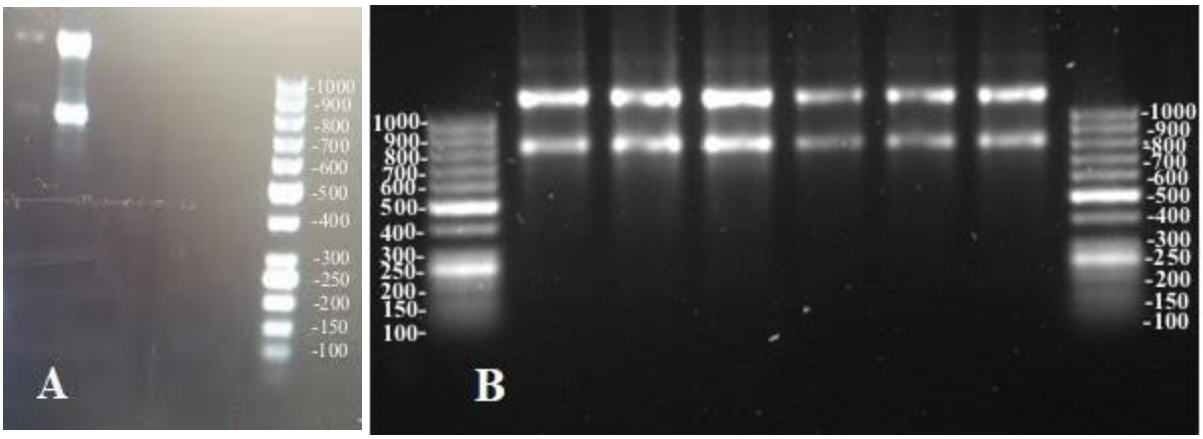

Fig 3.3 Extracted and purified RNA run on 1 % agarose in TAE buffer showing the intensity and integrity of the two bands (23s and 16s). Both pictures show bright, separated bands with different intensities. A) The picture shows two samples; the first one with very low intensity, that is, with low RNA product, and the second sample with very dense bands. B) The picture shows extracted RNAs from different biofilm samples. Both pictures show intact RNA which is ready for the subsequent steps. The gel was run at 5 V/cm

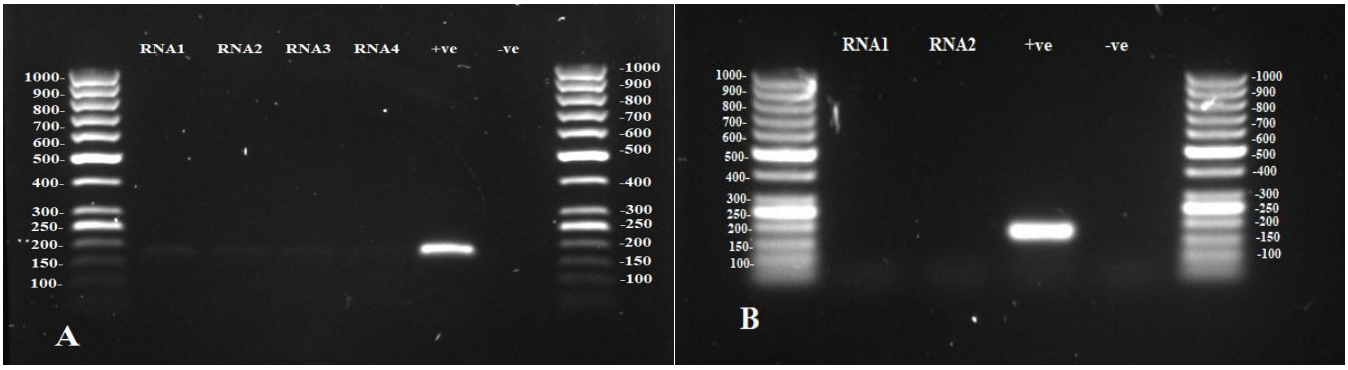

Fig 3.4 Gel electrophoresis (1 % agarose in TAE buffer) showing the purity of the extracted *E. coli* CTX-M-15's RNA samples (RNA 1 and RNA 2) after DNase treatment and PCR reaction. Electrophoresis results show the PCR products in which RNA samples used as the template after being treated with DNase to confirm the complete DNA digestion from the samples. A) The picture shows light bands (198bp) after DNase treatment, which indicates that there is still a small amount of contaminating DNA within the RNA sample. B) The picture

shows no bands for RNA 1 and 2, which means that both are free from contaminating DNA. The positive control (+ve) template was the *E. coli* CTX-M-15 genome DNA, and the negative control (-ve) had no template added. Primers used were the 16s rRNA as mentioned in 3.2.3. The gel was run at 5 V/cm

3.3.2 Primers specificities

The primers used in this work were tested for their specificities using end-point PCR with cDNA as the template for the reaction, and a Tm of 55 °C. Primers that showed a single band after running on agarose gel were selected for further qPCR expression analysis (Fig 3.5).

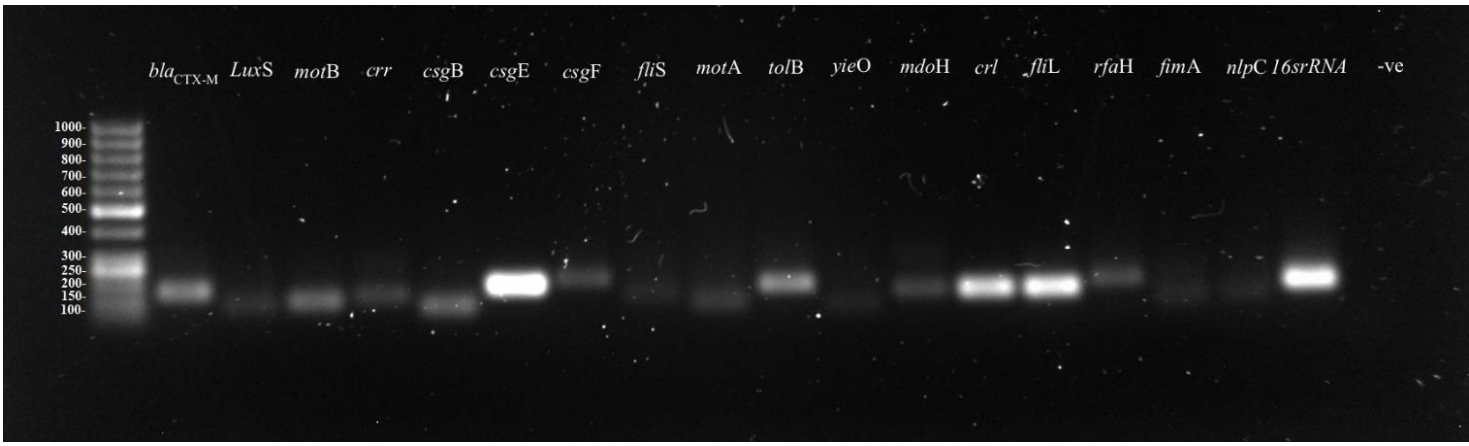

Fig 3.5 PCR products of cDNA of the biofilm-related and quorum-sensing genes plus the housekeeping gene (16s rRNA) after running on 1 % agarose in TAE buffer. This experiment was performed before qPCR to confirm that the specific selected gene is expressing by showing a product (band) which comes from its cDNA that was added as the template for the PCR reaction mixture. Negative control was the 16s rRNA primers, which shows no bands. 5 V/cm.

3.3.3 Primers efficiencies

The efficiency values for primers used for the gene expression analysis in this chapter ranged from ~92 % to ~106 %, which was within the range mentioned in 3.2.6 (80-120 %). The efficiency of Fig 3.6 below was ~100.5 % (Table 3.2).

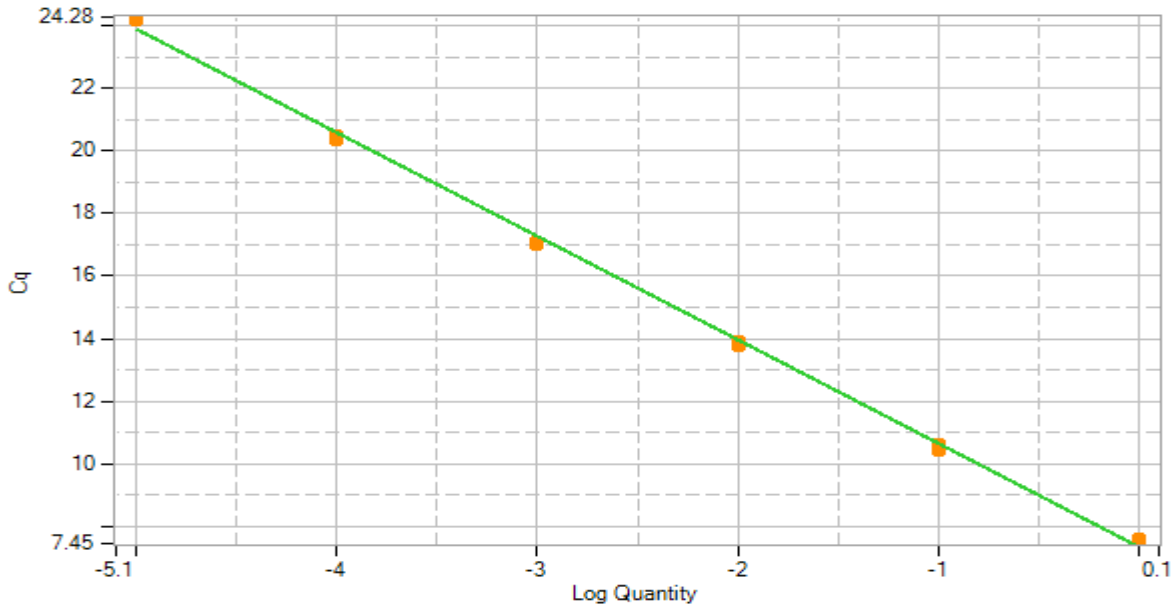

Fig 3.6 Example of a standard curve for the mdoH gene primers. Primer efficiency was calculated using serial dilutions of amplicons. In this example, each dot is composed of triplicate of the reaction mixture.

Table 3.2 The primers' efficiencies used in the qPCR study. Serial dilutions of amplicons used to calculate the efficiencies. An efficiency of 80-120 % was accepted.

Primer	Efficiency in AB (%)	Efficiency in LB (%)
16s	96.698	101.538
crr	98.869	103.4
*csg*B	96.563	105.816
*csg*E	93.201	103.839
*csg*F	95.639	99.799
$bla_{\text{CTX-M}}$	92.552	100.43
*fli*S	103.003	103.711
*Lux*S	95.621	93.764
*mdo*H	100.464	101.211
*mot*A	92.65	100.017
*mot*B	95.428	102.344
*tol*B	97.712	106.246
*yie*O	99.759	98.293

3.3.4 Expression levels of biofilm-associated genes quantified by qPCR

The expression of 12 of the selected genes in both media AB and LB which were associated with biofilm formation were compared using the Cq values which showed significant differences among all genes and at every time-point of the selected growth stages. The mean

Cq values ranged from 15.45 to 31.84. The standard deviation of Cq values for each gene was less than 0.5. The comparative relative expression of the selected 12 genes at each growth stage of biofilm formation for the *E. coli* CTX-M-15 grown in AB and LB were calculated relative to the calibration samples (Table 3.3). In this experiment, not all genes worked in both media and gave a single peak in the melting curve analysis, that is, some gave the standard one peak in one medium but not in the other. Therefore, those genes that did not give a single peak were excluded from expression comparison in this chapter but kept for the other comparison in the next chapter where they gave an acceptable result.

Table 3.3 Fold change in mRNA level of antibiotic resistance coding gene, AI-2-related genes, and biofilm-related genes in *E. coli* CTX-M-15 grown in LB and AB broth at different time-points of 12, 24, and 48 h. Downward arrows indicate significantly decreased gene expression and upward arrows indicate significantly increased gene expression when *P*-value < 0.05 (target sample differ to control). * indicates the target sample is not different from control (*P*-value > 0.05).

Gene	Fold Change in level of biofilm genes					
	AB			LB		
	12 h	24 h	48 h	12 h	24 h	48 h
16s (the reference gene)	1	1	1	1	1	1
crr (D-glucosamine phosphotransferase system permease activity)	0.05↓	0.18↓	0.05↓	0.54↓	1.26↑	0.34↓
*csg*B (Curlin nucleator protein)	0.19↓	419.76↑	1.19*	0.66↓	97.10↑	59.89↑
*csg*E (Predicted transport protein)	0.11↓	3.96↑	0.17↓	1.08↑	39.49↑	3.03↑
*csg*F (Predicted transport protein)	0.08↓	4.00↑	0.13↓	1.60↑	24.68↑	2.63↑
$bla_{\text{CTX-M}}$ (β-lactam resistance)	0.15↓	0.13↓	0.03↓	0.33↓	0.23↓	0.12↓
*fli*S (Flagellar protein potentiates polymerization)	0.07↓	0.55↓	0.10↓	0.05↓	0.06↓	0.01↓
*Lux*S (AI-2 synthase)	0.02↓	0.08↓	0.60↓	0.69*	1.75↑	0.25↓

*mdo*H (Glucan biosynthesis: glycosyl transferase)	0.04↓	0.19↓	0.05↓	0.52↓	2.41↑	0.37↓
*mot*A (a component of proton conductor of flagella motor)	0.49↓	0.74*	0.38↓	0.07↓	0.13↓	0.01↓
*mot*B (Protein rotates flagellar motor)	0.11↓	0.29↓	0.22↓	0.07↓	0.22↓	0.01↓
*tol*B (Periplasmic protein)	0.04↓	0.31↓	0.04↓	0.56↓	1.05*	0.15↓
*yie*O (Predicted multidrug or homocysteine efflux system)	0.09↓	0.43↓	0.34↓	0.09↓	0.41↓	0.06↓

All genes were downregulated at 12 h of growth in AB, while only two gave a significant upregulation in LB broth. Results in Table 3.3 represent qPCR values calibrated with 6 h of growth. In order to get a comprehensive overview for all selected genes' upregulations and downregulations, relative expressions of all genes were plotted into line charts, and the *p*-value was calculated for each time-point comparison to find out whether the upregulation and downregulation were significant (Fig 3.7).

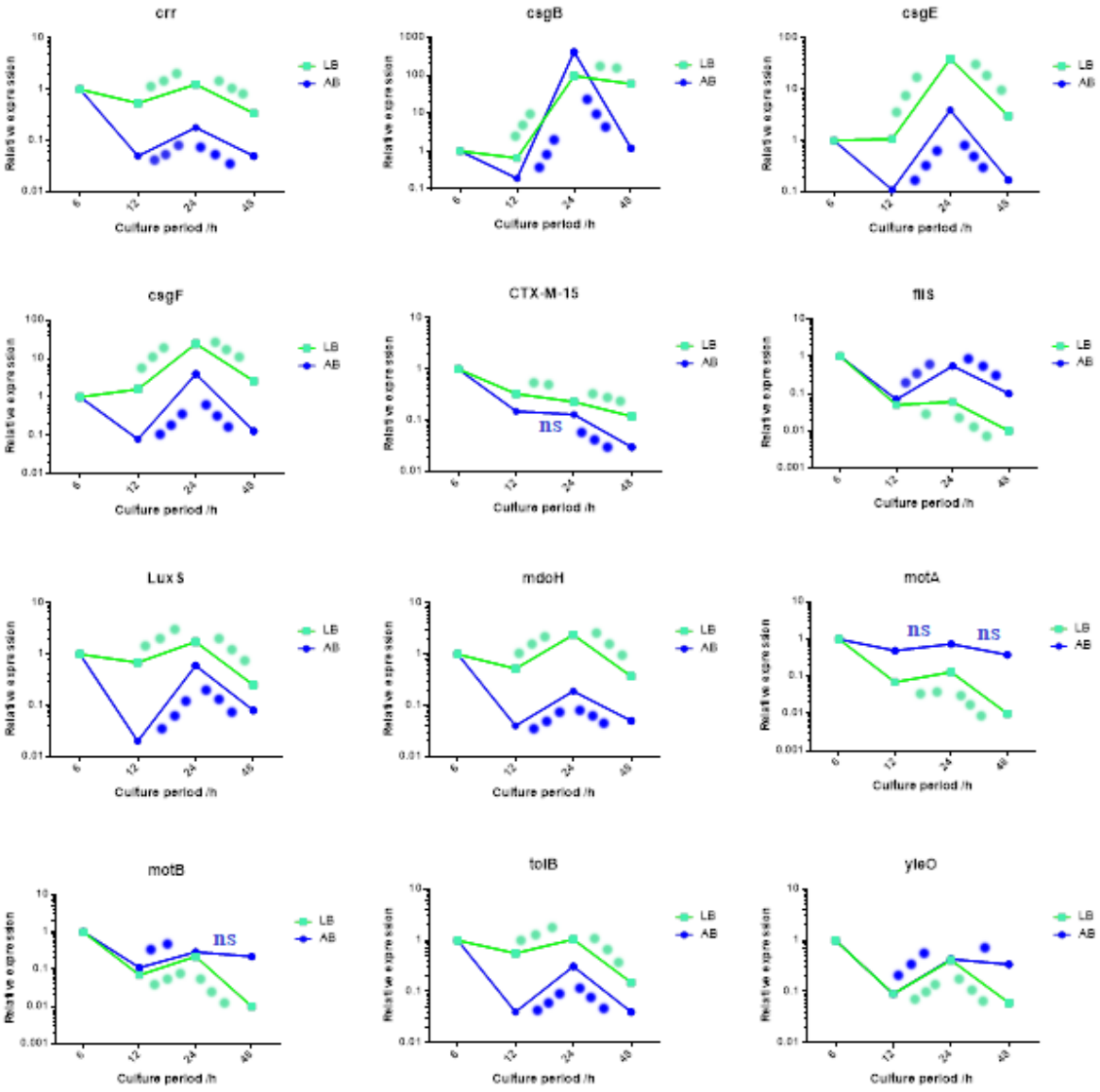

Fig 3.7 The fluctuation of the transcriptional level of the selected genes (*crr, csgB, csgE, csgF, bla*$_{CTX-M}$*, fliS, Lux*S, *mdoH, motA, motB, tolB, and yieO*) of *E. coli* CTX-M-15 growing in AB and LB broths at four time-points (X-axis). Total RNA was isolated from 6, 12, 24, and 48 h of static incubation cultures from both AB and LB broths, and the relative expression levels of all of the above 12 genes were compared by qPCR (relative plotted against log 10, Y-axis). Data represent two independent experiments. Green lines represent gene expression in LB, and blue lines represent gene expression in AB. A t-test was used to detect the significant

difference in genes' upregulations and downregulations between 12-24 and 24-48 h. Green dots refer to LB, and blue dots refer to AB. • p = 0.01-0.05, •• p = 0.001-0.01, ••• p = < 0.001.

As shown in Fig 3.7, all genes were downregulated at 12 h, then upregulated at 24 h to go back to downregulation after 48 h of growth, which coincides with the phenotypic results observed during the biofilm development, with the exception of *csgE* and *csgF* in LB medium (as they slightly upregulated at 12 h) and $bla_{CTX\text{-}M}$ (as its level continued downward by time). Cq value of each gene has been plotted to get a clear picture of the expression level in each medium at each time-point (Fig 3.8 and 3.9). Cq values also correlate with biofilm development. A lower Cq value means higher expression and vice versa.

.

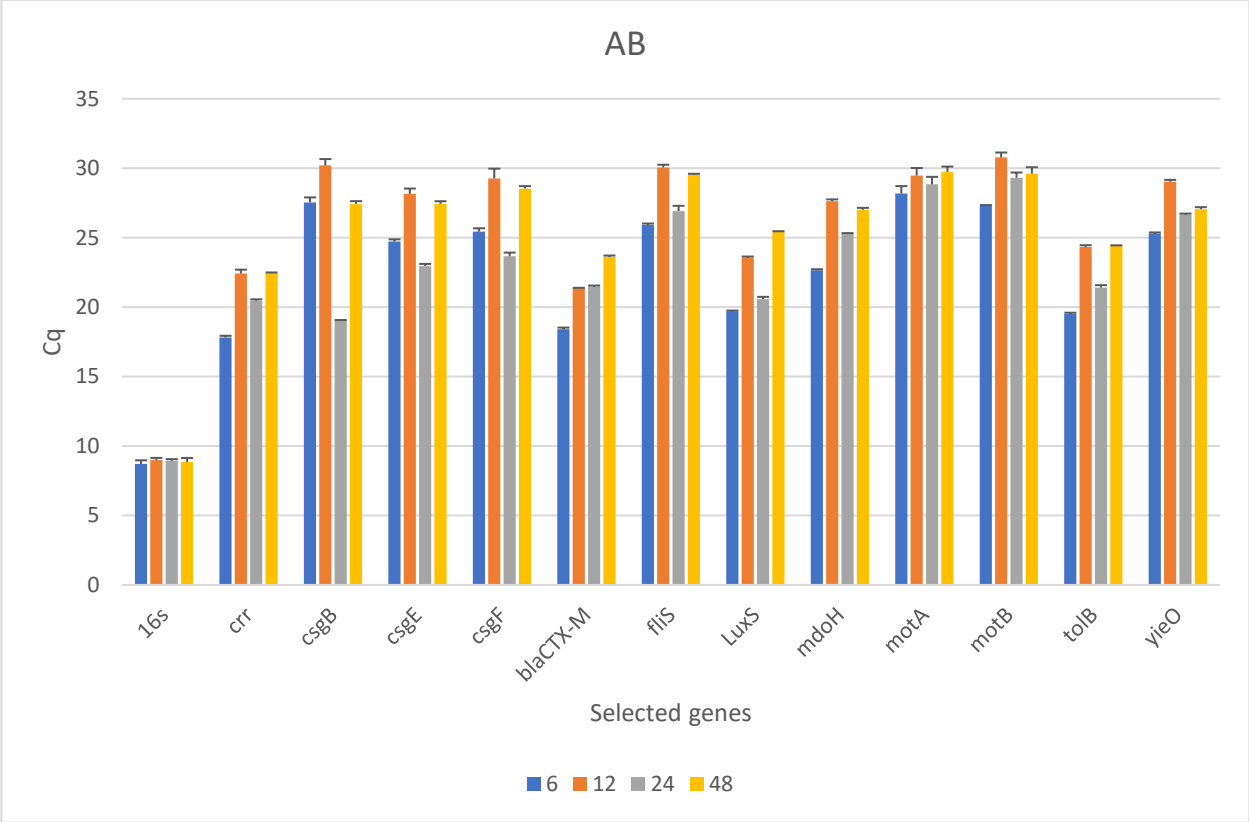

Fig 3.8 The variations in Cq value of each of the selected genes which represent the copy number of the target gene as measured by RT-qPCR. High Cq value indicates a low copy number of the gene, while the low Cq value indicates a high copy number of the gene. Each color of the columns represents a specific time-point of growth in AB medium. The experiment was done in three technical replicates, and data represent the means of those biological replicates. Error bars represent the standard deviation of the triplicates.

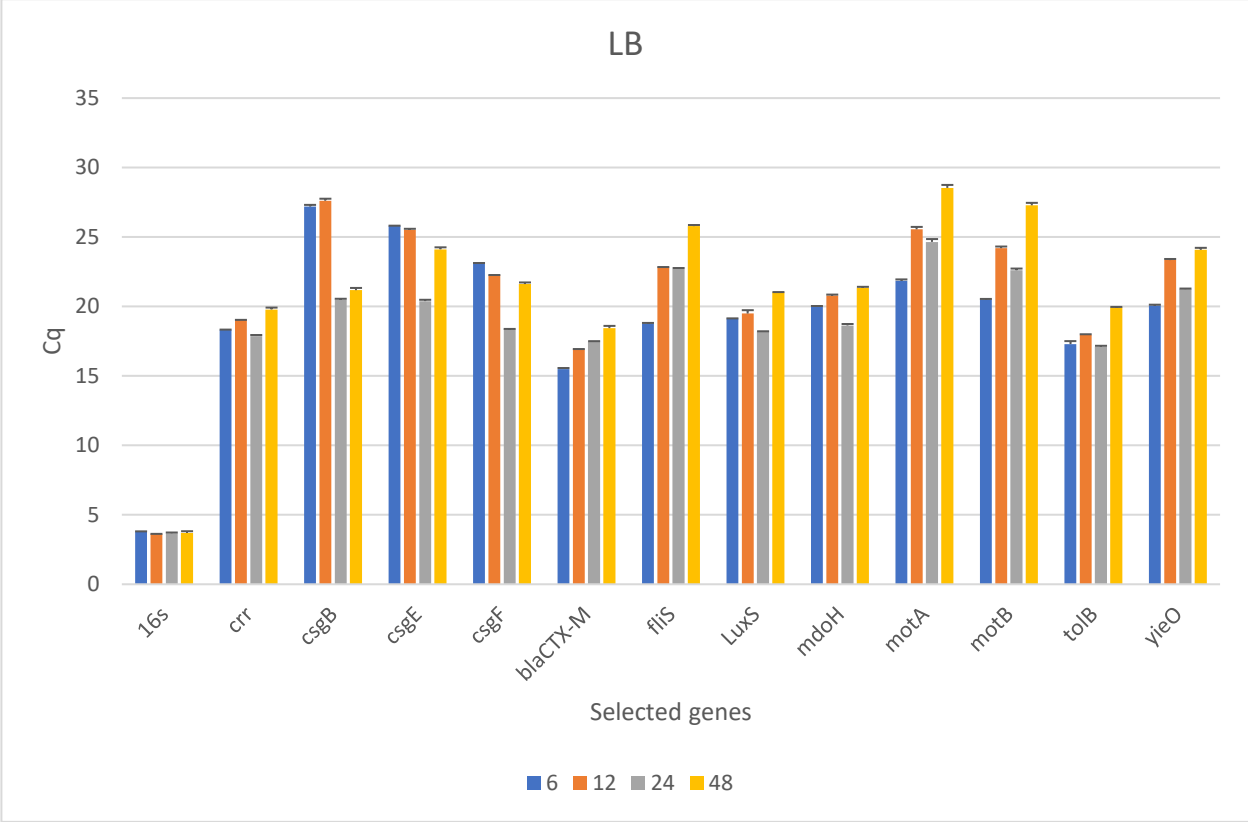

Fig 3.9 The variations in Cq value of each of the selected genes which represent the copy number of the target gene as measured by RT-qPCR. High Cq value indicates a low copy number of the gene, while the low Cq value indicates a high copy number of the gene. Each color of the columns represents a specific time-point of growth in LB medium. The experiment was done in three technical replicates, and data represent the means of those biological replicates. Error bars represent the standard deviation of the mean.

The expression of the selected genes at 12 h, 24 h, and 48 h was compared with that at 6 h to give a relative expression values for the selected time-points and for both media AB and LB, as shown in Fig 3.10 and 3.11

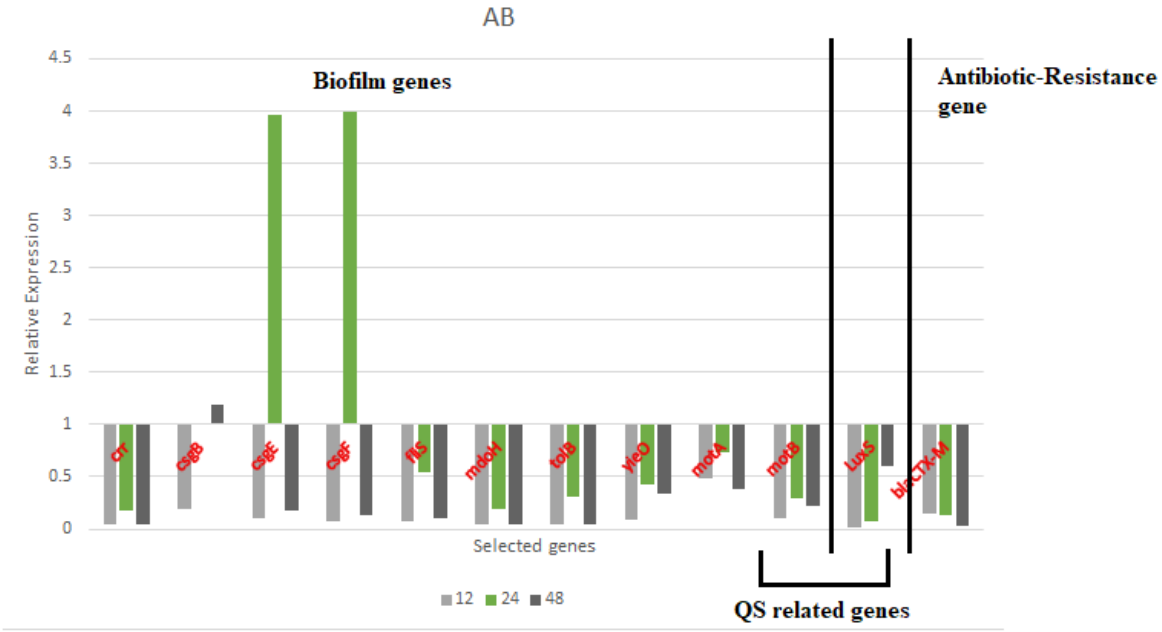

Fig 3.10 *E. coli* CTX-M-15 selected genes' fold change at 12 h, 24 h, and 48 h of growth in AB broth.

**csg*B fold change at 24 h is shown separately on Fig 3.12.

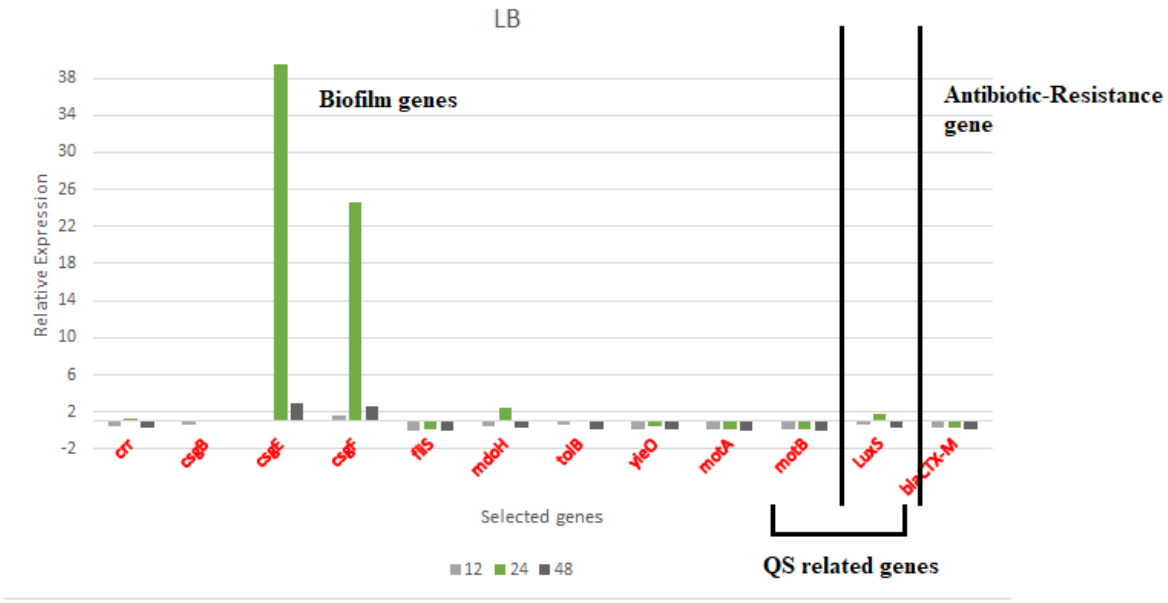

Fig 3.11 *E. coli* CTX-M-15 selected genes' fold change at 12 h, 24 h, and 48 h of growth in LB broth.

**csg*B fold change at 24 h and 48 h is shown separately on Fig 3.12.

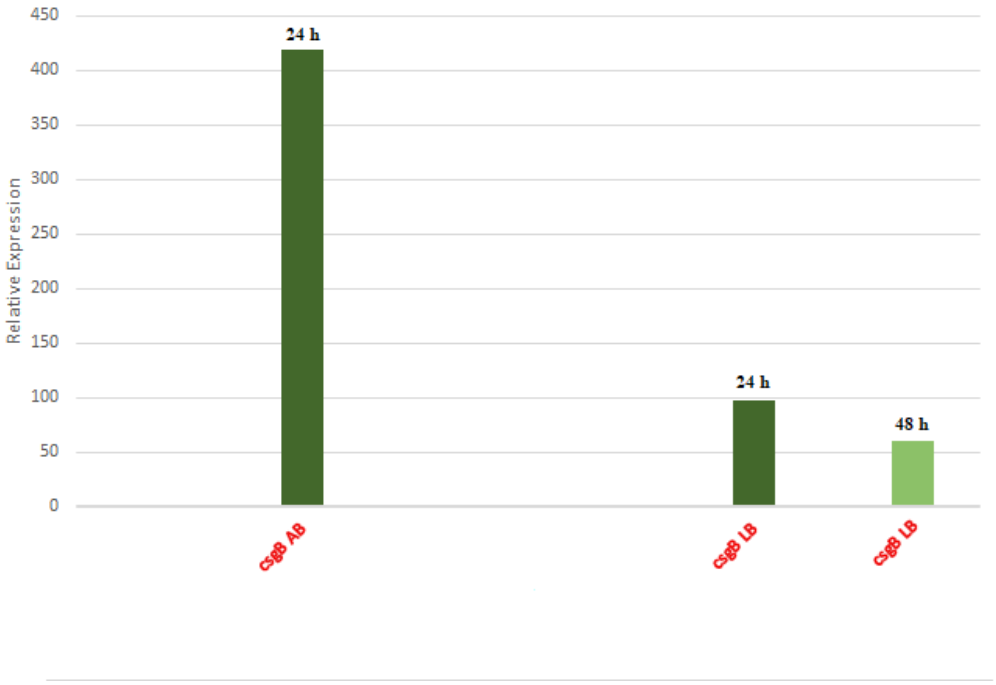

Fig 3.12 Fold change of *csg*B in AB at 24 h and LB at 24 h and 48 h in *E. coli* CTX-M-15.

3.4 Discussion

The molecular mechanism of biofilm formation in *E. coli*, as well as its relationship with antimicrobial resistance, are poorly understood, and there are limited studies dealing with expression profiles of biofilm-related genes during biofilm formation stages, along with the expression of resistance genes. This chapter tries to link between the level of formed biofilm at each selected time-point of *E. coli* CTX-M-15 growing in AB and LB broth, with the level of gene expression measured at those above-mentioned time-points, to find out whether there is a correlation between the formed biofilm and gene expression level at that specific time-

point, and to find out the connection of all of the above with the level of resistance during those time-points in different media.

A crystal violet method for measuring biofilm amount in four different time-points was used as a comparative analysis (as changes in biofilm amount were significant among the selected time-points for the same medium) with the gene expression in both media at the same four time-points. In comparison with DNA microarray analysis and qPCR results reported in other studies dealing with *E. coli* biofilms (Schembri et al, 2003; Niba et al, 2007), there were neither time-points nor relative quantification for the specific gene at the different stages of biofilm formation in the selected *E. coli* K-12 used for those studies. The previous chapter results showed two peaks of high OD_{570} values for both media, AB and LB, which can give an assumption that there were two cycles of biofilm formation (Fig 3.1).

Expression and upregulation of *csg*B, *csg*E, and *csg*F along with crystal violet OD_{570} results might give an indication for the timing of the attachment of bacterial cells to the surface, which is the first step in the biofilm formation process. *csg* gene clusters code for curli fibers and those clusters include two operons whose transcription is divergent; one operon encodes the *csgA*, *csgB* and *csgC* genes, while the other encodes *csgD*, *csgE*, *csgF*, and *csgG*. That might explain the difference in level and direction of expression obtained in this work (Hammar, 1996). Besides, results showed that media composition has a dramatic effect on timing and level of upregulation for those genes. The dramatic upregulation at 24 h for both media might indicate that this structure is a 3D mature biofilm and cells are on their initiation or through the detachment stage.

Relative expression of *fli*S with 6 h showed downregulation at 12 h, 24 h, and 48 h. There was a high significant upregulation at 24 h relative to 12 h in AB broth, while on LB it was slightly upregulated at the same time-point then dramatically downregulated. According to Fig 3.7, *fli*S has the highest level of expression at 6 h and 24 h (low Cq value). This might also suggest that those time-points with upregulations represent mature biofilms and cells are preparing for or at the detachment stage, as *fli*S has been reported to be indispensable for flagellation in *E. coli* and plays a significant role in motility (Kawagishi et al., 1992; Juhas et al., 2014).

Barrios et al. (2006) found that AI-2 induces biofilm formation in *E. coli*, increased biofilm thickness and mass, and minimized interstitial space between microcolonies. He also wrote that adding AI-2 increased biofilm biomass produced by *E. coli* up to 30-fold. Our findings in this research matched with Barrios et al. (2006) results as biofilm mass was the highest during LuxS upregulations (Fig 3.7).

As stated earlier, *mot*A and *mot*B are required for rotation of the flagellar motor, which is operated by H^+ ions gradient across the cytoplasmic membrane in *E. coli* (Sowa et al., 2014). There was upregulation for both at 6 h and 24 h in LB broth, which is consistent with biofilm level and with *fli*S as they all contribute to motility. Thus, in AB medium, the *mot*A was continuously expressed throughout growth during biofilm development. This was distinct only in AB broth, and this criterion might need further studies to get more knowledge about biofilms in poor media. It is not clear why there was no significant change in *mot*A expression level among 12 h, 24 h, and 48 h in AB, nor between 24 h and 48 h for *mot*B. However, this could be related to H^+ in the minimal media which is comprised mostly of salts.

As reported by Kjeldsen et al. (2014), analysis of $bla_{\text{CTX-M-1}}$ mRNA levels at different cefotaxime concentrations in antibiotic-resistant *E. coli* showed increased $bla_{\text{CTX-M-1}}$ expression when cefotaxime was present, and the expression of $bla_{\text{CTX-M-1}}$ was cefotaxime concentration-dependent regardless of the growth phase. Based on that, over time expression decrease in both media might be due to the lack of cefotaxime or any related antibiotic(s) that might trigger the upregulation of the gene of resistance.

crr showed a significant sequential up and down-regulation through the biofilm formation time-points and in both media. The upregulation timing at 6 h and 24 h synchronized with the peak of biofilm level clearly illustrates its role as being part of the phosphoenolpyruvate-dependent sugar phosphotransferase system, as many studies showed the role of this system in sugar transport, sugar phosphorylation, bacterial virulence, and biofilm formation (Saier Jr, 2015; Horng, 2018; Lazazzera, 2010).

*mdo*H expression was in the level of upregulation at 6 h and 24 h. This gene has been reported to be upregulated during biofilm formation (De Souza et al., 2004). This gene is involved in the biosynthesis of a protein called osmoregulated periplasmic glucan (OPG). OPG is required in the pathway of osmoregulated periplasmic glucan (OPG) biosynthesis, which is part of Glycan metabolism (UniProtKB, 2019a). Thus, these results might indicate that those time-points mentioned above and obtained from crystal violet assay represent real biofilm matrix.

Along with *crr* and *mdo*H expression, *tol*B also showed a zig-zag relative expression at 6 h and 24 h upregulation, at the peak of formed biofilm. *tol*B is part of the Tol-pal gene cluster which codes for seven genes. This gene cluster's encoded proteins seem to participate in

supporting the cell envelope integrity, but the precise task of the proteins in the cluster is still ambiguous. Mutation in this gene cluster yields a membrane with leaky functions, defects in cell division, and sensitivity to detergents and antibiotics (Lazzaroni et al, 1999; Vinés et al, 2005; Llamas et al, 2000) Accordingly, upregulation of this gene at those time-points might show the importance of maintaining cell integrity during biofilm maturation, as the cell is going to be released to the outside environment where it cannot be protected anymore by the biofilm layer. The same might apply for *yieO*, which is proposed to be a multidrug transporter gene (Kvist et al., 2008), as it also showed a zig-zag relative expression at 6 h and 24 h upregulation.

In summary, gene expression of biofilm-related and quorum sensing genes' results showed some synchronisation with the peaks in both media under the four different time-points, that is, the variation in the biofilm development correlates with the variation of related gene expression. (Fig 3.7 through 3.9).

The significance of this study comes as it illustrates not only genes that are expressed during biofilm formation but also shows their level of expression at different time-points. This might give more insights into the biofilm molecular biology which, in turn, might aid in finding a more efficient alternative medicine to treat biofilm-related infections or designing new drugs that target a specific time-point where the specific gene is upregulated or downregulated, a gene (or genes) whose expression plays a critical role in the biofilm formation process.

Chapter 4:

Effect of Manuka honey on biofilm forming related gene expression in *E. coli* CTX-M-15

4.1 Introduction

In this chapter, three types of Manuka honey (two from the same brand but differing in UMF and one from another brand) were tested for their antibacterial activity. Minimal inhibitory concentration (MIC), minimal biocidal concentration (MBC), and minimum biofilm elimination concentration (MBEC) were performed in order to determine the minimal concentration of the selected type that inhibit, stop the growth, and eliminate biofilm of the tested *E. coli* CTX-M-15 in AB broth respectively, as this broth mimics its natural environment as noted earlier (section 2.4).

There are not enough studies addressing Manuka honey and its effect on bacterial gene expression, especially in relation to biofilm and antibiotic-resistant genes. Therefore, this work focuses mainly on how Manuka honey affects the expression of genes associated with biofilm formation on specifically selected virulence genes that are related to biofilm formation, AI-2 controlled genes, and the gene responsible for the antibiotic-resistance $bla_{\text{CTX-M-15}}$ in the previously selected *E. coli* CTX-M-15. This might give an insight into the preferred target gene(s) for Manuka honey and, in turn, might aid in improving the best treatment and a better way to deliver it.

4.1.1 Aims and Objectives

Aim

The aim of this research was to test the antibacterial and antibiofilm ability of Manuka honey and to find out its effect on the level of gene expression of selected biofilm-related, quorum-sensing-controlled, and antibiotic-resistant genes in *E. coli* CTX-M-15.

Objectives

- to test the antibacterial activity of three different Manuka honey types by measuring their zone of inhibition with *E. coli* CTX-M-15
- to determine the MIC, MBC, and MBEC of the selected Manuka honey type
- to measure the gene expression level of biofilm related genes, AI-2 controlled genes, and $bla_{\text{CTX-M-15}}$ using the qPCR technique

4.2 Materials and methods

4.2.1 Antibacterial activity of Manuka honey

Three types of undiluted Manuka honey were tested for their antibacterial activity against *E. coli* CTX-M-15, two belonged to the same brand (Manuka Pharm®) but with different UMF and the other one belonged to a different brand (Steens™), using agar well diffusion assay and according to Boorn et al., 2010. Manuka Pharm® 24+ UMF and Manuka Pharm® 20+ UMF were purchased from Leicestershire, UK, while Steens™ Raw 24+ UMF Manuka honey was ordered online from New Zealand. 24+ UMF contained approximately 1122 mg/kg MGO (Steenshoney.com, 2019), while 20+ UMF contained approximately 829 mg/kg MGO (Wallace et al., 2010). Briefly, MHA plates were prepared and inoculated with 0.5 McFarland bacterial suspension (Absorbance was measured at 625 nm and ranged between 0.08 and 0.13) from overnight-grown *E. coli* CTX-M-15 in NB, and a sterile cork borer of 6 mm was used to make wells on each plate by completely removing the plug of agar right down to the plastic petri dish. 120 µl undiluted Manuka honey (which is the entire well size) was poured into each well to completely fill the entire well size, and the entire group was incubated overnight at 37°C. After incubation, the zone of inhibition was measured and recorded. This assay was performed in triplicate.

4.2.2 Minimum inhibitory concentration of Manuka honey

This was done using the microbroth dilution assay (% w/v) and according to Qamar et al., 2018 with modifications. A loopful of *E. coli* CTX-M-15 colonies was inoculated into 5 ml

of LB and incubated overnight at 37°C in a static incubator. After incubation, cultures were adjusted to achieve 0.5 McFarland in AB medium (to mimic the natural site of *E. coli* CTX-M-15 infection, section 2.4), then further diluted 1:100 with AB broth to achieve 1×10^5 colony forming units (CFU)/ml. Serial dilutions of Steens Manuka honey were prepared in a sterile AB broth as a diluent to maintain ingredients concentrations. A 1 g/ml stock solution of Steens Manuka honey (50 %) was created. Serial dilutions in triplicates of the following concentrations (45, 40, 35, 30, 25, 20, 15, 10, 9, 8, 7, 6, 5, 4, 3, 2, and 1 %) were created using AB broth. 100 µl of each of the Manuka honey dilution was added in 96 wells, flat bottom microtiter plate (Thermo Fisher Scientific), and 100 µl of the previously diluted bacterial suspension was added into each well for the above dilutions. Positive control contained AB broth with bacterial suspension and negative control contained only AB broth. All procedures were done in three biological replicates, and each biological replicate consisted of three technical replicates. The microtiter plate was incubated at 37°C for 24 h, after incubation, the MIC was calculated by comparison of each well with the positive and the negative controls wells by monitoring each well for having turbidity or being a clear using naked eye.

4.2.3 Minimum bactericidal concentration (MBC)

Minimum bactericidal concentration (% w/v) was performed to determine the lowest concentration of Manuka honey required to kill the antibiotic-resistant *E. coli* CTX-M-15. It is the first dilution with no growth on an agar plate (Sykes and Rankin, 2013). A 10 µl sample from microtiter plate wells of no visible growth was taken and plated on a nutrient agar plate

and incubated at 37 ^{0}C for 24 h. After incubation, plates were examined, and any colony developed was scored as bacterial growth while no colonies developed was scored as no bacterial growth. All procedures were done in three biological replicates, and each biological replicate consisted of three technical replicates.

4.2.4 Minimum biofilm elimination concentration (MBEC)

In order to determine the lowest concentration of Manuka honey required to inhibit the formation of biofilm of the antibiotic-resistant *E. coli* CTX-M-15, the minimum biofilm elimination concentration was determined using the micro broth dilution method (% w/v) and according to Camplin and Maddocks (2014) with modifications. A loopful of *E. coli* CTX-M-15 colonies was inoculated into 5 ml of LB and incubated overnight at 37°C in a static incubator. After incubation, cultures were diluted to an OD_{600} of 0.01 in AB medium. Serial dilutions of Steens Manuka honey were prepared in a sterile AB broth as a diluent with positive controls (AB broth with bacterial suspension) and negative controls (only AB broth). Microtiter plates were prepared and incubated at 37°C for 24 h. After incubation, the broth was carefully drawn, and the wells were washed three times using a sterile PBS. Bacteria in wells were fixed by adding 200 µl of 99 % methanol for 15 min, then discarded and left to dry in an inverted position for 30 min at room temperature. 200 µl of 2 % crystal violet was used to stain each well for 5 min at room temperature. Excess stain was rinsed with sterilized distilled water. The remaining dye was re-solubilized with 160 µl of 33 % glacial acetic acid and left at room temperature for 30 min. Finally, optical density (OD_{570}) for each well was measured using SpectraMax Plus 384 Spectrophotometer (Molecular Devices LLC). This

experiment was performed with three biological replicates, and each biological replicate consisted of three technical replicates.

4.2.5 Biofilm formation assay using AB broth with 2 % Manuka honey

2 % w/v of Steens Manuka honey was used to test the antibiofilm activity against *E. coli* CTX-M-15 grown in 6 wells TCPs in AB broth as, at this concentration, there is still a biofilm that can be produced and a significant difference in gene expression could be noticed, as there was a significant difference in biofilm produced after addition of 2 % Manuka honey compared with the biofilm without Manuka. The procedure was carried out as previously mentioned in 2.2.8 with the addition of 2 % w/v of Manuka honey and for three biological replicates. OD_{570} for each well was measured using Helios Gamma UV-Vis spectrophotometer and compared to the one grown on AB broth TCPs.

4.2.6 Gene expression analysis on the effect of Manuka honey on the expression of biofilm-forming genes and AI-2 controlled genes

4.2.6.1 RNA isolation and cDNA synthesis

In order to compare the gene expressions between Manuka-treated and untreated samples, *E. coli* CTX-M-15 was inoculated twice into 20 ml of AB broth, once with 2 % Manuka honey and once with AB broth alone and according to the protocol of Wasfi et al. (2016) with

modifications. A volume of 20 ml of Manuka honey was prepared in AB broth at a sub-inhibitory concentration (2 %) in Corning 50 ml centrifuge tubes (Sigma-Aldrich). An overnight culture of *E. coli* CTX-M-15 grown on LB was diluted 1:100 and grown on LB to mid-exponential phase. 500 µl of this culture was used to inoculate the 20 ml of Manuka honey solution and the AB broth and incubated at 37°C with shaking at 70 rpm for 3 h. After incubation, tubes were centrifuged at 10000 x g for 10 min and supernatant was decanted by pulling it using a pipette and keeping 2 ml of supernatant to maintain cell viability and not to degrade their RNA by adding the 2 volumes of RNAprotect Bacteria Reagent (Qiagen), vortexed immediately for 5 s, and incubated for 5 min at room temperature. The mixture was pelleted by centrifugation at 10000 x g for 10 min, supernatant was decanted, and pellets were stored for a short period at -15°C awaiting RNA extraction.

4.2.6.2 RNA extraction using Qiagen RNeasy Mini Kit

RNA extraction was performed as previously mentioned in 3.2.2 and 3.2.3.

4.2.6.3 Conversion of RNA to complementary DNA (cDNA)

Conversion of RNA to cDNA was performed as previously mentioned in 3.2.4.

4.2.7 Quantitative real-time PCR

The qPCR analysis was conducted using the Thermo Scientific™ PikoReal™ Real-Time PCR System. Reaction volumes and amplification conditions were the same as previously

mentioned in 3.2.7. No-template control and no-reverse transcriptase control were included. For each sample (treated and untreated), three technical replicates were used. All primer pairs' amplification efficiency was evaluated using tenfold dilutions of pooled cDNA. Analysis followed MIQE guidelines (Bustin et al., 2009).

4.2.7.1 No-reverse transcriptase

A no-reverse transcriptase control was used in triplicate for each of the treated and untreated sample by using the eluted pure RNA after the DNase treatment step without conversion into cDNA.

4.2.7.2 Validation of the reference genes

As mentioned in 3.2.9, 16s rRNA was chosen for potential stability as a reference gene by running qPCR for the treated and untreated in triplicate for each. A change in Ct value among the selected stages of less than 0.5 was accepted (Reid, 2018).

4.2.8 Data analysis using the relative standard curve method

The untreated growth was used as the calibration sample to calculate the expression of the selected biofilm forming genes and AI-2 controlled genes in AB broth. The X-fold change in the level of transcription was calculated using the relative standard curve method. Standard curves were made for both target and reference genes. Data were analysed using equations

from Pikoreal software user manual (Thermo Scientific) that were put into an excel sheet, and calculations for each gene studied were performed.

4.3 Results

4.3.1 Antibacterial activity of Manuka honey

This test was performed to determine the antibacterial activity of each of the tested Manuka honey brands by measuring the diameter of its inhibition zone. As expected, Manuka with UMF of +24 gave a significantly higher inhibition zone than the one of +20 (p-value <0.01). Steens +24 gave a noticeably higher inhibition zone than Manuka Pharm +24 (p-value <0.01). Table 4.1 below shows the mean values of the inhibition zone for the three brands.

Table 4.1 Inhibition zone of Manuka honey measured in millimetres. Numbers in the inhibition zone column represent the mean values of triplicates ± standard deviation of the mean.

Manuka brands	Inhibition zone
Manuka Pharm +20	11.6 ± 0.12
Manuka Pharm +24	14.4 ± 0.06
Steens +24	20.5 ± 0.1

4.3.2 Minimum inhibitory, bactericidal, and biofilm elimination concentration of Manuka honey

Those tests (MIC, MBC, and MBEC) were performed to determine the minimal concentration of the selected Manuka honey required to cease the growth, kill, and eliminate biofilm of *E. coli* CTX-M-15, respectively. Manuka honey Steens +24 was used to measure the tests above as it gave the highest inhibition zone. To calculate the results, the mode was applied. Results showed that the MIC was at Manuka concentration of 6 %, where no well showed any turbidity. The MBC was at the concentration of 8 %, at which no growth showed on any of the nine agar plates. The MBEC, according to the absorbency measurements, was the well with 5 % concentration of Manuka honey, where there was no statistical difference in OD_{570} values with the control wells (p-value < 0.01). Table 4.2 show the results for MBC.

Table 4.2 MBC data for Manuka honey on *E. coli* CTX-M-15. Three biological replicates were done with three technical replicates for each. N, no growth. G, growth.

	Replicate	Biological 1	Biological 2	Biological 3	
8 %	1	**G**	**N**	**N**	MBC
	2	**N**	**N**	**N**	
	3	**N**	**N**	**N**	
7 %	1	**G**	**N**	**N**	
	2	**N**	**G**	**G**	
	3	**G**	**N**	**G**	
6 %	1	**G**	**G**	**G**	
	2	**G**	**G**	**G**	
	3	**G**	**G**	**G**	

4.3.3 Biofilm formation assay using AB broth with 2 % Manuka honey

MBEC results in section 4.3.2 showed that below 5 % Manuka honey there is still some amount of biofilm that can be detected, and results in Fig 4.1 showed that treatment with 2 % Manuka honey led to a significant fold decrease in biofilm density (Table 4.3). Therefore, to study the molecular mechanism of Manuka honey and its effect on the selected gene expression, 2 % was adopted for this purpose. Fig 4.1 below illustrates the difference in biofilm density for the four time-points with and without Manuka treatment (2 %).

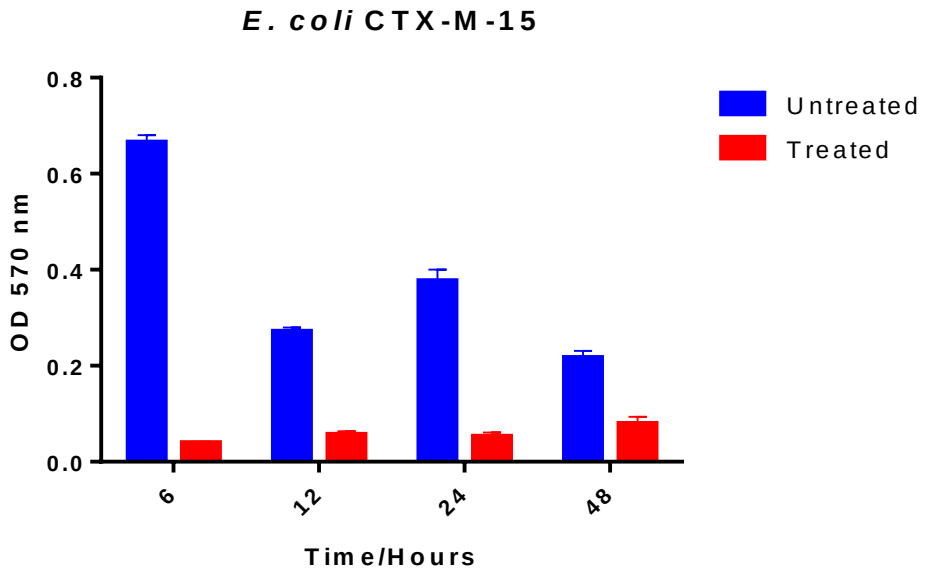

Fig 4.1 The significant reduction (p-value < 0.01) in biofilm formation after treatment of *E. coli* CTX-M-15 with 2 % Manuka honey. The graph shows the density of measured biofilm using OD_{570} for *E. coli* CTX-M-15 grown in AB broth treated with 2 % Manuka (red columns) and untreated (blue columns). Error bars represent the standard deviation of the mean.

Table 4.3 The significant fold decrease in biofilm density in comparison between the 2 % Manuka honey treated and untreated *E. coli* CTX-M-15

Time/Hours	Approximate number of fold reduction
6	17
12	5
24	7
48	3

4.3.4 RNA integrity and stability

As previously illustrated in 3.3.1, extracted RNA samples from treated and untreated AB broth were run on agarose gel, and the sample that showed intense bands of 16S and 23S rRNA indicated that the RNA in that sample was intact and not degraded. Also, the extracted RNA from both broths showed satisfactory quality and quantity.

4.3.5 Primers efficiencies

The efficiency values for primers used for the gene expression analysis in this chapter ranged from ~95 % to ~107 %, which was within the range mentioned in 3.2.6 (80-120 %). (Table 4.4).

Table 4.4 The primers' efficiencies used in the qPCR study. Serial dilutions of amplicons used to calculate the efficiencies. An efficiency of 80-120 % was accepted.

Gene	Efficiency (%)
16s	107.953
crl	96.887
crr	96.418
csgB	103.256
*csg*E	102.052
*csg*F	107.567
$bla_{\text{CTX-M}}$	97.939
*fim*A	99.546
*fli*L	98.021
fliS	99.581
luxS	101.897
motA	96.907
motB	101.912
*nlp*C	96.012
*rfa*H	99.605
*tol*B	97.613
*yie*O	95.009

4.3.6 Expression levels of Manuka-treated and untreated *E. coli* CTX-M-15 virulence, AI-2 controlled, and antibiotic-resistance genes

The expression level of 16 of the selected genes in both Manuka-treated and untreated AB broth were compared using the Ct values which showed significant differences among all genes in the comparison between treated and untreated. The mean Ct values for untreated AB broth ranged from 13.20 to 26.06, while for 2 % Manuka-treated ranged from 15.55 to 26.38. The standard deviation of Ct values for each gene and for both treated and untreated was less than 0.5.

Fig 4.2 shows the average Cq values as a measure of expression for these 17 genes for treated and untreated *E. coli* CTX-M-15. As can be seen clearly in this figure, treatment with 2 % Manuka caused a significant change (p-value < 0.05) in Cq values, either increasing or decreasing, which indicates a decrease and increase in gene expression, sequentially.

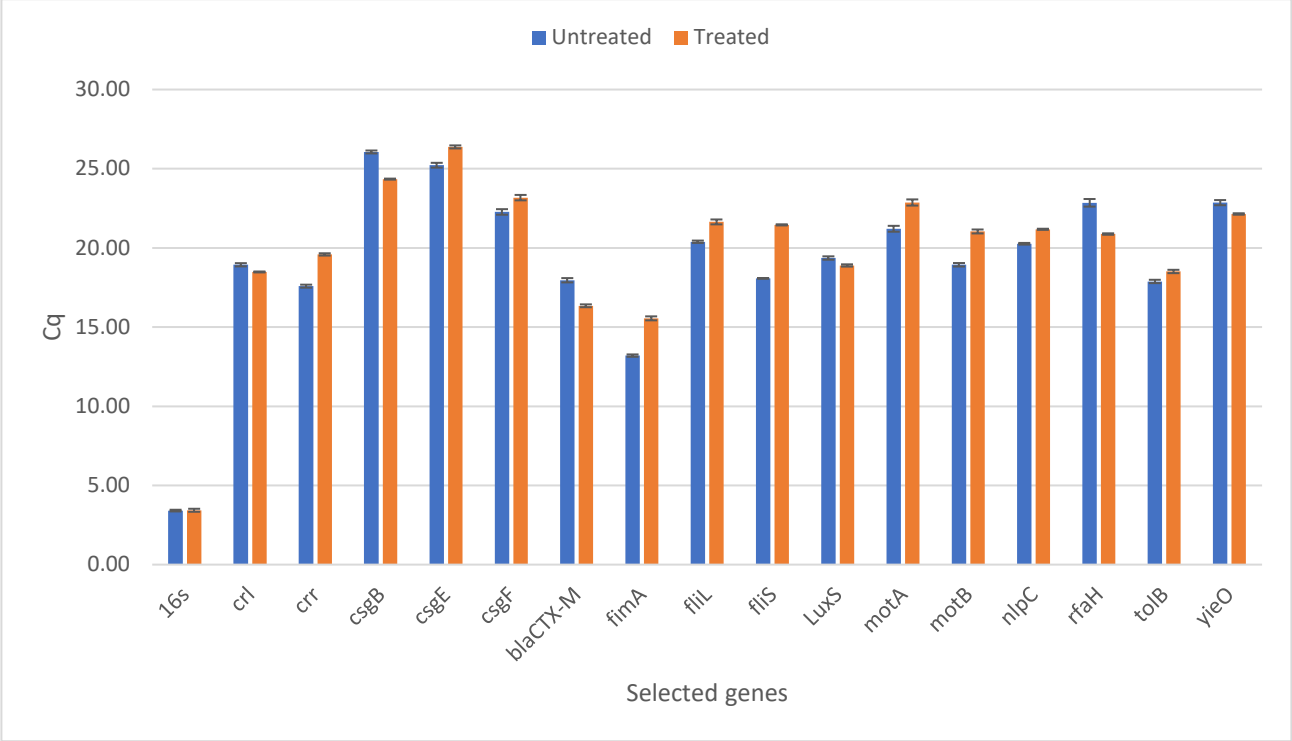

Fig 4.2 The comparison between the Cq values of Manuka-treated and untreated *E. coli* CTX-M-15 selected genes that represent the copy number of the target gene as measured by RT-qPCR. High Cq value indicates a low copy number of the gene, while the low Cq value indicates a high copy number of the gene. Manuka honey upregulated some genes (decreased their Cq value) and downregulated others (increased their Cq values). The experiment was done in three technical replicates, and data represent the means of those technical replicates. Error bars represent the standard deviation of the triplicates. (p-value < 0.05).

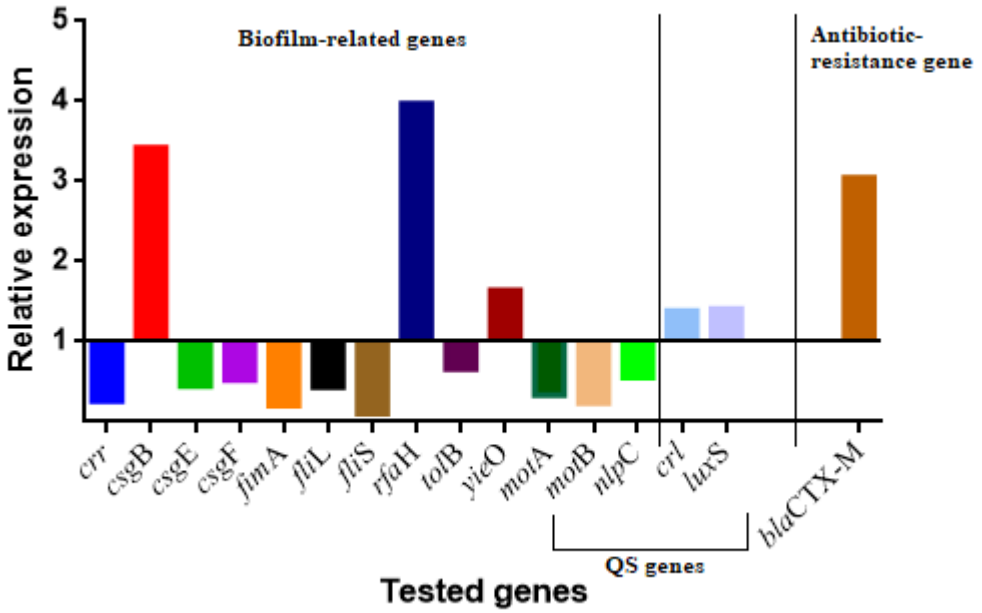

Fig 4.3 Bar chart shows the expression fold change (upregulation and downregulation) of the selected virulence genes, antibiotic-resistant gene, and AI-2 related genes in *E. coli* CTX-M-15 after treatment with 2 % Manuka in AB broth. The expression's fold change results were normalized against the reference gene 16s rRNA and then were taken away from one to show the genes were upregulated and downregulated.

Table 4.5 Fold change in mRNA level of the selected virulence genes, antibiotic-resistant gene, and AI-2 related genes in *E. coli* CTX-M-15 after treatment with 2 % Manuka in AB broth. REF indicates reference gene. TRG indicates target gene; downward arrows indicate significantly decreased gene expression and upward arrows indicate significantly increased gene expression when *P*-value <0.05 (target sample differ to control).

Gene	2 % Manuka
16s (the reference gene)	1
crl (Sigma factor-binding protein)	1.38↑
crr (D-glucosamine phosphotransferase system permease activity)	0.26↓
*csg*B (Curlin nucleator protein)	3.42↑
*csg*E (Predicted transport protein)	0.45↓
*csg*F (Predicted transport protein)	0.52↓
$bla_{\text{CTX-M}}$ (β-lactam resistance)	3.05↑
*fim*A (a major Type 1 subunit fimbrin)	0.20↓
*fli*L (Flagellar biosynthesis protein)	0.43↓
*fli*S (Flagellar protein potentiates polymerization)	0.10↓
*Lux*S (AI-2 synthase)	1.41↑
*mot*A (Proton conductor component of flagella motor)	0.33↓
*mot*B (Protein that rotates flagellar motor)	0.23↓
*nlp*C (Lipoprotein)	0.55↓
*rfa*H (DNA-binding transcriptional antiterminator)	3.97↑
*tol*B (Periplasmic protein)	0.66↓
*yie*O (Predicted homocysteine or multidrug efflux system)	1.64↑

As shown in Fig 4.3 and Table 4.5, 2 % Manuka honey caused a significant downregulation (p-value < 0.05) in expression for the genes *crr*, *csg*E, *csg*F, *fim*A, *fli*L, *fliS*, *motA*, *motB*, *nlp*C, and *tol*B, while *crl*, *csgB*, $bla_{\text{CTX-M}}$, *luxS*, *rfa*H, and *yie*O were significantly upregulated (p-value < 0.05).

4.4 Discussion

This work investigated the robust effect of Manuka honey by elucidating its inhibitory, biocidal, biofilm inhibition activity, and its mechanism of action against specific genes related to biofilm formation of *E. coli* CTX-M-15, the most prevalent antibiotic-resistant strains in the UK related to UTIs, and tried to find a good alternative for the current global issue of antibiotic resistance by testing the activity of Manuka honey concerning its inhibitory, biocidal, antibiofilm, and molecular mechanism effect on gene expression. This is the first study to detect the effect of Manuka honey on the antibiotic-resistant *E. coli* CTX-M-15 that represents a rapidly evolving issue in the UK (Woodford et al., 2004).

Many studies showed that plenty of genes are involved in biofilm formation and quorum-sensing in UPEC. Hence, downregulating these genes' expression could add to the efficiency of antibiotic treatment and could reduce the likelihood of treatment failure (Wasfi et al., 2016). Three brands of Manuka honey were tested for their antibacterial activity using the agar well diffusion method.

In this work, Steens™ Raw 24+ showed a significantly higher inhibition zone than Manuka Pharm® 24+, though both have the same UMF. Kwakman et al. (2011) showed that, after

neutralization of its MGO, the antimicrobial activity of Manuka honey against *Staphylococcus aureus* was reduced to a level of a honey-equivalent sugar solution. This indicated that MGO was responsible for Manuka's honey potent antibacterial activity against *Staphylococcus aureus*. Moreover, they showed that 2-fold higher concentrations of MGO neutralized manuka honey was required to kill *P. aeruginosa,* while against *E. coli* the Manuka's honey activity was not affected by neutralization of its MGO. The researchers deduced that MGO is not fully responsible for Manuka honey's non-peroxide antimicrobial activity, and it might be due to polyphenols or other components. This might explain why Steens™ Raw 24+ gave a significantly higher inhibition than Manuka Pharm® 24+, though both have the same UMF. Another study done by Lu et al. (2013 and 2014), who worked on many types of honey (including Manuka honey, alone and blended), and found that Manuka with the lowest MGO had the highest antibacterial activity against *E. coli*, *Bacillus subtilis*, and *S. aureus*, also confirmed the above conclusion. Paramasivan et al. (2014) reported that honeys from different geographical and floral sources show different effectiveness in antimicrobial activity even if they contain the same level of MGO, and this might be due to their differences in phenolic content. Results of this study were close to another study done by Idris and Afegbua (2017), which utilized the effect of Manuka honey on four ESBL *E. coli* different isolates which showed a mean zone of inhibition range between 16 and 18.4 mm.

In this research, MIC, MBC, and MBEC were performed using AB broth. The reason was to measure the effect of Manuka honey antibacterial activity against the tested antibiotic-resistant strain in a media mimicking its natural site of infection in which there is a low

concentration of nutrients. Besides, AB broth was pre-selected to perform the following experiments regarding the gene expression analysis and the comparison of biofilm with and without Manuka honey for the tested strain. Despite the difference in media composition, MIC results of this study, which was 6 % w/v, were highly similar to another study done by Anand et al. (2019), who performed MIC test on Mueller Hinton Broth (MHB), and the result on *E. coli* was 6.25 % w/v, while the MBC result of this study, which was 8 %, did not match with the study mentioned above, in which the MBC was 12.5 %. This could be due to the nutrient content of MHB, which is more enriched compared to AB which, in turn, might give much growth support (Mast group, 2019), or the difference in Manuka's antimicrobial contents.

MBEC results showed that biofilm formation was eliminated at a concentration of 5 % of Manuka honey. To study the effect of Manuka honey of genetic expression for the genes related to biofilm formation, a concentration of 2 % (less than 5 %, which can significantly reduce biofilm formation but not eliminate it), was selected for further analysis.

Several genes have been shown to play a role in *E. coli* virulence related to biofilm formation, and some are controlled by a quorum-sensing mechanism. Therefore, modulating the level of expression of those genes might add to the efficacy of antimicrobial therapy. Because of this, 12 genes related to biofilm formation, three genes related to and controlled by a quorum-sensing mechanism, and one gene responsible for the antimicrobial resistance in *E. coli* CTX-M-15 were selected, and their differential gene expression profiles in response to exposure to 2 % Manuka honey were determined using qPCR.

Many genes which were selected in this work (*crr*, *csg*B, *csg*E, *csg*F, *fim*A, *fli*L, *fli*S, *mot*A, *mot*B, *nlp*C, *rfa*H, *tol*B, and *yie*O) have been shown to be involved in the biofilm formation process in *E. coli* (Niba et al., 2007). Results from Table 3.3 and Fig 3.7 showed those genes were upregulated during biofilm formation. Current results show that *crr*, *csg*E, *csg*F, *fim*A, *fli*L, *fli*S, motA, motB, nlpC, and *tol*B were downregulated after 2 % Manuka honey treatment, whereas *csg*B, *rfa*H, and *yie*O were upregulated.

crl codes for a protein that binds to σs/RpoS, a sigma factor for stress response (Cavaliere and Norel, 2016). Since Manuka honey has been reported to display its antimicrobial effect through imposing high osmolarity to the microbial environment by its high sugar content to hinder the microbial growth (Mandal and Mandal, 2011), and since high osmolarity is a burden for microbial cells that drive their stress responses mechanisms of action (Moat et al., 2003), stress response genes would therefore be switched on to cope with this environmental stress. Results showed an upregulation of *crl* after Manuka honey treatment, and this might confirm its vital role in stress response.

Among the tested *csg* gene cluster, results showed that *csg*B has been upregulated, while the other tested genes *csg*E and *csg*F were downregulated. As mentioned before, both *csg*E and *csg*F are in one operon while *csg*B is in another operon, and each are regulated independently (Hammar et al., 1996; Barnhart and Chapman, 2006). Arnqvist et al. (1992) reported that *crl* stimulates transcription of *csg*BA operon through its promoter, and results of this work showed the upregulation of *csg*B, along with the upregulation of *crl*. Thus, results of this study agreed with those of Arnqvist et al., and that might explain the upregulation of *csg*B but not *csg*E and *csg*F.

Environmental factors, like osmolarity and pH, influence *lux*S expression (Delisa et al., 2001; Jeon et al., 2005). As stated above, Manuka honey imposes high osmolarity due to its sugar content. This might explain the upregulation of *lux*S after 2 % Manuka treatment. Besides, *crl*, which is controlled by AI-2, was also upregulated as stated above. This might elucidate the up-regulatory effect of stress conditions on specific co-related genes' expressions.

*rfa*H has been shown to repress biofilm formation by reduction of antigen 43 (Ag43) level. Ag43 mediated auto aggregation and biofilm formation, and it is encoded by *flu*, and *rfa*H has been shown to indirectly downregulate the expression of *flu* (Beloin et al., 2006). In these results, treatment with 2 % Manuka upregulated the expression of *rfa*H.

*yie*O is a multidrug transporter gene and was shown to be upregulated along with other multidrug transporter and stress-related genes in a study done by Kvist et al. (2008) during biofilm formation, and the same study reported that the biofilm formation process exerts hard pressure on the cells due to the intracellular stress conditions. There is no available study confirming the exact function of its protein. In the previous results chapter, *yieO* was upregulated during the anabolic stage of biofilm (the peak). In this chapter, *yie*O was upregulated after treatment with 2 % Manuka honey. Thus, stress imposed by Manuka honey and probably the osmotic stress which induced stress-related genes could explain the upregulation of *yie*O. Multidrug efflux systems were reported to show abilities to transport various structurally unrelated drugs and other compounds and thus aid in drug resistance (Hayashi et al., 2014; Andersen et al., 2015). *yie*O belongs to the major facilitator super family with a transmembrane transport activity under the multidrug efflux system (UniProtKB, 2019d). Despite being specific to antibiotics, most efflux pumps are multidrug

transporters which can pump a wide range of unrelated compounds and hence, significantly contribute to multidrug resistance (Yilmaz et al., 2014; Andersen et al., 2015).

Although there was no cefotaxime nor any related antibiotic added to the medium, qPCR results showed the upregulation of *bla*$_{\text{CTX-M}}$, the gene of resistance, after 2 % Manuka treatment. Brudzynski and Sjaarda (2014) have examined the effects of Canadian honeys on ampicillin-resistant and ampicillin-sensitive *E. coli* strains. Results showed that both strains were sensitive to honey and displayed the same level of cell shape change, cytotoxicity, and endotoxin release. They concluded that both honey and ampicillin (which is a β–lactam antibiotic) induced similar structural changes to LPS and cell wall, and that this ability underlies antibacterial activities of both agents. Those effects resembled the action of β-lactam antibiotics. So, in this study, Manuka honey might produce similar action as Canadian honeys by targeting the bacterial cell wall and, accordingly, upregulate *bla*$_{\text{CTX-M}}$ expression in an attempt for the latter to overcome the damaging effect on cell wall. However, another study done on *P. aeruginosa* exploring the effect of Manuka honey on its structure showed that cells were lysed, and SEM images showed short cells with cell surface abnormalities (Henriques et al., 2011). According to Brudzynski and Sjaarda's explanation, Manuka and Canadian honeys have different cellular targets, and the Canadian honeys killed *P. aeruginosa* in a shorter time than Manuka did in the Henriques et al. study. In contrast to Brudzynski and Sjaarda's findings, the upregulation of *bla*$_{\text{CTX-M}}$ up to three folds might support the idea that Manuka's mechanism of action could resemble the one of β-lactam antibiotics, bearing in mind that the previous studies used different bacterial genera.

Nevertheless, more research on this topic needs to be undertaken before the association between *bla*$_{CTX-M}$ upregulation and Manuka treatment is more clearly understood.

Another explanation for *bla*$_{CTX-M}$ upregulation is the effect of osmotic stress induced by Manuka's high sugar content. Antibiotic resistance genes were evolved from genes having other functions and roles, and genes coding for multidrug resistance (MDR) transport proteins are among them (Cohen, 2014). In the responses to hyperosmotic stress, general stress regulators in *E. coli* such as RpoS and regulators of quorum-sensing collaborate and promote the overexpression of MDR transporters (Yang et al., 2006). Based on this, the above-mentioned factors promoting expression of MDR transporters might still be involved in *bla*$_{CTX-M}$ expression and upregulation.

What was noticeable in this study is that *mot*B which is under AI-2 control which has a role in biofilm formation (Delisa et al., 2001; Niba et al., 2007) was downregulated after 2 % Manuka honey treatment, thought *lux*S was upregulated. This might indicate that Manuka honey targets the biofilm-related genes. Thus, the current qPCR findings may suggest that the tested Manuka honey can prevent or disrupt *E. coli* CTX-M-15 biofilm. Our experimental results bear a close resemblance to those of Wasfi et al. (2016), who tested three types of honeys, and stated that all the tested honeys repressed biofilm-promoting genes and activated the expression of biofilm repressor genes.

In summary, by comparing OD_{570} values between the treated and untreated *E. coli* CTX-M-15, 2 % Manuka honey-treated cells showed a dramatic reduction of biofilm density. The obtained Cq values from the qPCR reaction of both treated and untreated samples clearly demonstrated that biofilm-related genes were downregulated. Accordingly, the antibiofilm

activity of Manuka honey might be due to its selective targeted actions against biofilm genes. Therefore, Manuka honey could be an effective alternative solution for the global issue of antibiotic-resistance and biofilm eradication.

Chapter 5:

Overall Discussion and Conclusion

This work has demonstrated how biofilm density can be changed over four selected time-points for two types of antibiotic-resistant bacterial species, *E. coli* and *K. pneumoniae*, compared with their wild-type species. The biofilms were found in higher densities in antibiotic-resistant strains than in non-resistant strains, which could be the reason why those strains have developed resistance as a biofilm confers resistance or tolerance. In addition, biofilm is a field where bacteria can exchange their genetic materials including resistance traits (Tenover, 2006).

E. coli CTX-M-15 showed a variable ability to form a biofilm over the four time-points in the different media, which indicates its ability to adapt to many environmental conditions. This might explain why it is the most abundant UTI-causing strain in the UK (Hall and Mah, 2017; Gebreyohannes et al., 2019). qPCR data showed that gene expression is correlated with biofilm development for both media, which means that *E. coli* CTX-M-15 can adapt to any environmental condition. This has created an urgent need to search for suitable antimicrobial therapy; hence, Manuka honey was suggested and tested for its antimicrobial and antibiofilm ability as it has not been tested against this antibiotic-resistant strain.

Chapter 6:

Future work

Further work should include the examination of *E. coli* CTX-M-15 biofilm during the four time-points using a scanning electron microscope or confocal microscope to detect and exactly identify the biofilm stages during the four time-points regarding initial attachment, microcolony formation, biofilm maturation, and dispersion. Above all, this should give a better picture of any cellular damage imposed by Manuka honey.

It is also recommended that biofilm densities for antibiotic-resistant strains with other types of ESBLs, such as PER and VEB-1 and carbapenemase SME and VIM, be measured, including other families of beta-lactamases, such as inhibitor-resistant and AmpC beta-lactamases (Chaibi et al., 1999; Queenan and Bush, 2007; Jacoby, 2009; Paterson and Bonomo, 2005).

References

Abidi, S. H., Sherwani, S. K., Siddiqui, T. R., Bashir, A., & Kazmi, S. U. (2013). Drug resistance profile and biofilm forming potential of *Pseudomonas aeruginosa* isolated from contact lenses in Karachi-Pakistan. *BMC ophthalmology*, 13(1), 57.

Adams, C. J., Boult, C. H., Deadman, B. J., Farr, J. M., Grainger, M. N., Manley-Harris, M., & Snow, M. J. (2008). Isolation by HPLC and characterisation of the bioactive fraction of New Zealand manuka (Leptospermum scoparium) honey. *Carbohydrate research*, 343(4), 651-659.

Ahmed, M. N., Porse, A., Sommer, M. O. A., Høiby, N., & Ciofu, O. (2018). Evolution of antibiotic resistance in biofilm and planktonic Pseudomonas aeruginosa populations exposed to subinhibitory levels of ciprofloxacin. *Antimicrobial agents and chemotherapy*, 62(8), e00320-18.

Alba, J., Ishii, Y., Thomson, K., Moland, E. S., & Yamaguchi, K. (2005). Kinetics study of KPC-3, a plasmid-encoded class A carbapenem-hydrolyzing β-lactamase. *Antimicrobial agents and chemotherapy*, 49(11), 4760-4762.

Al-Mayahie, S. M. (2013). Phenotypic and genotypic comparison of ESBL production by vaginal Escherichia coli isolates from pregnant and non-pregnant women. *Annals of clinical microbiology and antimicrobials*, 12(1), 7.

Alsterlund, R., Carlsson, B., Gezelius, L., Haeggman, S., & Olsson-Liljequist, B. (2009). Multiresistant CTX-M-15 ESBL-producing Escherichia coli in southern Sweden: Description of an outbreak. *Scandinavian journal of infectious diseases*, 41(6-7), 410-415.

Alteri, C. J., & Mobley, H. L. (2015). Metabolism and fitness of urinary tract pathogens. *Microbiology spectrum*, 3(3).

Alvarez-Suarez, J. M., Gasparrini, M., Forbes-Hernández, T. Y., Mazzoni, L., & Giampieri, F. (2014). The composition and biological activity of honey: a focus on Manuka honey. *Foods*, 3(3), 420-432.

Ambler, R. P., Coulson, A. F., Frere, J. M., Ghuysen, J. M., Joris, B., Forsman, M., ... & Waley, S. G. (1991). A standard numbering scheme for the class A beta-lactamases. *Biochemical Journal*, 276(Pt 1), 269.

Aminov, R. I. (2010). A brief history of the antibiotic era: lessons learned and challenges for the future. *Frontiers in microbiology*, 1, 134.

Anand, S., Deighton, M., Livanos, G., Morrison, P. D., Pang, E. C., & Mantri, N. (2019). Antimicrobial activity of Agastache honey and characterization of its bioactive compounds in comparison with important commercial honeys. *Frontiers in microbiology*, 10, 263.

Andersen, J. L., He, G. X., Kakarla, P., KC, R., Kumar, S., Lakra, W. S., Mukherjee, M.M., Ranaweera, I., Shrestha, U., Tran, T. & Varela, M. F. (2015). Multidrug efflux pumps from Enterobacteriaceae, Vibrio cholerae and Staphylococcus aureus bacterial food pathogens. *International journal of environmental research and public health*, 12(2), 1487-1547.

Anderson, G. G., Dodson, K. W., Hooton, T. M., & Hultgren, S. J. (2004). Intracellular bacterial communities of uropathogenic Escherichia coli in urinary tract pathogenesis. *Trends in microbiology*, 12(9), 424-430.

Antibiotic research UK (2019). [Online] Available from: https://www.antibioticresearch.org.uk/about-antibiotic-resistance/bacterial-infections/common-bacterial-infections/?gclid=CjwKCAiAi4fwBRBxEiwAEO8_Hs2Nv48SVCqgiZcWKartCkROkZXaVnHlvCjv8Ok5PrtN_wMXyyMkyxoCEosQAvD_BwE

API20E (2010). *Identification system for Enterobacteriaceae and other non-fastidious Gram-negative rods* [Online] BioMérieux, Inc. Available from: http://biomanufacturing.org/uploads/files/587872707301898351-api20einstructions.pdf [Accessed 11/04 2016].

Arnqvist, A., Olsén, A., Pfeifer, J., Russell, D. G., & Normark, S. (1992). The Crl protein activates cryptic genes for curli formation and fibronectin binding in *Escherichia coli* HB101. *Molecular microbiology*, 6(17), 2443-2452.

Atshan, S. S., Shamsudin, M. N., Karunanidhi, A., van Belkum, A., Lung, L. T. T., Sekawi, Z., Nathan, J.J., Ling, K.H., Seng, J.S.C., Ali, A.M. & Abduljaleel, S. A. (2013). Quantitative PCR analysis of genes expressed during biofilm development of methicillin resistant Staphylococcus aureus (MRSA). Infection, genetics and evolution, 18, 106-112.

Attmannspacher, U., Scharf, B. E., & Harshey, R. M. (2008). FliL is essential for swarming: motor rotation in absence of FliL fractures the flagellar rod in swarmer cells of Salmonella enterica. *Molecular microbiology*, 68(2), 328-341.

Ayhan, N., Başbuğ, N., & Oztürk, S. (1988). Causative agents of urinary tract infections and sensitivity to antibiotics. *Mikrobiyoloji bulteni*, 22(3), 215-221.

Balestrino, D., Haagensen, J. A., Rich, C., & Forestier, C. (2005). Characterization of type 2 quorum sensing in Klebsiella pneumoniae and relationship with biofilm formation. *Journal of bacteriology*, 187(8), 2870-2880.

Barnhart, M. M., & Chapman, M. R. (2006). Curli biogenesis and function. Annu. Rev. Microbiol., 60, 131-147.

Barrios, A. F. G., Zuo, R., Hashimoto, Y., Yang, L., Bentley, W. E., & Wood, T. K. (2006). Autoinducer 2 controls biofilm formation in Escherichia coli through a novel motility quorum-sensing regulator (MqsR, B3022). Journal of bacteriology, 188(1), 305-316.

Basak, S., Rajurkar, M. N., Attal, R. O., & Mallick, S. K. (2013). Biofilms: a challenge to medical fraternity in infection control. *In Infection Control*. IntechOpen.

Bassler, B. L., & Losick, R. (2006). Bacterially speaking. *Cell*, 125(2), 237-246.

Baty, A. M., Eastburn, C. C., Diwu, Z., Techkarnjanaruk, S., Goodman, A. E., & Geesey, G. G. (2000a). Differentiation of chitinase-active and non-chitinase-active subpopulations of a marine bacterium during chitin degradation. *Appl. Environ. Microbiol*., 66(8), 3566-3573.

Baty, A. M., Eastburn, C. C., Techkarnjanaruk, S., Goodman, A. E., & Geesey, G. G. (2000b). Spatial and temporal variations in chitinolytic gene expression and bacterial biomass production during chitin degradation. *Appl. Environ. Microbiol*., 66(8), 3574-3585.

Bauernfeind, A., Schweighart, S., & Grimm, H. (1990). A new plasmidic cefotaximase in a clinical isolate of Escherichia coli. *Infection*, 18(5), 294-298.

Bauernfeind, A., Holley, M., Jungwirth, R., Mangold, P., Röhnisch, T., Schweighart, S., Wilhelm, R., Casellas, J.M. & Goldberg, M. (1992). A new plasmidic cefotaximase from patients infected with Salmonella typhimurium. *Infection*, 20(3), 158-163.

Becraft, E. D., Cohan, F. M., Kühl, M., Jensen, S. I., & Ward, D. M. (2011). Fine-scale distribution patterns of Synechococcus ecological diversity in microbial mats of Mushroom Spring, Yellowstone National Park. *Appl. Environ. Microbiol*., 77(21), 7689-7697.

Bedenic, B., Randegger, C., Boras, A., & Haechler, H. (2001). Comparison of five different methods for detection of SHV extended-spectrum β-lactamases. *Journal of chemotherapy*, 13(1), 24-33.

Bedenic, B., Vranes, J., Mihaljevic, L. J., Tonkic, M., Sviben, M., Plecko, V., & Kalenic, S. (2007). Sensitivity and specificity of various β-lactam antibiotics and phenotypical methods for detection of TEM, SHV and CTX-M extended-spectrum β-lactamases. *Journal of chemotherapy*, 19(2), 127-139.

Beehan, D. P., Wolfsdorf, K., Elam, J., Krekeler, N., Paccamonti, D., & Lyle, S. K. (2015). The evaluation of biofilm-forming potential of Escherichia coli collected from the equine female reproductive tract. *Journal of Equine Veterinary Science*, 35(11-12), 935-939.

Behzadi, P., & Behzadi, E. (2008). The microbial agents of urinary tract infections at central laboratory of Dr. Shariati Hospital, Tehran, Iran. *Turk Klin Tip Bilim*, 28(4), 445.

Beloin, C., Michaelis, K., Lindner, K., Landini, P., Hacker, J., Ghigo, J. M., & Dobrindt, U. (2006). The transcriptional antiterminator RfaH represses biofilm formation in *Escherichia coli*. *Journal of bacteriology*, 188(4), 1316-1331.

BioSurface Technologies Corp (2016) *CDC Biofilm Reactor* [Online]. Available from: https://biofilms.biz/?gclid=Cj0KCQiAl5zwBRCTARIsAIrukdMOqyppZR9bWfTsGmVmydfUAgDWb_MQI5BAqJNcaPqS5wO10O5RnDIaAocHEALw_wcB [Accessed 11/04 2016].

Bjarnsholt, T. (2013). The role of bacterial biofilms in chronic infections. *Apmis*, 121, 1-58.

Boles, B. R., Thoendel, M., & Singh, P. K. (2004). Self-generated diversity produces "insurance effects" in biofilm communities. *Proceedings of the National Academy of Sciences*, 101(47), 16630-16635.

Bonnet, R. (2004). Growing group of extended-spectrum β-lactamases: the CTX-M enzymes. *Antimicrobial agents and chemotherapy*, 48(1), 1-14.

Boorn, K. L., Khor, Y. Y., Sweetman, E., Tan, F., Heard, T. A., & Hammer, K. A. (2010). Antimicrobial activity of honey from the stingless bee *Trigona carbonaria* determined by agar diffusion, agar dilution, broth microdilution and time-kill methodology. *Journal of applied microbiology*, 108(5), 1534-1543.

Boyd, D. A., Tyler, S., Christianson, S., McGeer, A., Muller, M. P., Willey, B. M., Bryce, E., Gardam, M., Nordmann, P. & Mulvey, M. R. (2004). Complete nucleotide sequence of

a 92-kilobase plasmid harboring the CTX-M-15 extended-spectrum beta-lactamase involved in an outbreak in long-term-care facilities in Toronto, Canada. *Antimicrobial agents and chemotherapy*, 48(10), 3758-3764.

Braithwaite, R. A., & McEvoy, L. A. (2005). Marine biofouling on fish farms and its remediation. *Advances in marine biology*, 47, 215-252.

Branda, S. S., González-Pastor, J. E., Ben-Yehuda, S., Losick, R., & Kolter, R. (2001). Fruiting body formation by Bacillus subtilis. *Proceedings of the National Academy of Sciences*, 98(20), 11621-11626.

Bratu, S., Landman, D., Alam, M., Tolentino, E., & Quale, J. (2005). Detection of KPC carbapenem-hydrolyzing enzymes in Enterobacter spp. from Brooklyn, *New York. Antimicrobial agents and chemotherapy*, 49(2), 776-778.

Brudzynski, K., & Sjaarda, C. (2014). Antibacterial compounds of Canadian honeys target bacterial cell wall inducing phenotype changes, growth inhibition and cell lysis that resemble action of β-lactam antibiotics. *PLoS One*, 9(9), e106967.

Brun-Buisson, C., Philippon, A., Ansquer, M., Legrand, P., Montravers, F., & Duval, J. (1987). Transferable enzymatic resistance to third-generation cephalosporins during nosocomial outbreak of multiresistant Klebsiella pneumoniae. *The Lancet*, 330(8554), 302-306.

BSAC (2015). *BSAC Methods for Antimicrobial Susceptibility Testing*. In: BSAC (ed.).

Bush, K., & Fisher, J. F. (2011). Epidemiological expansion, structural studies, and clinical challenges of new β-lactamases from gram-negative bacteria. *Annual review of microbiology*, 65, 455-478.

Bush, K., Jacoby, G. A., & Medeiros, A. A. (1995). A functional classification scheme for beta-lactamases and its correlation with molecular structure. *Antimicrobial agents and chemotherapy*, 39(6), 1211.

Bustin, S. A., Benes, V., Garson, J. A., Hellemans, J., Huggett, J., Kubista, M., Mueller, R., Nolan, T., Pfaffl, M.W., Shipley, G.L. & Vandesompele, J. (2009). The MIQE guidelines: minimum information for publication of quantitative real-time PCR experiments. *Clinical chemistry*, 55(4), 611-622.

Byarugaba, D. K. (2005). Antimicrobial resistance and its containment in developing countries. In *Antibiotic Policies* (pp. 617-647). Springer, Boston, MA.

Cai, T., Nesi, G., Mazzoli, S., Meacci, F., Lanzafame, P., Caciagli, P., Mereu, L., Tateo, S., Malossini, G., Selli, C. & Bartoletti, R. (2015). Asymptomatic bacteriuria treatment is associated with a higher prevalence of antibiotic resistant strains in women with urinary tract infections. *Clinical Infectious Diseases*, 61(11), 1655-1661.

Camilli, A., & Bassler, B. L. (2006). Bacterial small-molecule signaling pathways. *Science*, 311(5764), 1113-1116.

Camplin, A. L., & Maddocks, S. E. (2014). Manuka honey treatment of biofilms of *Pseudomonas aeruginosa* results in the emergence of isolates with increased honey resistance. *Annals of clinical microbiology and antimicrobials*, 13(1), 19.

Cantón, R., González-Alba, J. M., & Galán, J. C. (2012). CTX-M enzymes: origin and diffusion. *Frontiers in Microbiology*, 3: 110.

Cappuyns, A. M., Bernaerts, K., Vanderleyden, J., & Van Impe, J. F. (2009). A dynamic model for diauxic growth, overflow metabolism, and AI-2-mediated cell–cell communication of Salmonella Typhimurium based on systems biology concepts. *Biotechnology and bioengineering*, 102(1), 280-293.

Castanheira, M., Deshpande, L. M., Mathai, D., Bell, J. M., Jones, R. N., & Mendes, R. E. (2011). Early dissemination of NDM-1-and OXA-181-producing Enterobacteriaceae in Indian hospitals: report from the SENTRY Antimicrobial Surveillance Program, 2006-2007. *Antimicrobial agents and chemotherapy*, 55(3), 1274-1278.

Cavaliere, P., & Norel, F. (2016). Recent advances in the characterization of Crl, the unconventional activator of the stress sigma factor σS/RpoS. Biomolecular concepts, 7(3), 197-204.

Centres for Disease Control and Prevention (US). (2013). *Antibiotic resistance threats in the United States, 2013*. Centres for Disease Control and Prevention, US Department of Health and Human Services.

Cepas, V., López, Y., Munoz, E., Rolo, D., Ardanuy, C., Martí, S., Xercavins, D., Horcajada, J. P., Bosch, J., & Soto, S. M. (2019). Relationship Between Biofilm Formation and Antimicrobial Resistance in Gram-Negative Bacteria. Microbial Drug Resistance, 25(1), 72-79.

Ceri, H., Olson, M. E., Stremick, C., Read, R. R., Morck, D., & Buret, A. (1999). The Calgary Biofilm Device: new technology for rapid determination of antibiotic susceptibilities of bacterial biofilms. *Journal of clinical microbiology*, 37(6), 1771-1776.

Chaibi, E. B., Sirot, D., Paul, G., & Labia, R. (1999). Inhibitor-resistant TEM β-lactamases: phenotypic, genetic and biochemical characteristics. Journal of Antimicrobial Chemotherapy, 43(4), 447-458.

Chervoneva, I., Li, Y., Schulz, S., Croker, S., Wilson, C., Waldman, S. A., & Hyslop, T. (2010). Selection of optimal reference genes for normalization in quantitative RT-PCR. *BMC bioinformatics*, 11(1), 253.

Chimileski, S., Franklin, M. J., & Papke, R. T. (2014). Biofilms formed by the archaeon Haloferax volcanii exhibit cellular differentiation and social motility, and facilitate horizontal gene transfer. *BMC biology*, 12(1), 65.

Chimileski, S., Franklin, M. J., & Papke, R. T. (2014). Biofilms formed by the archaeon Haloferax volcanii exhibit cellular differentiation and social motility, and facilitate horizontal gene transfer. *BMC biology*, 12(1), 65.

Cho, H. H., Kwon, K. C., Kim, S., Park, Y., & Koo, S. H. (2018). Association between biofilm formation and antimicrobial resistance in carbapenem-resistant Pseudomonas aeruginosa. Annals of Clinical & Laboratory Science, 48(3), 363-368.

Ciofu, O., Rojo-Molinero, E., Macià, M. D., & Oliver, A. (2017). Antibiotic treatment of biofilm infections. Apmis, 125(4), 304-319.

Clarke, M. B., & Sperandio, V. (2006). LuxS-dependent regulation of Escherichia coli. *Bacterial Cell-to-Cell Communication: Role in Virulence and Pathogenesis*, 11.

Clarkson, C. (2015). *Beta Lactam Pharmacology*. [Online] Available from: http://tmedweb.tulane.edu/pharmwiki/doku.php/beta_lactam_working_rough_draft_-_not_ready_for_prime_time?rev=1440091333

Codjoe, F. S., & Donkor, E. S. (2018). Carbapenem resistance: a review. *Medical Sciences*, 6(1), 1.

Coenye, T., & Nelis, H. J. (2010). In vitro and in vivo model systems to study microbial biofilm formation. *Journal of microbiological methods*, 83(2), 89-105.

Coetser, S. E., & Cloete, T. E. (2005). Biofouling and biocorrosion in industrial water systems. *Critical reviews in microbiology*, 31(4), 213-232.

Cohen, B. E. (2014). Functional linkage between genes that regulate osmotic stress responses and multidrug resistance transporters: challenges and opportunities for antibiotic discovery. Antimicrobial agents and chemotherapy, 58(2), 640-646.

Collins, C. H. (2004). Collins and Lyne's Microbiological Methods, 8P th P edition. *Arnold, a member of the Hodder Headling group London* UK.

Cooper, R. A., Jenkins, L., Henriques, A. F. M., Duggan, R. S., & Burton, N. F. (2010). Absence of bacterial resistance to medical-grade manuka honey. *European journal of clinical microbiology & infectious diseases*, 29(10), 1237-1241.

Corehtash, Z. G., Ahmad Khorshidi, F. F., Akbari, H., & Aznaveh, A. M. (2015). Biofilm formation and virulence factors among *Pseudomonas aeruginosa* isolated from burn patients. *Jundishapur journal of microbiology*, 8(10).

Costerton, J. W., Cheng, K. J., Geesey, G. G., Ladd, T. I., Nickel, J. C., Dasgupta, M., & Marrie, T. J. (1987). Bacterial biofilms in nature and disease. *Annual Reviews in Microbiology*, 41(1), 435-464.

Costerton, J. W., Stewart, P. S., & Greenberg, E. P. (1999). Bacterial biofilms: a common cause of persistent infections. science, 284(5418), 1318-1322.

Coulthurst, S. J., Kurz, C. L., & Salmond, G. P. (2004). luxS mutants of Serratia defective in autoinducer-2-dependent 'quorum sensing'show strain-dependent impacts on virulence and production of carbapenem and prodigiosin. *Microbiology*, 150(6), 1901-1910.

Crémet, L., Corvec, S., Batard, E., Auger, M., Lopez, I., Pagniez, F., Dauvergne, S. & Caroff, N. (2013). Comparison of three methods to study biofilm formation by clinical strains of Escherichia coli. *Diagnostic microbiology and infectious disease*, 75(3), 252-255.

Culture collections (2013a). *Antimicrobial Resistance Reference Strains* [Online]. Public Health England. Available from: https://www.phe-culturecollections.org.uk/products/bacteria/antimicrobialresistancereferencestrains.aspx [Accessed 14/02 2016].

Culture collections (2013b). *Bacteria and Mycoplasmas Detail* [Online]. Public Health England. Available from: https://www.phe-

culturecollections.org.uk/products/bacteria/detail.jsp?refId=NCTC+12241&collection=nctc [Accessed 14/02 2016].

Culture collections (2013c). *Bacteria Collection: Klebsiella pneumoniae subsp. pneumoniae* [Online]. Public Health England. Available from: https://www.phe-culturecollections.org.uk/products/bacteria/detail.jsp?refId=NCTC+9633&collection=nctc [Accessed 11/04 2016].

Curtis, S. J., & Epstein, W. O. L. F. G. A. N. G. (1975). Phosphorylation of D-glucose in Escherichia coli mutants defective in glucosephosphotransferase, mannosephosphotransferase, and glucokinase. *Journal of Bacteriology*, 122(3), 1189-1199.

Datta, N., & Kontomichalou, P. (1965). Penicillinase synthesis controlled by infectious R factors in Enterobacteriaceae. *Nature*, 208(5007), 239-241.

Davey, M. E., & O'toole, G. A. (2000). Microbial biofilms: from ecology to molecular genetics. *Microbiol. Mol. Biol*. Rev., 64(4), 847-867.

De Souza, A. A., Takita, M. A., Coletta-Filho, H. D., Caldana, C., Yanai, G. M., Muto, N. H., de Oliveira, R. C., Nunes, L. R., & Machado, M. A. (2004). Gene expression profile of the plant pathogen Xylella fastidiosa during biofilm formation in vitro. FEMS Microbiology Letters, 237(2), 341-353.

Delcaru, C., Alexandru, I., Podgoreanu, P., Grosu, M., Stavropoulos, E., Chifiriuc, M. C., & Lazar, V. (2016). Microbial biofilms in urinary tract infections and prostatitis: etiology, pathogenicity, and combating strategies. *Pathogens*, 5(4), 65.

DeLisa, M. P., Wu, C. F., Wang, L., Valdes, J. J., & Bentley, W. E. (2001). DNA Microarray-Based Identification of Genes Controlled by Autoinducer 2-Stimulated Quorum Sensing in Escherichia coli. Journal of Bacteriology, 183(18), 5239-5247.

Dimou, V., Dhanji, H., Pike, R., Livermore, D. M., & Woodford, N. (2012). Characterization of Enterobacteriaceae producing OXA-48-like carbapenemases in the UK. *Journal of antimicrobial chemotherapy*, 67(7), 1660-1665.

Docquier, J. D., Calderone, V., De Luca, F., Benvenuti, M., Giuliani, F., Bellucci, L., Tafi, A., Nordmann, P., Botta, M., Rossolini, G.M. & Mangani, S. (2009). Crystal structure of the OXA-48 β-lactamase reveals mechanistic diversity among class D carbapenemases. *Chemistry & biology*, 16(5), 540-547.

Donlan, R. M., & Costerton, J. W. (2002). Biofilms: survival mechanisms of clinically relevant microorganisms. *Clinical microbiology reviews*, 15(2), 167-193.

Dunsmore, B. C., Jacobsen, A., Hall-Stoodley, L., Bass, C. J., Lappin-Scott, H. M., & Stoodley, P. (2002). The influence of fluid shear on the structure and material properties of sulphate-reducing bacterial biofilms. *Journal of Industrial Microbiology and Biotechnology*, 29(6), 347-353.

Ebie, M. Y., Kandakai-Olukemi, Y. T., Ayanbadejo, J., & Tanyigna, K. B. (2001). Urinary tract infections in a Nigerian military hospital. *Nigerian Journal of Microbiology*, 15(1), 31-37.

ECOMETAL (2011) *First HS report: Introduction and equipment* [Online]. Available from: http://www.ecometal.org/art-57/hygienic_surface_project_ecometal [Accessed 3 Apr. 2016].

Emery Pharma (2014) *Testing Antimicrobials Using Minimum Biofilm Eradication Concentration (MBEC)* [Online] Available from: https://emerypharma.com/blog/testing-antimicrobials-using-minimum-biofilm-eradication-concentration-mbec/ [Accessed 3 Apr. 2016].

Erb, A., Stürmer, T., Marre, R., & Brenner, H. (2007). Prevalence of antibiotic resistance in Escherichia coli: overview of geographical, temporal, and methodological variations. *European Journal of Clinical Microbiology & Infectious Diseases*, 26(2), 83-90.

Evans, B. A., & Amyes, S. G. (2014). OXA β-lactamases. *Clinical microbiology reviews*, 27(2), 241-263.

Eyoh, A. B., Toukam, M., Atashili, J., Fokunang, C., Gonsu, H., Lyonga, E. E., Mandi, H, Ikomey G, Mukwele, B., Mesembe, M., & Assoumou, M. C. O. (2014). Relationship between multiple drug resistance and biofilm formation in Staphylococcus aureus isolated from medical and non-medical personnel in Yaounde, Cameroon. *The Pan African medical journal*, 17.

Fattahi, S., Kafil, H. S., Nahai, M. R., Asgharzadeh, M., Nori, R., & Aghazadeh, M. (2015). Relationship of biofilm formation and different virulence genes in uropathogenic Escherichia coli isolates from Northwest Iran. *GMS hygiene and infection control*, 10.

Fisher, J. F., Meroueh, S. O., & Mobashery, S. (2005). Bacterial resistance to β-lactam antibiotics: compelling opportunism, compelling opportunity. *Chemical reviews*, 105(2), 395-424.

Flemming, H. C. (2002). Biofouling in water systems–cases, causes and countermeasures. *Applied microbiology and biotechnology*, 59(6), 629-640.

Flores-Mireles, A. L., Walker, J. N., Caparon, M., & Hultgren, S. J. (2015). Urinary tract infections: epidemiology, mechanisms of infection and treatment options. *Nature reviews microbiology*, 13(5), 269-284.

Fomda, B. A., Khan, A., & Zahoor, D. (2014). NDM-1 (New Delhi metallo beta lactamase-1) producing Gram-negative bacilli: Emergence & clinical implications. *The Indian journal of medical research*, 140(5), 672.

Franklin, M. J., Chang, C., Akiyama, T., & Bothner, B. (2015). New technologies for studying biofilms. *Microbiology spectrum*, 3(4).

Frère, J. M., Galleni, M., Bush, K., & Dideberg, O. (2005). Is it necessary to change the classification of β-lactamases?. *Journal of Antimicrobial Chemotherapy*, 55(6), 1051-1053.

Fuqua, C., Parsek, M. R., & Greenberg, E. P. (2001). Regulation of gene expression by cell-to-cell communication: acyl-homoserine lactone quorum sensing. *Annual review of genetics*, 35(1), 439-468.

Galeva, A., Moroz, N., Yoon, Y. H., Hughes, K. T., Samatey, F. A., & Kostyukova, A. S. (2014). Bacterial flagellin-specific chaperone FliS interacts with anti-sigma factor FlgM. *Journal of bacteriology*, 196(6), 1215-1221.

Garofalo, C. K., Hooton, T. M., Martin, S. M., Stamm, W. E., Palermo, J. J., Gordon, J. I., & Hultgren, S. J. (2007). Escherichia coli from urine of female patients with urinary tract infections is competent for intracellular bacterial community formation. *Infection and immunity*, 75(1), 52-60.

Garrec, H., Drieux-Rouzet, L., Golmard, J. L., Jarlier, V., & Robert, J. (2011). Comparison of nine phenotypic methods for detection of extended-spectrum β-lactamase production by Enterobacteriaceae. *Journal of clinical microbiology*, 49(3), 1048-1057.

Gebreyohannes, G., Nyerere, A., Bii, C., & Sbhatu, D. B. (2019). Challenges of intervention, treatment, and antibiotic resistance of biofilm-forming microorganisms. *Heliyon*, 5(8), e02192.

Gelens, L., Hill, L., Vandervelde, A., Danckaert, J., & Loris, R. (2013). A general model for toxin-antitoxin module dynamics can explain persister cell formation in E. coli. *PLoS computational biology*, 9(8), e1003190.

Goeres, D. M., Hamilton, M. A., Beck, N. A., Buckingham-Meyer, K., Hilyard, J. D., Loetterle, L. R., Lorenz, L.A., Walker, D.K. & Stewart, P. S. (2009). A method for growing a biofilm under low shear at the air–liquid interface using the drip flow biofilm reactor. *Nature protocols*, 4(5), 783.

Goeres, D. M., Loetterle, L. R., Hamilton, M. A., Murga, R., Kirby, D. W., & Donlan, R. M. (2005). Statistical assessment of a laboratory method for growing biofilms. *Microbiology*, 151(3), 757-762.

Goncalves, D., Cecilio, P., & Ferreira, H. (2013). First detection of OXA-48-like producing Acinetobacter baumannii in the faecal flora of nursing home residents in Northern Portugal. *In Twenty-third European Congress of Clinical Microbiology and Infectious Diseases, Berlin, Germany.*

Greenberg, E. P., Hastings, J. W., & Ulitzur, S. (1979). Induction of luciferase synthesis in Beneckea harveyi by other marine bacteria. *Archives of Microbiology*, *120*(2), 87-91.

Gurung, J., Khyriem, A. B., Banik, A., Lyngdoh, W. V., Choudhury, B., & Bhattacharyya, P. (2013). Association of biofilm production with multidrug resistance among clinical isolates of Acinetobacter baumannii and Pseudomonas aeruginosa from intensive care unit. *Indian journal of critical care medicine: peer-reviewed, official publication of Indian Society of Critical Care Medicine*, 17(4), 214.

Hall, C. W., & Mah, T. F. (2017). Molecular mechanisms of biofilm-based antibiotic resistance and tolerance in pathogenic bacteria. *FEMS microbiology reviews*, 41(3), 276-301.

Hall-Stoodley, L., Costerton, J. W., & Stoodley, P. (2004). Bacterial biofilms: from the natural environment to infectious diseases. *Nature reviews microbiology*, 2(2), 95.

Hammar, M. R., Arnqvist, A., Bian, Z., Olsén, A., & Normark, S. (1995). Expression of two csg operons is required for production of fibronectin-and congo red-binding curli polymers in Escherichia coli K-12. *Molecular microbiology*, 18(4), 661-670.

Hammar, M., Bian, Z., & Normark, S. (1996). Nucleator-dependent intercellular assembly of adhesive curli organelles in Escherichia coli. *Proceedings of the National Academy of Sciences*, 93(13), 6562-6566

Hancock, V., Witsø, I. L., & Klemm, P. (2011). Biofilm formation as a function of adhesin, growth medium, substratum and strain type. *International Journal of Medical Microbiology*, 301(7), 570-576.

Hansen, S. K., Rainey, P. B., Haagensen, J. A., & Molin, S. (2007). Evolution of species interactions in a biofilm community. *Nature*, 445(7127), 533.

Hassett, D. J., Ma, J. F., Elkins, J. G., McDermott, T. R., Ochsner, U. A., West, S. E., Huang, C.T., Fredericks, J., Burnett, S., Stewart, P.S. & McFeters, G. (1999). Quorum sensing in Pseudomonas aeruginosa controls expression of catalase and superoxide dismutase genes and mediates biofilm susceptibility to hydrogen peroxide. *Molecular microbiology*, 34(5), 1082-1093.

Hayashi, K., Fukushima, A., Hayashi-Nishino, M., & Nishino, K. (2014). Effect of methylglyoxal on multidrug-resistant *Pseudomonas aeruginosa*. *Frontiers in microbiology*, 5, 180.

Henriques, A. F., Jenkins, R. E., Burton, N. F., & Cooper, R. A. (2011). The effect of manuka honey on the structure of Pseudomonas aeruginosa. *European journal of clinical microbiology & infectious diseases*, 30(2), 167-171.

Herzberg, M., Kaye, I. K., Peti, W., & Wood, T. K. (2006). YdgG (TqsA) controls biofilm formation in Escherichia coli K-12 through autoinducer 2 transport. *Journal of bacteriology*, 188(2), 587-598.

Hooton, T. M., & Stamm, W. E. (1997). Diagnosis and treatment of uncomplicated urinary tract infection. *Infectious Disease Clinics*, 11(3), 551-581.

Horng, Y. T., Wang, C. J., Chung, W. T., Chao, H. J., Chen, Y. Y., & Soo, P. C. (2018). Phosphoenolpyruvate phosphotransferase system components positively regulate Klebsiella biofilm formation. *Journal of microbiology, immunology and infection*, 51(2), 174-183.

Huang, C. T., Mcfeters, G. A., & Stewart, P. S. (1996). Evaluation of physiological staining, cryoembedding and autofluorescence quenching techniques on fouling biofilms. *Biofouling*, 9(4), 269-277.

Idris, A. R., & Afegbua, S. L. (2017). Single and joint antibacterial activity of aqueous garlic extract and Manuka honey on extended-spectrum beta-lactamase-producing Escherichia coli. *Transactions of The Royal Society of Tropical Medicine and Hygiene*, 111(10), 472-478.

Jacoby, G. A. (1997). Extended-spectrum β-lactamases and other enzymes providing resistance to oxyimino-β-lactams. *Infectious disease clinics of North America*, 11(4), 875-887.

Jacoby, G. A. (2009). AmpC β-lactamases. Clinical microbiology reviews, 22(1), 161-182.

Jamal, M., Ahmad, W., Andleeb, S., Jalil, F., Imran, M., Nawaz, M. A., Hussain, T., Ali, M., Rafiq, M. & Kamil, M. A. (2018). Bacterial biofilm and associated infections. Journal of the Chinese Medical Association, 81(1), 7-11.

Janin and Pierre, R. (1976). *Uspto patent full-text and image database* [Online]. Avaliable from http://patft.uspto.gov/netacgi/nph-Parser?Sect1=PTO1&Sect2=HITOFF&d=PALL&p=1&u=%2Fnetahtml%2FPTO%2Fsrch

num.htm&r=1&f=G&l=50&s1=3936356.PN.&OS=PN/3936356&RS=PN/3936356 [Accessed 19 July 2019].

Jeon, B., Hirayama, K., & Itoh, K. (2005). Production of the autoinducer-2 signalling molecule in Escherichia coli-monoassociated mice. *Microbial ecology in health and disease*, 17(4), 212-215.

Johnston, M., McBride, M., Dahiya, D., Owusu, R. K., & Nigam, P. S. N. (2018). Antibacterial activity of Manuka honey and its components: An overview. *AIMS Microbiology*, 4(4), 655-664.

Juhas, M., Evans, L. D., Frost, J., Davenport, P. W., Yarkoni, O., Fraser, G. M., & Ajioka, J. W. (2014). Escherichia coli flagellar genes as target sites for integration and expression of genetic circuits. PloS one, 9(10), e111451.

Juhna, T., Birzniece, D., Larsson, S., Zulenkovs, D., Sharipo, A., Azevedo, N. F., Menard-Szczebara, F., Castagnet, S., Feliers, C. & Keevil, C. W. (2007). Detection of Escherichia coli in biofilms from pipe samples and coupons in drinking water distribution networks. *Appl. Environ. Microbiol.*, 73(22), 7456-7464.

Kaper, J. B., & Sperandio, V. (2005). Bacterial cell-to-cell signaling in the gastrointestinal tract. *Infection and immunity*, 73(6), 3197-3209.

Kapoor, G., Saigal, S., & Elongavan, A. (2017). Action and resistance mechanisms of antibiotics: A guide for clinicians. *Journal of anaesthesiology, clinical pharmacology*, 33(3), 300.

Karim, A., Poirel, L., Nagarajan, S., & Nordmann, P. (2001). Plasmid-mediated extended-spectrum β-lactamase (CTX-M-3 like) from India and gene association with insertion sequence IS Ecp1. *FEMS microbiology letters*, 201(2), 237-241.

Kawagishi, I., Müller, V., Williams, A. W., Irikura, V. M., & Macnab, R. M. (1992). Subdivision of flagellar region III of the Escherichia coli and Salmonella typhimurium chromosomes and identification of two additional flagellar genes. Microbiology, 138(6), 1051-1065.

Kim, W., Racimo, F., Schluter, J., Levy, S. B., & Foster, K. R. (2014). Importance of positioning for microbial evolution. *Proceedings of the National Academy of Sciences*, 111(16), E1639-E1647.

Kim, W., Tengra, F. K., Young, Z., Shong, J., Marchand, N., Chan, H. K., Pangule, R.C., Parra, M., Dordick, J.S., Plawsky, J.L. & Collins, C. H. (2013). Spaceflight promotes biofilm formation by Pseudomonas aeruginosa. *PloS one*, 8(4), e62437.

Kjeldsen, T. S., Overgaard, M., Nielsen, S. S., Bortolaia, V., Jelsbak, L., Sommer, M., Guardabassi, L., & Olsen, J. E. (2014). CTX-M-1 β-lactamase expression in Escherichia coli is dependent on cefotaxime concentration, growth phase and gene location. *Journal of Antimicrobial Chemotherapy*, 70(1), 62-70.

Kleerebezem, M., Quadri, L. E., Kuipers, O. P., & De Vos, W. M. (1997). Quorum sensing by peptide pheromones and two-component signal-transduction systems in Gram-positive bacteria. *Molecular microbiology*, 24(5), 895-904.

Knothe, H., Shah, P., Krcmery, V., Antal, M., & Mitsuhashi, S. (1983). Transferable resistance to cefotaxime, cefoxitin, cefamandole and cefuroxime in clinical isolates of Klebsiella pneumoniae and Serratia marcescens. *Infection*, 11(6), 315-317.

Kotra, L. P., & Mobashery, S. (1998). β-Lactam antibiotics, β-lactamases and bacterial resistance. *Bulletin de l'Institut Pasteur*, 96(3), 139-150.

Kozera, B., & Rapacz, M. (2013). Reference genes in real-time PCR. *Journal of applied genetics*, 54(4), 391-406.

Kralik, P., & Ricchi, M. (2017). A basic guide to real time PCR in microbial diagnostics: definitions, parameters, and everything. *Frontiers in microbiology*, 8, 108.

Kubista, M., Andrade, J. M., Bengtsson, M., Forootan, A., Jonák, J., Lind, K., Sindelka, R., Sjöback, R., Sjögreen, B., Strömbom, L. & Ståhlberg, A. (2006). The real-time polymerase chain reaction. *Molecular aspects of medicine*, 27(2-3), 95-125.

Kumarasamy, K. K., Toleman, M. A., Walsh, T. R., Bagaria, J., Butt, F., Balakrishnan, R., Chaudhary, U., Doumith, M., Giske, C.G., Irfan, S. & Krishnan, P. (2010). Emergence of a new antibiotic resistance mechanism in India, Pakistan, and the UK: a molecular, biological, and epidemiological study. *The Lancet infectious diseases*, 10(9), 597-602.

Kunduru, M. R., & Pometto, A. L. (1996). Continuous ethanol production byZymomonas mobilis andSaccharomyces cerevisiae in biofilm reactors. *Journal of industrial microbiology*, 16(4), 249-256.

Kvist, M., Hancock, V., & Klemm, P. (2008). Inactivation of efflux pumps abolishes bacterial biofilm formation. *Appl. Environ. Microbiol*., 74(23), 7376-7382.

Kwakman, P. H., Te Velde, A. A., De Boer, L., Vandenbroucke-Grauls, C. M., & Zaat, S. A. (2011). Two major medicinal honeys have different mechanisms of bactericidal activity. PloS one, 6(3), e17709.

Lawrence, J. R., Korber, D. R., Hoyle, B. D., Costerton, J. W., & Caldwell, D. E. (1991). Optical sectioning of microbial biofilms. *Journal of bacteriology*, 173(20), 6558-6567.

Lazazzera, B. A. (2010). The phosphoenolpyruvate phosphotransferase system: as important for biofilm formation by Vibrio cholerae as it is for metabolism in Escherichia coli. *Journal of bacteriology*, 192(16), 4083-4085.

Lazzaroni, J. C., Germon, P., Ray, M. C., & Vianney, A. (1999). The Tol proteins of Escherichia coli and their involvement in the uptake of biomolecules and outer membrane stability. FEMS microbiology letters, 177(2), 191-197.

Lee, A. S. Y., & Song, K. P. (2005). LuxS/autoinducer-2 quorum sensing molecule regulates transcriptional virulence gene expression in Clostridium difficile. *Biochemical and biophysical research communications*, 335(3), 659-666.

Lee, J. H., Regmi, S. C., Kim, J. A., Cho, M. H., Yun, H., Lee, C. S., & Lee, J. (2011). Apple flavonoid phloretin inhibits Escherichia coli O157: H7 biofilm formation and ameliorates colon inflammation in rats. *Infection and immunity*, 79(12), 4819-4827.

Lenz, A. P., Williamson, K. S., Pitts, B., Stewart, P. S., & Franklin, M. J. (2008). Localized gene expression in Pseudomonas aeruginosa biofilms. *Appl. Environ. Microbiol*., 74(14), 4463-4471.

Leung, V., Loo, V. G., Frenette, C., Domingo, M. C., Bourgault, A. M., Mulvey, M. R., & Robson, H. G. (2012). First Canadian outbreak of Enterobacteriaceae-expressing Klebsiella pneumoniae carbapenemase type 3. Canadian Journal of Infectious Diseases and Medical Microbiology, 23(3), 117-120.

Levin-Reisman, I., Ronin, I., Gefen, O., Braniss, I., Shoresh, N., & Balaban, N. Q. (2017). Antibiotic tolerance facilitates the evolution of resistance. Science, 355(6327), 826-830.

Lewandowski, Z., Walser, G., & Characklis, W. G. (1991). Reaction kinetics in biofilms. Biotechnology and bioengineering, 38(8), 877-882.

Li, B., Qiu, Y., Zhang, J., Huang, X., Shi, H., & Yin, H. (2018). Real-time study of rapid spread of antibiotic resistance plasmid in biofilm using microfluidics. *Environmental science & technology*, 52(19), 11132-11141.

Li, J., Attila, C., Wang, L., Wood, T. K., Valdes, J. J., & Bentley, W. E. (2007). Quorum sensing in Escherichia coli is signaled by AI-2/LsrR: effects on small RNA and biofilm architecture. Journal of bacteriology, 189(16), 6011-6020.

Li, X. Z., Webb, J. S., Kjelleberg, S., & Rosche, B. (2006). Enhanced benzaldehyde tolerance in Zymomonas mobilis biofilms and the potential of biofilm applications in fine-chemical production. *Appl. Environ. Microbiol*., 72(2), 1639-1644.

Liakopoulos, A., Mevius, D., & Ceccarelli, D. (2016). A review of SHV extended-spectrum β-lactamases: neglected yet ubiquitous. *Frontiers in microbiology*, 7, 1374.

Livak, K. J., & Schmittgen, T. D. (2001). Analysis of relative gene expression data using real-time quantitative PCR and the $2^{-\Delta\Delta CT}$ method. *methods*, 25(4), 402-408.

Livermore, D. M., & Woodford, N. (2000). Carbapenemases: a problem in waiting?. *Current opinion in microbiology*, 3(5), 489-495.

Livermore, D. M., & Woodford, N. (2006). The β-lactamase threat in Enterobacteriaceae, Pseudomonas and Acinetobacter. *Trends in microbiology*, 14(9), 413-420.

Llamas, M. A., Ramos, J. L., & Rodríguez-Herva, J. J. (2000). Mutations in Each of the tol Genes of Pseudomonas putida Reveal that They Are Critical for Maintenance of Outer Membrane Stability. Journal of bacteriology, 182(17), 4764-4772.

Lu, J., Carter, D. A., Turnbull, L., Rosendale, D., Hedderley, D., Stephens, J., Gannabathula, S., Steinhorn, G., Schlothauer, R.C., Whitchurch, C.B. & Harry, E. J. (2013). The effect of New Zealand kanuka, manuka and clover honeys on bacterial growth dynamics and cellular morphology varies according to the species. PloS one, 8(2), e55898.

Lu, J., Turnbull, L., Burke, C. M., Liu, M., Carter, D. A., Schlothauer, R. C., Whitchurch, C.B. & Harry, E. J. (2014). Manuka-type honeys can eradicate biofilms produced by Staphylococcus aureus strains with different biofilm-forming abilities. PeerJ, 2, e326.

Lupo, A., Papp-Wallace, K. M., Sendi, P., Bonomo, R. A., & Endimiani, A. (2013). Non-phenotypic tests to detect and characterize antibiotic resistance mechanisms in Enterobacteriaceae. Diagnostic microbiology and infectious disease, 77(3), 179-194.

Mah, T. F. C., & O'Toole, G. A. (2001). Mechanisms of biofilm resistance to antimicrobial agents. *Trends in microbiology*, 9(1), 34-39.

Mandal, M. D., & Mandal, S. (2011). Honey: its medicinal propelrty and antibacterial activity. Asian Pacific Journal of Tropical Biomedicine, 1(2), 154-160.

MAST, G. (2015*). ESBL and AmpC Detection Disc Sets*. In: LTD., M. G. (ed.). Bootle: Mast House.

Matsumoto, Y. O. S. H. I. M. I., Ikeda, F. U. M. I. A. K. I., Kamimura, T. O. S. H. I. A. K. I., Yokota, Y. O. S. H. I. K. O., & Mine, Y. A. S. U. H. I. R. O. (1988). Novel plasmid-mediated beta-lactamase from Escherichia coli that inactivates oxyimino-cephalosporins. *Antimicrobial agents and chemotherapy*, 32(8), 1243-1246.

Mavric, E., Wittmann, S., Barth, G., & Henle, T. (2008). Identification and quantification of methylglyoxal as the dominant antibacterial constituent of Manuka (Leptospermum scoparium) honeys from New Zealand. *Molecular nutrition & food research*, 52(4), 483-489.

Mazzariol, A., Bazaj, A., & Cornaglia, G. (2017). Multi-drug-resistant Gram-negative bacteria causing urinary tract infections: a review. Journal of Chemotherapy, 29(sup1), 2-9.

McLoone, P., Warnock, M., & Fyfe, L. (2016). Honey: A realistic antimicrobial for disorders of the skin. Journal of Microbiology, Immunology and Infection, 49(2), 161-167.

Meletis, G. (2016). Carbapenem resistance: overview of the problem and future perspectives. *Therapeutic advances in infectious disease*, 3(1), 15-21.

Merritt, J., Qi, F., Goodman, S. D., Anderson, M. H., & Shi, W. (2003). Mutation of luxS affects biofilm formation in Streptococcus mutans. *Infection and immunity*, 71(4), 1972-1979.

Miller, M. B., & Bassler, B. L. (2001). Quorum sensing in bacteria. *Annual Reviews in Microbiology*, 55(1), 165-199.

Miriagou, V., Cornaglia, G., Edelstein, M., Galani, I., Giske, C. G., Gniadkowski, M., Malamou-Lada, E., Martinez-Martinez, L., Navarro, F., Nordmann, P. & Peixe, L. (2010). Acquired carbapenemases in Gram-negative bacterial pathogens: detection and surveillance issues. *Clinical microbiology and infection*, 16(2), 112-122.

Moat, A. G., Foster, J. W., & Spector, M. P. (Eds.). (2003). Microbial physiology. John Wiley & Sons.

Munoz-Price, L. S., De La Cuesta, C., Adams, S., Wyckoff, M., Cleary, T., McCurdy, S. P., Huband, M.D., Lemmon, M.M., Lescoe, M., Dibhajj, F.B. & Hayden, M. K. (2010). Successful eradication of a monoclonal strain of Klebsiella pneumoniae during a K. pneumoniae carbapenemase-producing K. pneumoniae outbreak in a surgical intensive care unit in Miami, Florida. *Infection Control & Hospital Epidemiology*, 31(10), 1074-1077.

Niba, E. T. E., Naka, Y., Nagase, M., Mori, H., & Kitakawa, M. (2007). A genome-wide approach to identify the genes involved in biofilm formation in E. coli. DNA research, 14(6), 237-246.

Nickerson, C. A., Ott, C. M., Wilson, J. W., Ramamurthy, R., & Pierson, D. L. (2004). Microbial responses to microgravity and other low-shear environments. *Microbiol. Mol. Biol. Rev.*, 68(2), 345-361.

Nicolella, C., Van Loosdrecht, M. C. M., & Heijnen, J. J. (2000). Wastewater treatment with particulate biofilm reactors. *Journal of biotechnology*, 80(1), 1-33.

Niu, C., Robbins, C. M., Pittman, K. J., Osborn, J. L., Stubblefield, B. A., Simmons, R. B., & Gilbert, E. S. (2013). LuxS influences Escherichia coli biofilm formation through

autoinducer-2-dependent and autoinducer-2-independent modalities. *FEMS microbiology ecology*, 83(3), 778-791.

Niveditha, S., Pramodhini, S., Umadevi, S., Kumar, S., & Stephen, S. (2012). The isolation and the biofilm formation of uropathogens in the patients with catheter associated urinary tract infections (UTIs). Journal of clinical and diagnostic research: JCDR, 6(9), 1478.

Nivens, D. E., Ohman, D. E., Williams, J., & Franklin, M. J. (2001). Role of alginate and its O acetylation in formation of Pseudomonas aeruginosa microcolonies and biofilms. *Journal of bacteriology*, 183(3), 1047-1057.

Notake, S., Matsuda, M., Tamai, K., Yanagisawa, H., Hiramatsu, K., & Kikuchi, K. (2013). Detection of IMP metallo-β-lactamase in carbapenem-nonsusceptible Enterobacteriaceae and non-glucose-fermenting Gram-negative rods by immunochromatography assay. *Journal of clinical microbiology*, 51(6), 1762-1768.

Obiogbolu, C. H., Okonko, I. O., Anyamere, C. O., Adedeji, A. O., Akanbi, A. O., Ogun, A. A., Ejembi, J. & Faleye, T. O. C. (2009). Incidence of urinary tract infections (UTIs) among pregnant women in Akwa metropolis, Southeastern Nigeria. *Sci Res Essays*, 4(8), 820-824.

Ohtani, K., Hayashi, H., & Shimizu, T. (2002). The luxS gene is involved in cell–cell signalling for toxin production in Clostridium perfringens. *Molecular microbiology*, 44(1), 171-179.

Olaitan, P. B., Adeleke, O. E., & Iyabo, O. O. (2007). Honey: a reservoir for microorganisms and an inhibitory agent for microbes. African health sciences, 7(3).

O'Toole, G. A. (2011). Microtiter dish biofilm formation assay. JoVE (Journal of Visualized Experiments), (47), e2437.

O'Toole, G. A., & Kolter, R. (1998a). Flagellar and twitching motility are necessary for Pseudomonas aeruginosa biofilm development. *Molecular microbiology*, 30(2), 295-304.

O'Toole, G. A., & Kolter, R. (1998b). Initiation of biofilm formation in Pseudomonas fluorescens WCS365 proceeds via multiple, convergent signalling pathways: a genetic analysis. *Molecular microbiology*, 28(3), 449-461.

Oxford, N. D. E. C. (2014). Diagnostic Evidence Co-operative Oxford.

Paramasivan, S., Drilling, A. J., Jardeleza, C., Jervis-Bardy, J., Vreugde, S., & Wormald, P. J. (2014, March). Methylglyoxal-augmented manuka honey as a topical anti–Staphylococcus aureus biofilm agent: safety and efficacy in an in vivo model. In International forum of allergy & rhinology (Vol. 4, No. 3, pp. 187-195).

Parsek, M. R., & Singh, P. K. (2003). Bacterial biofilms: an emerging link to disease pathogenesis. *Annual Reviews in Microbiology*, 57(1), 677-701.

Partridge, J. D., Nieto, V., & Harshey, R. M. (2015). A new player at the flagellar motor: FliL controls both motor output and bias. *MBio*, 6(2), e02367-14.

Paterson, D. L., & Bonomo, R. A. (2005). Extended-spectrum β-lactamases: a clinical update. *Clinical microbiology reviews*, 18(4), 657-686.

Pereira, C. S., Thompson, J. A., & Xavier, K. B. (2013). AI-2-mediated signalling in bacteria. *FEMS microbiology reviews*, *37*(2), 156-181.

Petersen, M. L. (2018). Biofilm Formation of *Escherichia coli* from Surface Soils is Influenced by Variation in Cell Envelope, Iron Metabolism, and Attachment Factor Genes (Doctoral dissertation, North Dakota State University).

Poirel, L., Benouda, A., Hays, C., & Nordmann, P. (2011). Emergence of NDM-1-producing Klebsiella pneumoniae in Morocco. *Journal of Antimicrobial Chemotherapy*, 66(12), 2781-2783.

Poirel, L., Héritier, C., Podglajen, I., Sougakoff, W., Gutmann, L., & Nordmann, P. (2003). Emergence in Klebsiella pneumoniae of a chromosome-encoded SHV β-lactamase that compromises the efficacy of imipenem. *Antimicrobial agents and chemotherapy*, 47(2), 755-758.

Poirel, L., Héritier, C., Tolün, V., & Nordmann, P. (2004). Emergence of oxacillinase-mediated resistance to imipenem in Klebsiella pneumoniae. *Antimicrobial agents and chemotherapy*, 48(1), 15-22.

Poirel, L., Kämpfer, P., & Nordmann, P. (2002). Chromosome-encoded Ambler class A β-lactamase of Kluyvera georgiana, a probable progenitor of a subgroup of CTX-M extended-spectrum β-lactamases. *Antimicrobial agents and chemotherapy*, 46(12), 4038-4040.

Poirel, L., Pitout, J. D., & Nordmann, P. (2007). Carbapenemases: molecular diversity and clinical consequences. *Future Microbiol*, 2, 501-12.

Poirel, L., Potron, A., & Nordmann, P. (2012). OXA-48-like carbapenemases: the phantom menace. *Journal of Antimicrobial Chemotherapy*, 67(7), 1597-1606.

Pratt, L. A., & Kolter, R. (1998). Genetic analysis of Escherichia coli biofilm formation: roles of flagella, motility, chemotaxis and type I pili. *Molecular microbiology*, 30(2), 285-293.

Pratt, L. A., & Silhavy, T. J. (1998). Crl stimulates RpoS activity during stationary phase. Molecular microbiology, 29(5), 1225-1236.

Prigent-Combaret, C., Vidal, O., Dorel, C., & Lejeune, P. (1999). Abiotic surface sensing and biofilm-dependent regulation of gene expression in Escherichia coli. *Journal of bacteriology*, 181(19), 5993-6002.

Prouty, A. M., Schwesinger, W. H., & Gunn, J. S. (2002). Biofilm Formation and Interaction with the Surfaces of Gallstones by Salmonella spp. *Infection and immunity*, 70(5), 2640-2649.

Qamar, M. U., Saleem, S., Toleman, M. A., Saqalein, M., Waseem, M., Nisar, M. A., Khurshid, M., Taj, Z. & Jahan, S. (2018). In vitro and in vivo activity of Manuka honey against NDM-1-producing *Klebsiella pneumoniae* ST11. *Future microbiology*, 13(1), 13-26.

Queenan, A. M., & Bush, K. (2007). Carbapenemases: the versatile β-lactamases. *Clinical microbiology reviews*, 20(3), 440-458.

Rabaey, K., Rodríguez, J., Blackall, L. L., Keller, J., Gross, P., Batstone, D., Verstraete, W. & Nealson, K. H. (2007). Microbial ecology meets electrochemistry: electricity-driven and driving communities. *The ISME journal*, 1(1), 9.

Rabin, N., Zheng, Y., Opoku-Temeng, C., Du, Y., Bonsu, E., & Sintim, H. O. (2015). Biofilm formation mechanisms and targets for developing antibiofilm agents. Future medicinal chemistry, 7(4), 493-512.

Ramsing, N. B., Ferris, M. J., & Ward, D. M. (2000). Highly Ordered Vertical Structure ofSynechococcus Populations within the One-Millimeter-Thick Photic Zone of a Hot Spring Cyanobacterial Mat. *Appl. Environ. Microbiol*., 66(3), 1038-1049.

Rani, S. A., Pitts, B., & Stewart, P. S. (2005). Rapid diffusion of fluorescent tracers into Staphylococcus epidermidis biofilms visualized by time lapse microscopy. *Antimicrobial agents and chemotherapy*, 49(2), 728-732.

Rani, S. A., Pitts, B., Beyenal, H., Veluchamy, R. A., Lewandowski, Z., Davison, W. M., Buckingham-Meyer, K. & Stewart, P. S. (2007). Spatial patterns of DNA replication, protein synthesis, and oxygen concentration within bacterial biofilms reveal diverse physiological states. *Journal of bacteriology*, 189(11), 4223-4233.

Rasmussen, B. A., Bush, K., Keeney, D., Yang, Y., Hare, R., O'Gara, C., & Medeiros, A. A. (1996). Characterization of IMI-1 beta-lactamase, a class A carbapenem-hydrolyzing enzyme from Enterobacter cloacae. *Antimicrobial agents and chemotherapy*, 40(9), 2080-2086.

Rasmussen, K., & Lewandowski, Z. (1998). Microelectrode measurements of local mass transport rates in heterogeneous biofilms. *Biotechnology and Bioengineering*, 59(3), 302-309.

Reid, R. (2018) *Beta-lactam resistant urinary tract infections: prevalence, the development of rapid diagnostics and novel treatments*. Unpublished thesis (PhD.), De Montfort University.

Reisner, A., Krogfelt, K. A., Klein, B. M., Zechner, E. L., & Molin, S. (2006). In vitro biofilm formation of commensal and pathogenic Escherichia coli strains: impact of environmental and genetic factors. *Journal of bacteriology*, 188(10), 3572-3581.

Rice, L. B., Willey, S. H., Papanicolaou, G. A., Medeiros, A. A., Eliopoulos, G. M., Moellering, R. C., & Jacoby, G. A. (1990). Outbreak of ceftazidime resistance caused by extended-spectrum beta-lactamases at a Massachusetts chronic-care facility. *Antimicrobial agents and chemotherapy*, 34(11), 2193-2199.

Rinaudi, L. V., & Giordano, W. (2010). An integrated view of biofilm formation in rhizobia. *FEMS microbiology letters*, 304(1), 1-11.

Rolain, J. M., Parola, P., & Cornaglia, G. (2010). New Delhi metallo-beta-lactamase (NDM-1): towards a new pandemia?. *Clinical Microbiology and Infection*, 16(12), 1699-1701.

Ronald, A. (2002). The etiology of urinary tract infection: traditional and emerging pathogens. *The American journal of medicine*, 113(1), 14-19.

Rosen, D. A., Pinkner, J. S., Jones, J. M., Walker, J. N., Clegg, S., & Hultgren, S. J. (2008). Utilization of an intracellular bacterial community pathway in Klebsiella pneumoniae urinary tract infection and the effects of FimK on type 1 pilus expression. *Infection and immunity*, 76(7), 3337-3345.

Roux, A., Christophe beloin, and Jean-Marc Ghigo. 2010. Escherichia coli biofilms. *France: HAL Archives Ouvertes. PMCID: PMC2864707.*

Sahuquillo-Arce, J. M., Hernández-Cabezas, A., Yarad-Auad, F., Ibáñez-Martínez, E., Falomir-Salcedo, P., & Ruiz-Gaitán, A. (2015). Carbapenemases: a worldwide threat to antimicrobial therapy. *World Journal of Pharmacology*, 4(1), 75-95.

Saier Jr, M. H. (2015). The bacterial phosphotransferase system: new frontiers 50 years after its discovery. Journal of molecular microbiology and biotechnology, 25(2-3), 73-78

Schembri, M. A., Kjærgaard, K., & Klemm, P. (2003). Global gene expression in Escherichia coli biofilms. *Molecular microbiology*, 48(1), 253-267.

Singh, K., Mangold, K. A., Wyant, K., Schora, D. M., Voss, B., Kaul, K. L., Hayden, M.K., Chundi, V. & Peterson, L. R. (2012). Rectal screening for Klebsiella pneumoniae carbapenemases: comparison of real-time PCR and culture using two selective screening agar plates. *Journal of clinical microbiology*, 50(8), 2596-2600.

Singh, R., Paul, D., & Jain, R. K. (2006). Biofilms: implications in bioremediation. *Trends in microbiology*, 14(9), 389-397.

Singh, S., Singh, S. K., Chowdhury, I., & Singh, R. (2017). Understanding the mechanism of bacterial biofilms resistance to antimicrobial agents. *The open microbiology journal*, 11, 53.

Sirot, D., Sirot, J., Labia, R., Morand, A., Courvalin, P., Darfeuille-Michaud, A., Perroux, R. & Cluzel, R. (1987). Transferable resistance to third-generation cephalosporins in clinical isolates of Klebsiella pneumoniae: identification of CTX-1, a novel β-lactamase. *Journal of Antimicrobial Chemotherapy*, 20(3), 323-334.

Soto, S. M. (2014). Importance of biofilms in urinary tract infections: new therapeutic approaches. Advances in biology, 2014.

Soto, S. M., Smithson, A., Martinez, J. A., Horcajada, J. P., Mensa, J., & Vila, J. (2007). Biofilm formation in uropathogenic Escherichia coli strains: relationship with prostatitis, urovirulence factors and antimicrobial resistance. The Journal of urology, 177(1), 365-368.

Soto, S., Smithson, A., Horcajada, J. P., Martinez, J. A., Mensa, J. P., & Vila, J. (2006). Implication of biofilm formation in the persistence of urinary tract infection caused by uropathogenic Escherichia coli. Clinical Microbiology and infection, 12(10), 1034-1036.

Sowa, Y., Homma, M., Ishijima, A., & Berry, R. M. (2014). Hybrid-fuel bacterial flagellar motors in Escherichia coli. Proceedings of the National Academy of Sciences, 111(9), 3436-3441.

Sperandio, V., Mellies, J. L., Nguyen, W., Shin, S., & Kaper, J. B. (1999). Quorum sensing controls expression of the type III secretion gene transcription and protein secretion in enterohemorrhagic and enteropathogenic Escherichia coli. *Proceedings of the National Academy of Sciences*, 96(26), 15196-15201.

Sperandio, V., Torres, A. G., & Kaper, J. B. (2002). Quorum sensing Escherichia coli regulators B and C (QseBC): a novel two-component regulatory system involved in the regulation of flagella and motility by quorum sensing in E. coli. *Molecular microbiology*, 43(3), 809-821.

Standardization (2008) *Development of Latest Proposed Biofilm Standard Launched* [Online]. Available from: https://www.astm.org/SNEWS/MJ_2008/biofilm_mj08.html [Accessed 3 Apr. 2016].

Stapper, A. P., Narasimhan, G., Ohman, D. E., Barakat, J., Hentzer, M., Molin, S., Kharazmi, A., Høiby, N. & Mathee, K. (2004). Alginate production affects Pseudomonas aeruginosa biofilm development and architecture, but is not essential for biofilm formation. *Journal of medical microbiology*, 53(7), 679-690.

Steens (2019) STEENS UMF 24 (MGO 1122) Raw unpasteurized NZ Manuka honey 250 gram [Online] Available from: https://steenshoney.com/collections/umf-manuka-honey/products/steens-raw-manuka-honey-umf-24-cold-pressed?variant=29238086205484

Stepanović, S., Ćirković, I., Ranin, L., & S✓ vabić-Vlahović, M. (2004). Biofilm formation by Salmonella spp. and Listeria monocytogenes on plastic surface. *Letters in applied microbiology*, 38(5), 428-432.

Steward, C. D., Wallace, D., Hubert, S. K., Lawton, R., Fridkin, S. K., Gaynes, R. P., McGowan Jr, J.E. & Tenover, F. C. (2000). Ability of laboratories to detect emerging antimicrobial resistance in nosocomial pathogens: a survey of project ICARE laboratories. *Diagnostic microbiology and infectious disease*, 38(1), 59-67.

Stewart, P. S. (1996). Theoretical aspects of antibiotic diffusion into microbial biofilms. Antimicrobial agents and chemotherapy, 40(11), 2517-2522.

Stewart, P. S., & Costerton, J. W. (2001). Antibiotic resistance of bacteria in biofilms. *The lancet*, 358(9276), 135-138.

Stewart, P. S., & Franklin, M. J. (2008). Physiological heterogeneity in biofilms. *Nature Reviews Microbiology*, 6(3), 199.

Stewart, P. S., McFeters, G. A., & Huang, C. T. (2000). Biofilm control by antimicrobial agents. *In Biofilms II: Process analysis and applications* (pp. 373-405).

Stoodley, P., Sauer, K., Davies, D. G., & Costerton, J. W. (2002). Biofilms as complex differentiated communities. *Annual Reviews in Microbiology*, 56(1), 187-209.

Stoodley, P., Sauer, K., Davies, D. G., & Costerton, J. W. (2002). Biofilms as complex differentiated communities. *Annual Reviews in Microbiology*, 56(1), 187-209.

Stürenburg, E., Sobottka, I., Feucht, H. H., Mack, D., & Laufs, R. (2003). Comparison of BDPhoenix and VITEK2 automated antimicrobial susceptibility test systems for extended-spectrum beta-lactamase detection in Escherichia coli and Klebsiella species clinical isolates. *Diagnostic microbiology and infectious disease*, 45(1), 29-34.

Sturgis, J. N. (2001). Organisation and evolution of the tol-pal gene cluster. *Journal of molecular microbiology and biotechnology*, 3(1), 113-122.

Sturme, M. H., Kleerebezem, M., Nakayama, J., Akkermans, A. D., Vaughan, E. E., & De Vos, W. M. (2002). Cell to cell communication by autoinducing peptides in gram-positive bacteria. *Antonie Van Leeuwenhoek*, 81(1-4), 233-243.

Surette, M. G., & Bassler, B. L. (1998). Quorum sensing in Escherichia coli and Salmonella typhimurium. *Proceedings of the National Academy of Sciences*, 95(12), 7046-7050.

Surette, M. G., Miller, M. B., & Bassler, B. L. (1999). Quorum sensing in Escherichia coli, Salmonella typhimurium, and Vibrio harveyi: a new family of genes responsible for autoinducer production. *Proceedings of the National Academy of Sciences*, 96(4), 1639-1644.

Sykes, J. E., & Rankin, S. C. (2013). Isolation and identification of aerobic and anaerobic bacteria. *Canine and Feline Infectious Diseases. St. Louis: Elsevier Inc*, 17-28.

Sykes, R. B., & Bush, K. (1982). Physiology, biochemistry, and inactivation of β-lactamases. In *The Biology of Beta-Lactam Antibiotics* (pp. 155-207). Academic Press.

Tacconelli, E., Magrini, N., Kahlmeter, G., & Singh, N. (2017). Global priority list of antibiotic-resistant bacteria to guide research, discovery, and development of new antibiotics. World Health Organization, 27.

Taft, R. J., Pang, K. C., Mercer, T. R., Dinger, M., & Mattick, J. S. (2010). Non-coding RNAs: regulators of disease. *The Journal of Pathology: A Journal of the Pathological Society of Great Britain and Ireland*, 220(2), 126-139.

Tan, C. W., & Chlebicki, M. P. (2016). Urinary tract infections in adults. *Singapore medical journal*, 57(9), 485.

Tandogdu, Z., & Wagenlehner, F. M. (2016). Global epidemiology of urinary tract infections. *Current opinion in infectious diseases*, 29(1), 73-79.

Tenney, J., Hudson, N., Alnifaidy, H., Li, J. T. C., & Fung, K. H. (2018). Risk factors for aquiring multidrug-resistant organisms in urinary tract infections: a systematic literature review. *Saudi pharmaceutical journal*, 26(5), 678-684.

Tenover, F. C. (2006). Mechanisms of antimicrobial resistance in bacteria. The American journal of medicine, 119(6), S3-S10.

Thermo fisher scientific (2019) Introduction to Gene Expression: Getting Started Guide. [Online] Available from: https://www.thermofisher.com/uk/en/home/life-science/pcr/real-time-pcr/real-time-pcr-learning-center/gene-expression-analysis-real-time-pcr-information/introduction-gene-expression.html [Accessed 7 July 2019].

Tipper, D. J., & Strominger, J. L. (1965). Mechanism of action of penicillins: a proposal based on their structural similarity to acyl-D-alanyl-D-alanine. *Proceedings of the National Academy of Sciences of the United States of America*, 54(4), 1133.

Tyburski, J., Studzinska, A., Daca, P., & Tretyn, A. (2008). PCR in real time. The methods of data analysis. *Biotechnologia*, 1, 86-96.

Tzouvelekis, L. S., & Bonomo, R. A. (1999). SHV-type beta-lactamases. *Current pharmaceutical design*, 5(11), 847-864.

UniProtKB (2019a) *UniProtKB - B7LCG2 (OPGH_ECOLI)* [Online] Uniprot. Available from: https://www.uniprot.org/uniprot/B7LCG2 [Accessed 01/09/2019].

UniProtKB (2019b) *UniProtKB - P62517 (OPGH_ECOLI)* [Online] Uniprot. Available from: https://www.uniprot.org/uniprot/P62517 [Accessed 01/09/2019].

UniProtKB (2019c) *UniProtKB - P0A855 (TOLB_ECOLI)* [Online] Uniprot. Available from: https://www.uniprot.org/uniprot/P0A855 [Accessed 01/09/2019].

UniProtKB (2019d) *UniProtKB - Q1R4H8 (Q1R4H8_ECOUT)* [Online] Uniprot. Available from: https://www.uniprot.org/uniprot/Q1R4H8 [Accessed 01/09/2019].

UniProtKB (2019e) *UniProtKB - P0AF06 (MOTB_ECOLI)* [Online] Uniprot. Available from: https://www.uniprot.org/uniprot/P0AF06 [Accessed 01/09/2019].

UniProtKB (2019f) *UniProtKB - P24251 (CRL_ECOLI)* [Online] Uniprot. Available from: https://www.uniprot.org/uniprot/P24251 [Accessed 01/09/2019].

UniProtKB (2019g) *UniProtKB - P04128 (FIMA1_ECOLI)* [Online] Uniprot. Available from: https://www.uniprot.org/uniprot/P04128 [Accessed 01/09/2019].

UniProtKB (2019h) *UniProtKB - P0AFW0 (RFAH_ECOLI)* [Online] Uniprot. Available from: https://www.uniprot.org/uniprot/P0AFW0 [Accessed 01/09/2019].

University Hospital Southampton NHS Foundation Trust (2019) *Urinary tract infections*. Retrieved from https://www.uhs.nhs.uk/Media/Controlleddocuments/Patientinformation/Generalmedicine/Urinary-tract-infection-patient-information.pdf

Ventola, C. L. (2015). The antibiotic resistance crisis: part 1: causes and threats. *Pharmacy and therapeutics*, 40(4), 277.

Vieira, H. L., Freire, P., & Arraiano, C. M. (2004). Effect of Escherichia coli morphogene bolA on biofilms. *Appl. Environ. Microbiol*., 70(9), 5682-5684.

Vinés, E. D., Marolda, C. L., Balachandran, A., & Valvano, M. A. (2005). Defective O-antigen polymerization in tolA and pal mutants of Escherichia coli in response to extracytoplasmic stress. *Journal of bacteriology*, 187(10), 3359-3368.

Visavadia, B. G., Honeysett, J., & Danford, M. H. (2008). Manuka honey dressing: An effective treatment for chronic wound infections. *British Journal of Oral and Maxillofacial Surgery*, 46(1), 55-56.

Visick, K. L., & McFall-Ngai, M. J. (2000). An exclusive contract: specificity in the Vibrio fischeri-Euprymna scolopes partnership. *Journal of Bacteriology*, 182(7), 1779-1787.

Vlamakis, H., Aguilar, C., Losick, R., & Kolter, R. (2008). Control of cell fate by the formation of an architecturally complex bacterial community. *Genes & development*, 22(7), 945-953.

Vos, T., Barber, R. M., Bell, B., Bertozzi-Villa, A., Biryukov, S., Bolliger, I., Charlson, F., Davis, A., Degenhardt, L. & Dicker, D. (2015). Global Burden of Disease Study 2013 Collaborators. Global, regional, and national incidence, prevalence, and years lived with disability for 301 acute and chronic diseases and injuries in 188 countries, 1990–2013: A systematic analysis for the Global Burden of Disease Study 2013. *Lancet*, 386(9995), 743-800.

Vranic, S. M., Zatric, N., Rebic, V., Aljicevic, M., & Abdulzaimovic, A. (2017). The most frequent isolates from outpatients with urinary tract infection. *Materia socio-medica*, 29(1), 17.

Wallace, A., Eady, S., Miles, M., Martin, H., McLachlan, A., Rodier, M., Willis, J., Scott, R. & Sutherland, J. (2010). Demonstrating the safety of manuka honey UMF® 20+ in a human clinical trial with healthy individuals. *British journal of nutrition*, 103(7), 1023-1028.

Walsh, C. (2000). Molecular mechanisms that confer antibacterial drug resistance. *Nature*, 406(6797), 775.

Walsh, T. R. (2010). Emerging carbapenemases: a global perspective. *International journal of antimicrobial agents*, 36, S8-S14.

Walters, M., & Sperandio, V. (2006). Autoinducer 3 and epinephrine signaling in the kinetics of locus of enterocyte effacement gene expression in enterohemorrhagic Escherichia coli. *Infection and Immunity*, 74(10), 5445-5455.

Walther-Rasmussen, J., & Høiby, N. (2007). Class A carbapenemases. *Journal of Antimicrobial Chemotherapy*, 60(3), 470-482.

Wang, L., Li, J., March, J. C., Valdes, J. J., & Bentley, W. E. (2005). luxS-dependent gene regulation in Escherichia coli K-12 revealed by genomic expression profiling. Journal of bacteriology, 187(24), 8350-8360.

Wang, Z. W., & Chen, S. (2009). Potential of biofilm-based biofuel production. *Applied microbiology and biotechnology*, 83(1), 1-18.

Wasfi, R., Elkhatib, W. F., & Khairalla, A. S. (2016). Effects of selected Egyptian honeys on the cellular ultrastructure and the gene expression profile of *Escherichia coli*. *PloS one*, 11(3), e0150984.

Watanabe, M., Iyobe, S., Inoue, M., & Mitsuhashi, S. (1991). Transferable imipenem resistance in Pseudomonas aeruginosa. *Antimicrobial agents and chemotherapy*, 35(1), 147-151.

Watnick, P., & Kolter, R. (2000). Biofilm, city of microbes. *Journal of bacteriology*, 182(10), 2675-2679.

Weber, D. J., Raasch, R., & Rutala, W. A. (1999). Nosocomial infections in the ICU: the growing importance of antibiotic-resistant pathogens. *Chest*, 115(3), 34S-41S.

Weigel, N., Kukuruzinska, M. A., Nakazawa, A., Waygood, E. B., & Roseman, S. (1982). Sugar transport by the bacterial phosphotransferase system. Phosphoryl transfer reactions catalyzed by enzyme I of Salmonella typhimurium. *Journal of Biological Chemistry*, 257(23), 14477-14491.

Werner, E., Roe, F., Bugnicourt, A., Franklin, M. J., Heydorn, A., Molin, S., Pitts, B. & Stewart, P. S. (2004). Stratified growth in Pseudomonas aeruginosa biofilms. *Appl. Environ. Microbiol*., 70(10), 6188-6196.

Whitehead, N. A., Barnard, A. M., Slater, H., Simpson, N. J., & Salmond, G. P. (2001). Quorum-sensing in Gram-negative bacteria. *FEMS microbiology reviews*, 25(4), 365-404.

Willey, J. M., Sherwood, L., & Woolverton, C. J. (2008). *Prescott, Harley, and Klein's microbiology*. McGraw-Hill Higher Education.

Withers, H., Swift, S., & Williams, P. (2001). Quorum sensing as an integral component of gene regulatory networks in Gram-negative bacteria. *Current opinion in microbiology*, 4(2), 186-193.

Wolska, K. I., Grudniak, A. M., Rudnicka, Z., & Markowska, K. (2016). Genetic control of bacterial biofilms. *Journal of applied genetics*, 57(2), 225-238.

Wood, T. K., Barrios, A. F. G., Herzberg, M., & Lee, J. (2006). Motility influences biofilm architecture in Escherichia coli. *Applied microbiology and biotechnology*, 72(2), 361-367.

Woodford, N., Ward, M. E., Kaufmann, M. E., Turton, J., Fagan, E. J., James, D., Johnson, A.P., Pike, R., Warner, M., Cheasty, T. & Pearson, A. (2004). Community and hospital spread of Escherichia coli producing CTX-M extended-spectrum β-lactamases in the UK. *Journal of antimicrobial chemotherapy*, 54(4), 735-743.

Woodford, N., Zhang, J., Warner, M., Kaufmann, M. E., Matos, J., MacDonald, A., Brudney, D., Sompolinsky, D., Navon-Venezia, S. & Livermore, D. M. (2008). Arrival of Klebsiella pneumoniae producing KPC carbapenemase in the United Kingdom. *Journal of antimicrobial chemotherapy*, 62(6), 1261-1264.

World Health Organization (2017). [Online] Available from: https://www.who.int/news-room/detail/27-02-2017-who-publishes-list-of-bacteria-for-which-new-antibiotics-are-urgently-needed [Accessed 6 Jul. 2019].

World Health Organization (2018a). [Online] Available from: https://www.who.int/gpsc/information_centre/cauda-uti_eccmid.pdf [Accessed 6 Jul. 2019].

World Health Organization (2018b). [Online] Available from: https://www.who.int/news-room/fact-sheets/detail/antibiotic-resistance [Accessed 6 Jul. 2019].

Worthington, R. J., & Melander, C. (2013). Overcoming resistance to β-lactam antibiotics. *The Journal of organic chemistry*, 78(9), 4207-4213.

Xavier, K. B., & Bassler, B. L. (2003). LuxS quorum sensing: more than just a numbers game. *Current opinion in microbiology*, 6(2), 191-197.

Xi, C., Marks, D. L., Schlachter, S., Luo, W., & Boppart, S. A. (2006). High-resolution three-dimensional imaging of biofilm development using optical coherence tomography. *Journal of biomedical optics*, 11(3), 034001.

Xu, K. D., Franklin, M. J., Park, C. H., McFeters, G. A., & Stewart, P. S. (2001). Gene expression and protein levels of the stationary phase sigma factor, RpoS, in continuously-fed Pseudomonas aeruginosa biofilms. *FEMS microbiology letters*, 199(1), 67-71.

Xue, T., Yu, L., Shang, F., Li, W., Zhang, M., Ni, J., & Chen, X. (2016). The role of autoinducer 2 (AI-2) on antibiotic resistance regulation in an Escherichia coli strain isolated from a dairy cow with mastitis. *Journal of dairy science*, 99(6), 4693-4698.

Yang, S., Lopez, C. R., & Zechiedrich, E. L. (2006). Quorum sensing and multidrug transporters in Escherichia coli. *Proceedings of the National Academy of Sciences*, 103(7), 2386-2391.

Yigit, H., Queenan, A. M., Anderson, G. J., Domenech-Sanchez, A., Biddle, J. W., Steward, C. D., Alberti, S., Bush, K. & Tenover, F. C. (2001). Novel carbapenem-hydrolyzing β-lactamase, KPC-1, from a carbapenem-resistant strain of Klebsiella pneumoniae. *Antimicrobial agents and chemotherapy*, 45(4), 1151-1161.

Yilmaz, M. T., Tatlisu, N. B., Toker, O. S., Karaman, S., Dertli, E., Sagdic, O., & Arici, M. (2014). Steady, dynamic and creep rheological analysis as a novel approach to detect honey

adulteration by fructose and saccharose syrups: Correlations with HPLC-RID results. *Food Research International*, 64, 634-646.

Yong, D., Toleman, M. A., Giske, C. G., Cho, H. S., Sundman, K., Lee, K., & Walsh, T. R. (2009). Characterization of a new metallo-β-lactamase gene, blaNDM-1, and a novel erythromycin esterase gene carried on a unique genetic structure in Klebsiella pneumoniae sequence type 14 from India. *Antimicrobial agents and chemotherapy*, 53(12), 5046-5054.

Zaman, S. B., Hussain, M. A., Nye, R., Mehta, V., Mamun, K. T., & Hossain, N. (2017). A review on antibiotic resistance: alarm bells are ringing. *Cureus*, 9(6).

Zhao, W. H., & Hu, Z. Q. (2013). Epidemiology and genetics of CTX-M extended-spectrum β-lactamases in Gram-negative bacteria. *Critical reviews in microbiology*, 39(1), 79-101.

Zhou, J., Sharp, L. L., Tang, H. L., Lloyd, S. A., Billings, S., Braun, T. F., & Blair, D. F. (1998). Function of protonatable residues in the flagellar motor of Escherichia coli: a critical role for Asp 32 of MotB. *Journal of Bacteriology*, 180(10), 2729-2735.

Zhu, J., Miller, M. B., Vance, R. E., Dziejman, M., Bassler, B. L., & Mekalanos, J. J. (2002). Quorum-sensing regulators control virulence gene expression in Vibrio cholerae. *Proceedings of the National Academy of Sciences*, 99(5), 3129-3134.

Appendices

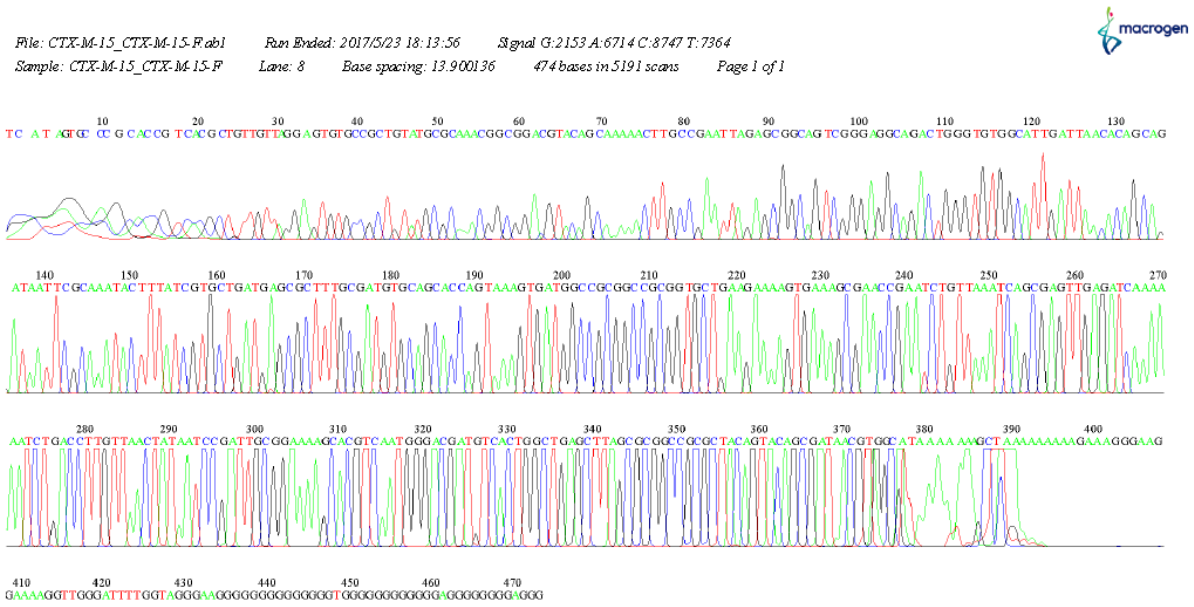

Fig 1.I CTX-M-15 gene sequence

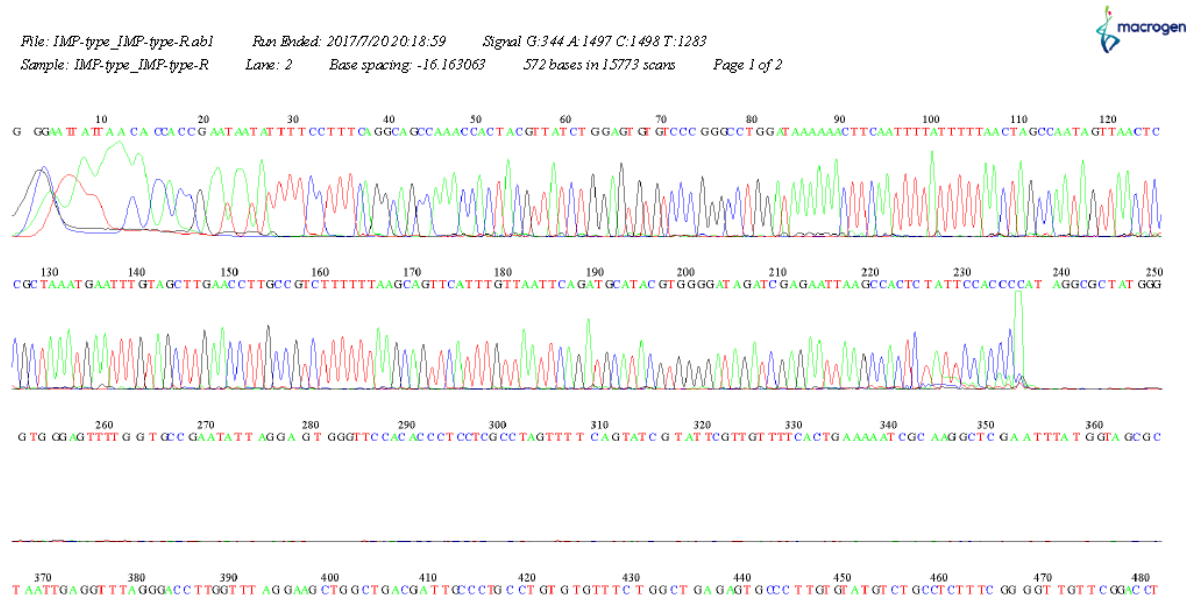

Fig 1.II IMP-type gene sequence

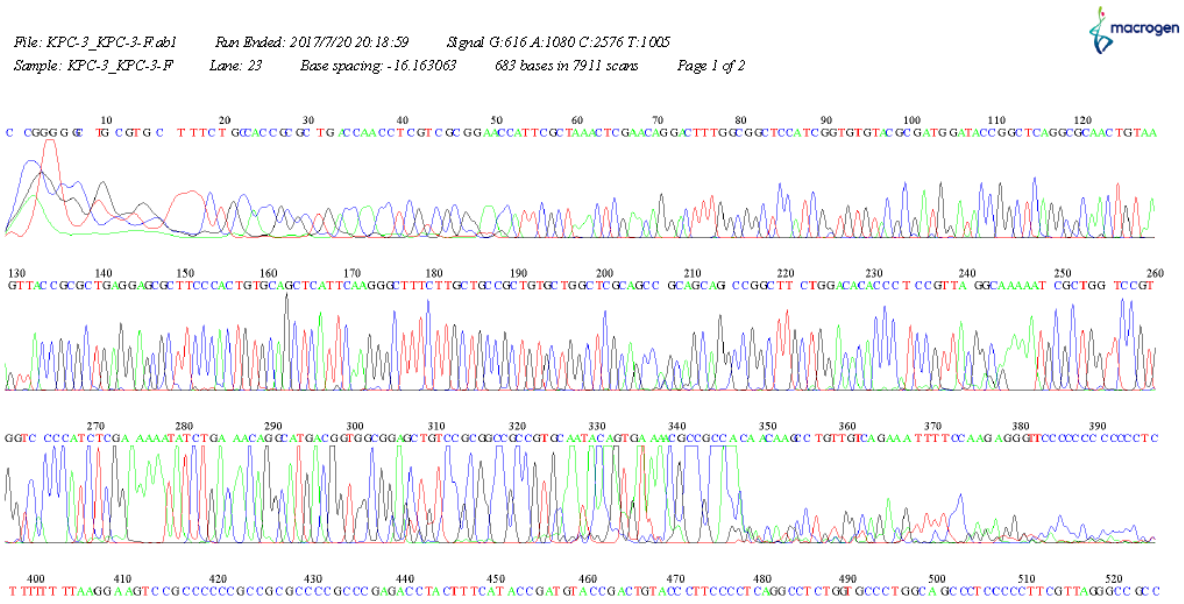

Fig 1.III KPC-3 gene sequence

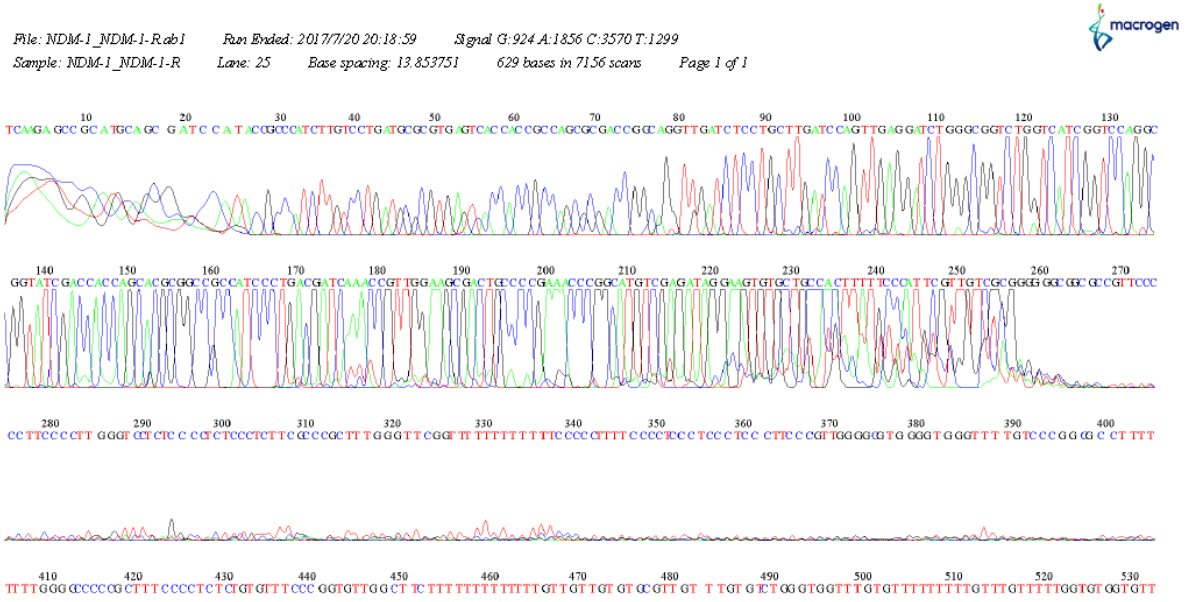

Fig 1.IV NDM-1 gene sequence

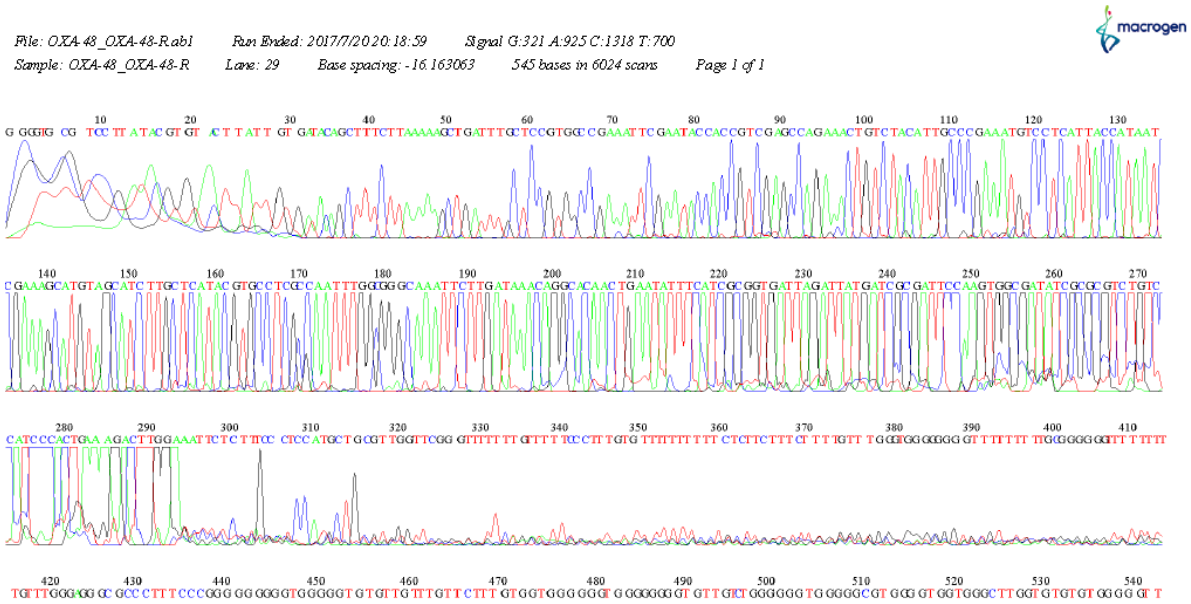

Fig 1.V OXA-48 gene sequence

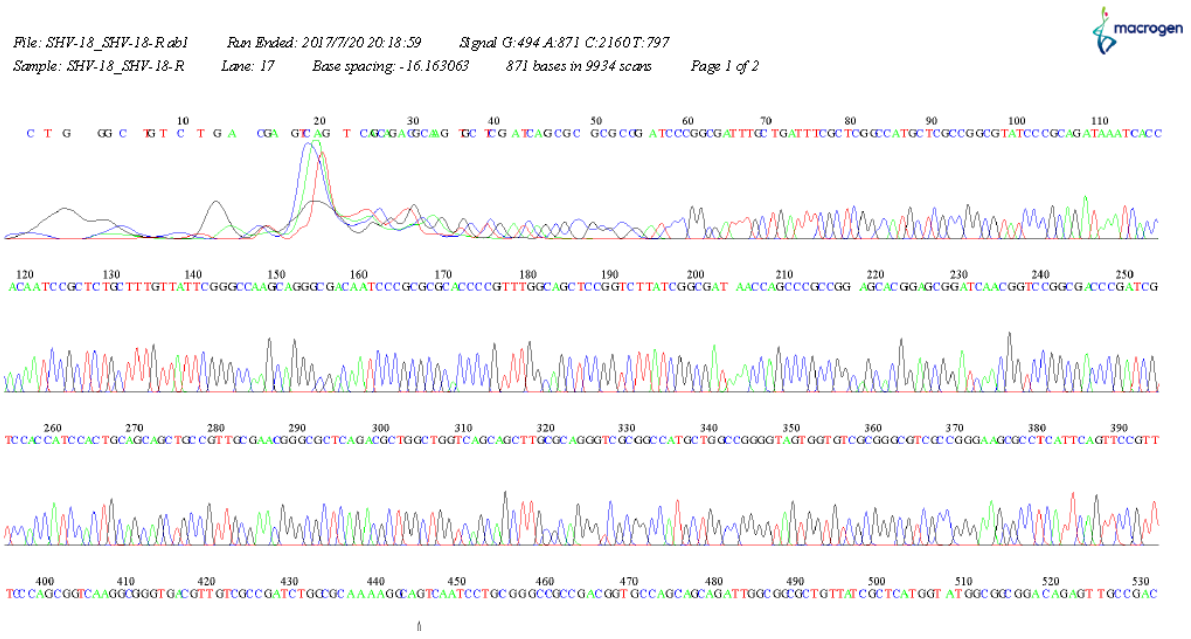

Fig 1.VI SHV-18 gene sequence

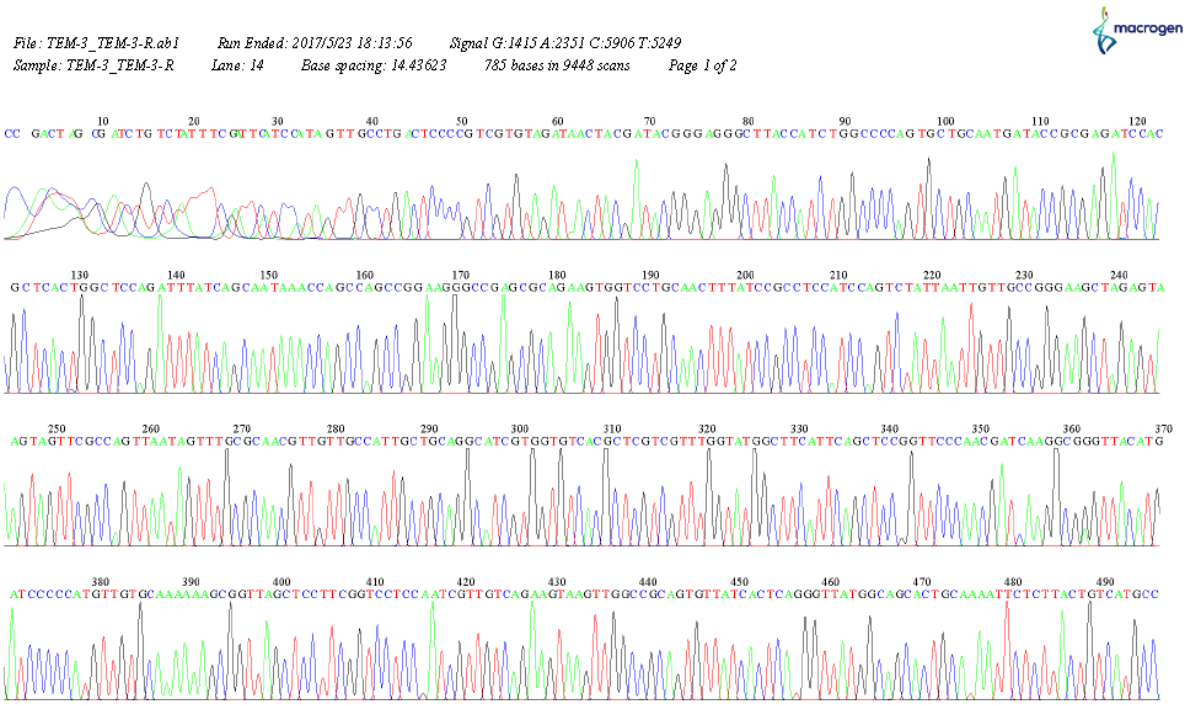

Fig 1.VII TEM-3 gene sequence

Appendix II

Table 2.I One-way ANOVA showing the significance of differences in biofilm density values among four growth stages (6, 12, 24, and 48 h) for *E. coli* strains grown in AB medium with static incubation. According to the data shown, all *E. coli* strains showed a significant difference in biofilm density values when comparing their growth between the four different time-points of growth.

Strain	mean 6 h	mean 12 h	mean 24 h	mean 48 h	*p*-value	significant ($p < 0.01$)
E. coli IMP-type	0.050	0.134	0.205	0.112	0.0006	Yes
E. coli CTX-M-15	0.665	0.271	0.376	0.216	< 0.0001	Yes
E. coli TEM-3	0.324	0.474	0.644	0.511	< 0.0001	Yes
E. coli 12241	0.041	0.097	0.131	0.059	0.0002	Yes

Table 2.II One-way ANOVA showing the significance of differences in biofilm density values among four growth stages (6, 12, 24, and 48 h) for *K. pneumoniae* strains grown in AB medium with static incubation. According to the data shown, all *K. pneumoniae* strains showed a significant difference in biofilm density values when comparing their growth between the four different time-points of growth.

Strain	mean 6 h	mean 12 h	mean 24 h	mean 48 h	*p*-value	significant ($p < 0.01$)
K. pneumoniae OXA-48	0.198	0.255	0.372	0.326	< 0.0001	Yes
K. pneumoniae SHV-18	0.169	0.197	0.154	0.185	0.0358	No
K. pneumoniae NDM-1	0.159	0.228	0.359	0.296	< 0.0001	Yes
K. pneumoniae KPC-3	0.227	0.267	0.414	0.284	< 0.0001	Yes
K. pneumoniae 9633	0.014	0.025	0.063	0.038	0.0010	Yes

Table 2.III One-way ANOVA showing the significance of differences in biofilm density values among four growth stages (6, 12, 24, and 48 h) for *E. coli* strains grown in AB medium with shaking incubation. According to the data shown, all *E. coli* strains showed a significant difference in biofilm density values when comparing their growth between the four different time-points of growth.

Strain	mean 6 h	mean 12 h	mean 24 h	mean 48 h	*p*-value	significant ($p < 0.01$)
E. coli IMP-type	0.039	0.055	0.082	0.024	< 0.0001	Yes
E. coli CTX-M-15	0.113	0.083	0.064	0.028	< 0.0001	Yes
E. coli TEM-3	0.038	0.049	0.089	0.044	< 0.0001	Yes
E. coli 12241	0.025	0.044	0.066	0.021	< 0.0001	Yes

Table 2.IV One-way ANOVA showing the significance of differences in biofilm density values among four growth stages (6, 12, 24, and 48 h) for *K. pneumoniae* strains grown in AB medium with shaking incubation. According to the data shown, all *K. pneumoniae* strains showed a significant difference in biofilm density values when comparing their growth between the four different time-points of growth.

Strain	mean 6 h	mean 12 h	mean 24 h	mean 48 h	*p*-value	significant ($p < 0.01$)
K. pneumoniae OXA-48	0.291	0.516	0.255	0.395	< 0.0001	Yes
K. pneumoniae SHV-18	0.196	0.370	0.171	0.291	< 0.0001	Yes
K. pneumoniae NDM-1	0.255	0.428	0.699	0.634	< 0.0001	Yes
K. pneumoniae KPC-3	0.312	0.498	0.715	0.493	< 0.0001	Yes
K. pneumoniae 9633	0.025	0.041	0.072	0.054	< 0.0001	Yes

Table 2.V One-way ANOVA showing the significance of differences in biofilm density values among four growth stages (6, 12, 24, and 48 h) for *E. coli* strains grown in LB medium with static incubation. According to the data shown, all *E. coli* strains showed a significant difference in biofilm density values when comparing their growth between the four different time-points of growth.

Strain	mean 6 h	mean 12 h	mean 24 h	mean 48 h	*p*-value	significant ($p < 0.01$)
E. coli IMP-type	0.478	0.406	0.342	0.181	< 0.0001	Yes
E. coli CTX-M-15	0.611	0.225	0.410	0.089	< 0.0001	Yes
E. coli TEM-3	0.511	0.376	0.270	0.081	< 0.0001	Yes
E. coli 12241	0.345	0.305	0.239	0.082	< 0.0001	Yes

Table 2.VI One-way ANOVA showing the significance of differences in biofilm density values among four growth stages (6, 12, 24, and 48 h) for *K. pneumoniae* strains grown in LB medium with static incubation. According to the data shown, all *K. pneumoniae* strains showed a significant difference in biofilm density values when comparing their growth between the four different time-points of growth.

Strain	mean 6 h	mean 12 h	mean 24 h	mean 48 h	*p*-value	significant ($p < 0.01$)
K. pneumoniae OXA-48	0.227	0.065	0.355	0.144	< 0.0001	Yes
K. pneumoniae SHV-18	0.428	0.293	0.562	0.328	< 0.0001	Yes
K. pneumoniae NDM-1	0.217	0.271	0.309	0.292	0.0006	Yes
K. pneumoniae KPC-3	0.370	0.456	0.505	0.473	< 0.0001	Yes
K. pneumoniae 9633	0.016	0.037	0.058	0.042	0.0081	Yes

Table 2.VII One-way ANOVA showing the significance of differences in biofilm density values among four growth stages (6, 12, 24, and 48 h) for *E. coli* strains grown in LB medium with shaking incubation. According to the data shown, all *E. coli* strains showed a significant difference in biofilm density values when comparing their growth between the four different time-points of growth.

Strain	mean 6 h	mean 12 h	mean 24 h	mean 48 h	*p*-value	significant ($p < 0.01$)
E. coli IMP-type	0.122	0.224	0.026	0.103	< 0.0001	Yes
E. coli CTX-M-15	0.614	0.601	0.179	0.072	< 0.0001	Yes
E. coli TEM-3	0.190	0.256	0.088	0.129	< 0.0001	Yes
E. coli 12241	0.100	0.173	0.012	0.082	< 0.0001	Yes

Table 2.VIII One-way ANOVA showing the significance of differences in biofilm density values among four growth stages (6, 12, 24, and 48 h) for *K. pneumoniae* strains grown in LB medium with shaking incubation. According to the data shown, all *K. pneumoniae* strains showed a significant difference in biofilm density values when comparing their growth between the four different time-points of growth.

Strain	mean 6 h	mean 12 h	mean 24 h	mean 48 h	*p*-value	significant ($p < 0.01$)
K. pneumoniae OXA-48	0.438	0.391	0.352	0.376	< 0.0001	Yes
K. pneumoniae SHV-18	0.412	0.357	0.268	0.294	< 0.0001	Yes
K. pneumoniae NDM-1	0.576	0.426	0.340	0.392	< 0.0001	Yes
K. pneumoniae KPC-3	0.624	0.547	0.456	0.500	< 0.0001	Yes
K. pneumoniae 9633	0.103	0.074	0.033	0.068	< 0.0001	Yes

Table 2.IX One-way ANOVA showing the significance of differences in biofilm density values among four growth stages (6, 12, 24, and 48 h) for *E. coli* strains grown in NB medium with static incubation. According to the data shown, all *E. coli* strains showed a significant difference in biofilm density values when comparing their growth between the four different time-points of growth.

Strain	mean 6 h	mean 12 h	mean 24 h	mean 48 h	*p*-value	significant ($p < 0.01$)
E. coli IMP-type	0.097	0.190	0.110	0.056	0.0001	Yes
E. coli CTX-M-15	0.310	0.350	0.209	0.237	< 0.0001	Yes
E. coli TEM-3	0.184	0.339	0.139	0.063	< 0.0001	Yes
E. coli 12241	0.074	0.117	0.076	0.046	0.0004	Yes

Table 2.X One-way ANOVA showing the significance of differences in biofilm density values among four growth stages (6, 12, 24, and 48 h) for *K. pneumoniae* strains grown in NB medium with static incubation. According to the data shown, all *K. pneumoniae* strains (except 9600) showed a significant difference in biofilm density values when comparing their growth between the four different time-points of growth.

Strain	mean 6 h	mean 12 h	mean 24 h	mean 48 h	*p*-value	significant ($p < 0.01$)
K. pneumoniae OXA-48	0.221	0.618	0.686	0.624	< 0.0001	Yes
K. pneumoniae SHV-18	0.452	0.646	0.735	0.643	< 0.0001	Yes
K. pneumoniae NDM-1	0.253	0.549	0.634	0.560	< 0.0001	Yes
K. pneumoniae KPC-3	0.462	0.785	0.884	0.815	< 0.0001	Yes
K. pneumoniae 9633	0.025	0.082	0.102	0.089	0.0011	Yes

Table 2.XI One-way ANOVA showing the significance of differences in biofilm density values among four growth stages (6, 12, 24, and 48 h) for *E. coli* strains grown in NB medium with shaking incubation. According to the data shown, all *E. coli* strains showed a significant difference in biofilm density values when comparing their growth between the four different time-points of growth.

Strain	mean 6 h	mean 12 h	mean 24 h	mean 48 h	*p*-value	significant ($p < 0.01$)
E. coli IMP-type	0.156	0.000	0.059	0.021	< 0.0001	Yes
E. coli CTX-M-15	0.320	0.127	0.069	0.028	< 0.0001	Yes
E. coli TEM-3	0.089	0.000	0.063	0.033	< 0.0001	Yes
E. coli 12241	0.073	0.000	0.047	0.015	0.0015	Yes

Table 2.XII One-way ANOVA showing the significance of differences in biofilm density values among four growth stages (6, 12, 24, and 48 h) for *K. pneumoniae* strains grown in NB medium with shaking incubation. According to the data shown, all *K. pneumoniae* strains showed a significant difference in biofilm density values when comparing their growth between the four different time-points of growth.

Strain	mean 6 h	mean 12 h	mean 24 h	mean 48 h	*p*-value	significant ($p < 0.01$)
K. pneumoniae OXA-48	0.413	0.200	0.287	0.219	< 0.0001	Yes
K. pneumoniae SHV-18	0.645	0.266	0.453	0.281	< 0.0001	Yes
K. pneumoniae NDM-1	0.628	0.324	0.548	0.373	< 0.0001	Yes
K. pneumoniae KPC-3	0.673	0.263	0.649	0.312	< 0.0001	Yes
K. pneumoniae 9633	0.110	0.051	0.090	0.061	0.0514	No

Standard curves for the calculation of the primer efficiency in AB broth

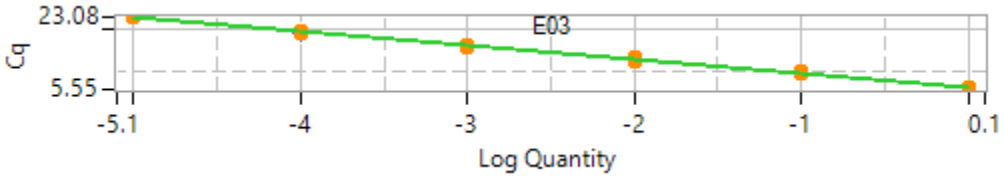

crr

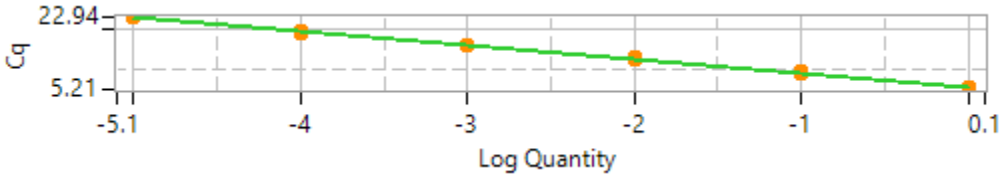

csgB

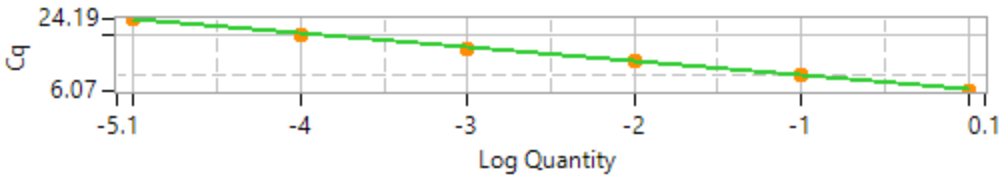

csgE

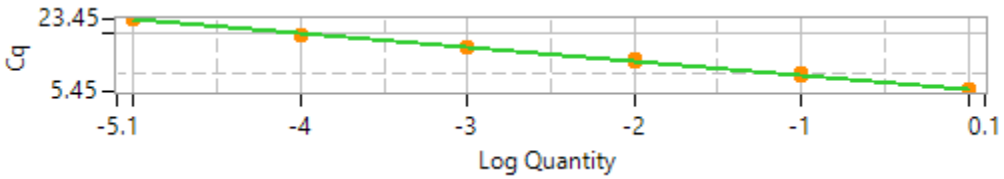

csgF

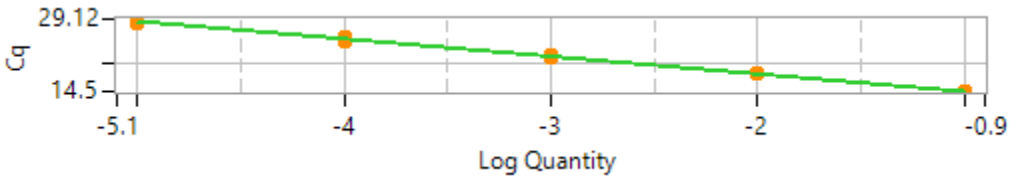

CTX-M-15

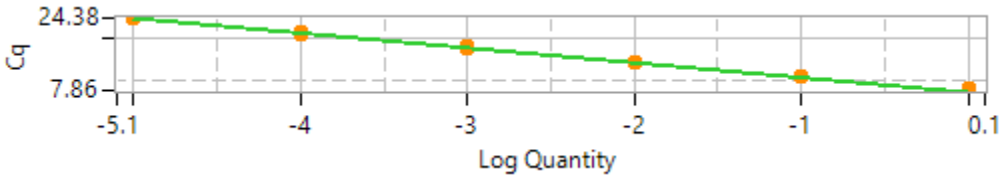

fliS

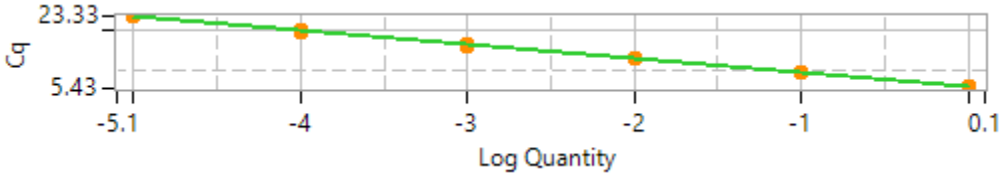

luxS

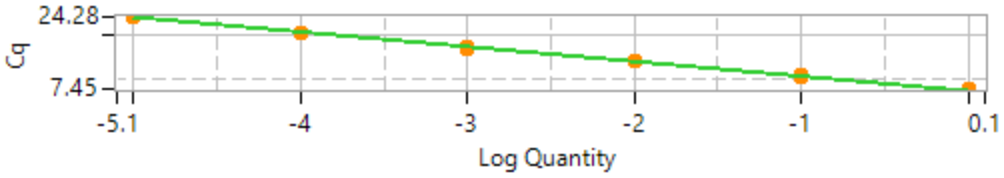

mdoH

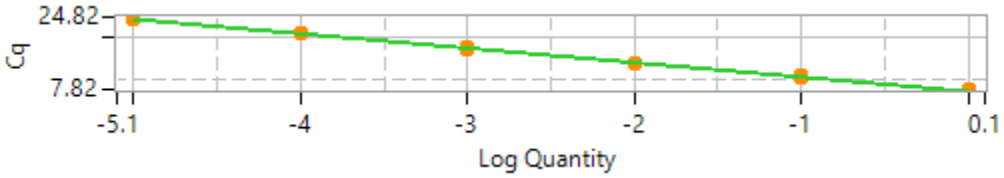

motA

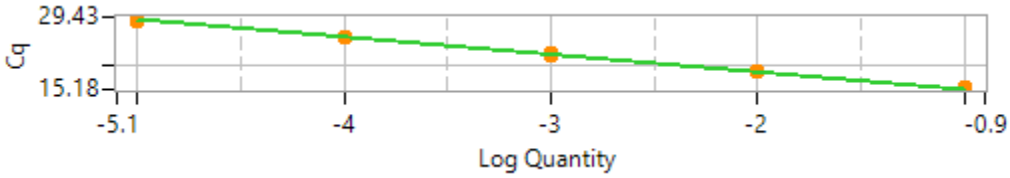

motB

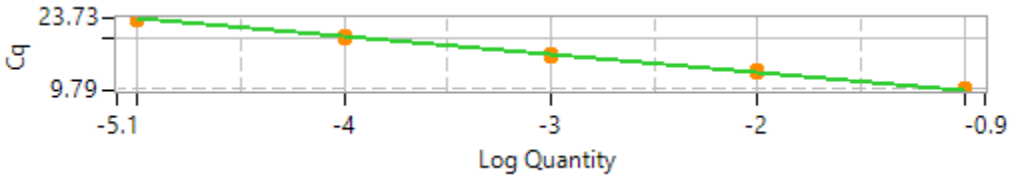
23.73
Cq
9.79
-5.1
-4
-3
-2
-0.9
Log Quantity

tolB

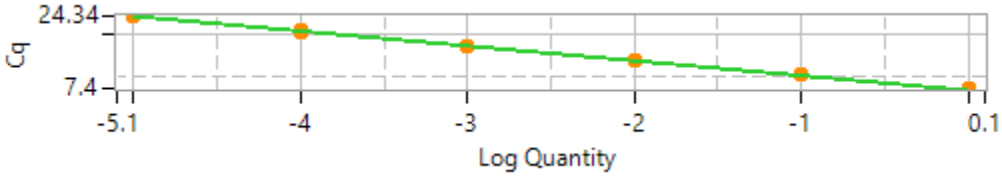
24.34
Cq
7.4
-5.1
-4
-3
-2
-1
0.1
Log Quantity

yieO

Standard curves for the calculation of the primer efficiency in LB broth

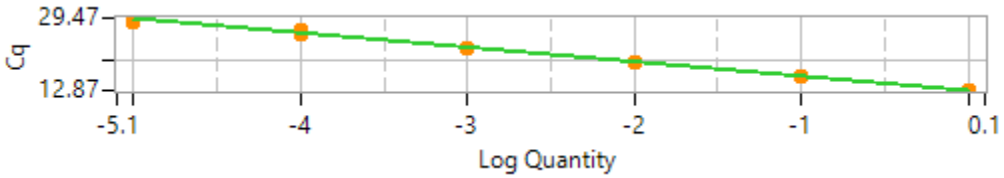

crr

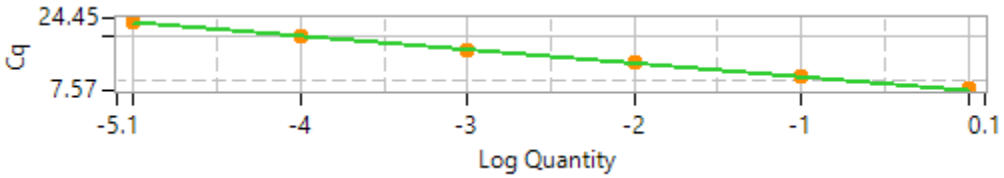

csgB

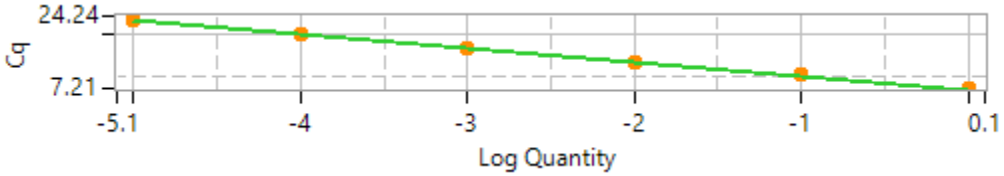

csgE

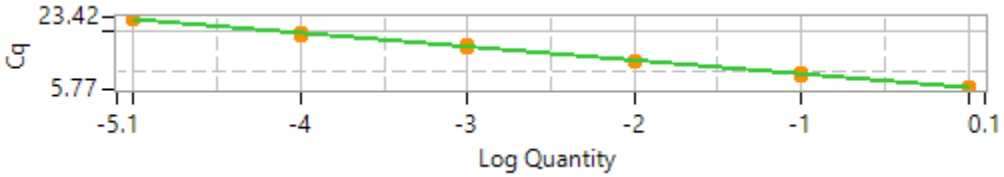

csgF

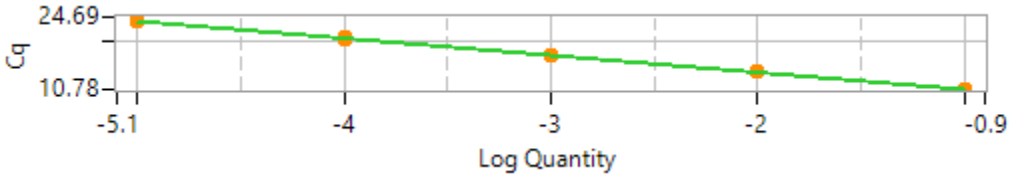

CTX-M-15

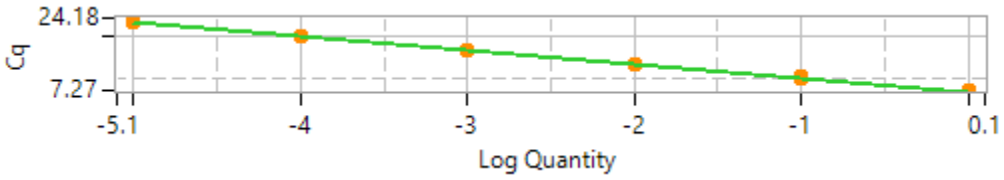

fliS

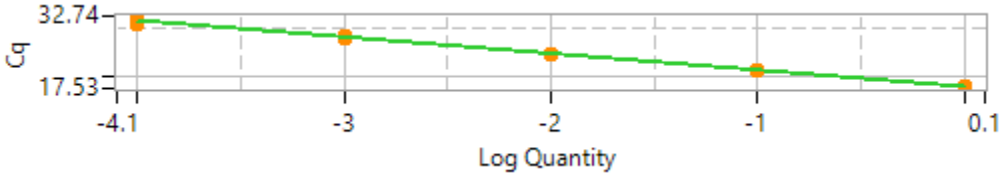

luxS

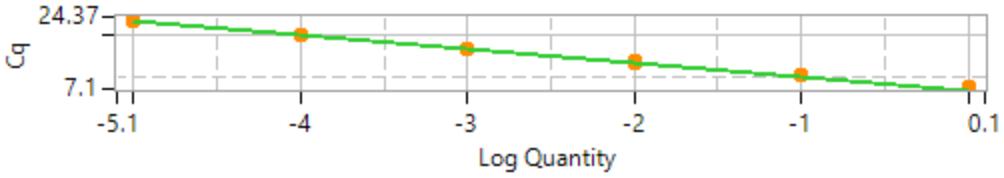

mdoH

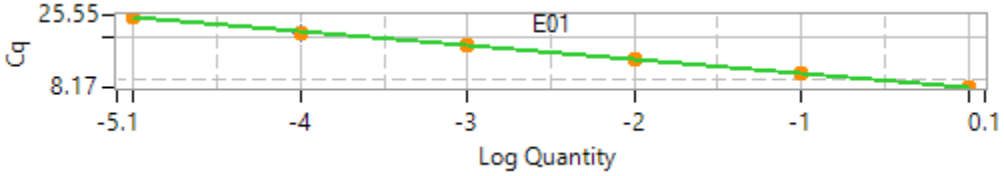

motA

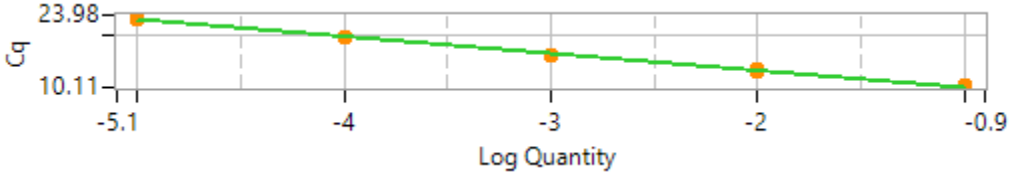

motB

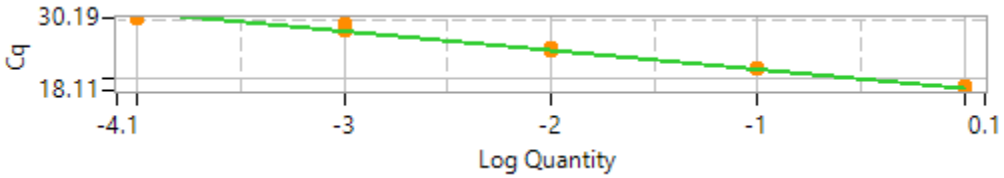
30.19
18.11
Cq
-4.1
-3
-2
-1
0.1
Log Quantity

tolB

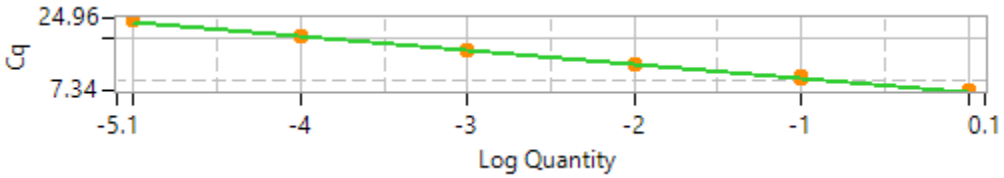
24.96
7.34
Cq
-5.1
-4
-3
-2
-1
0.1
Log Quantity

yieO

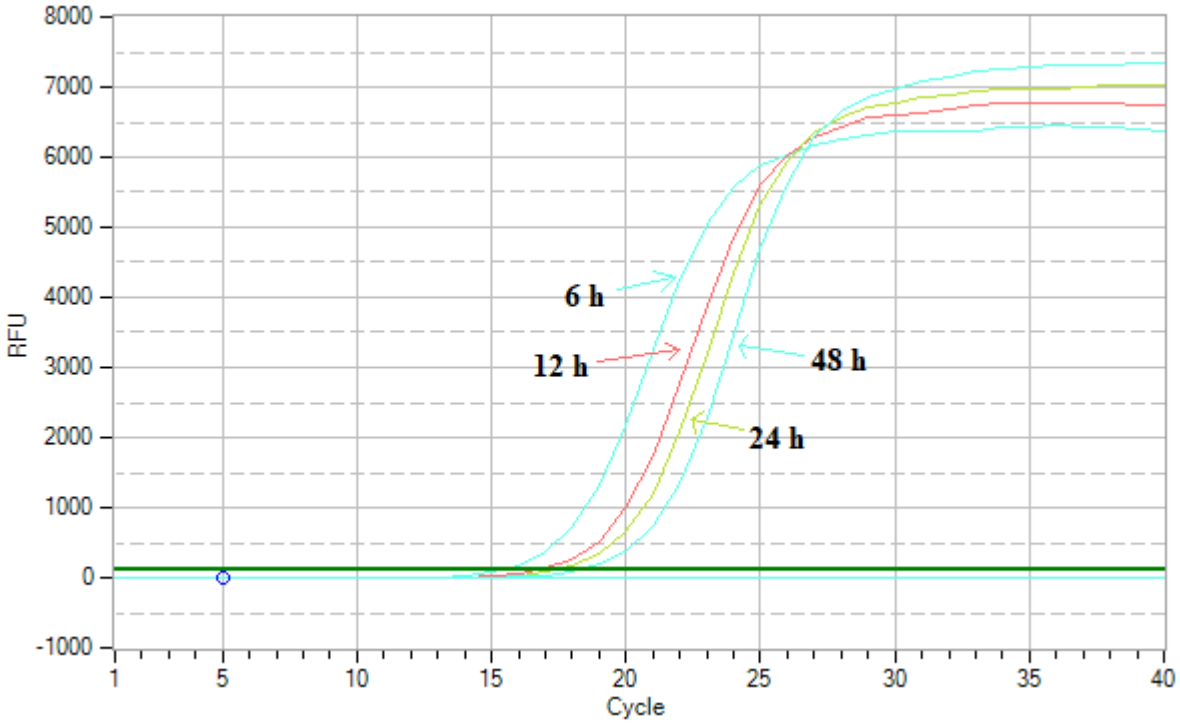

Example of a Ct value obtained from this study

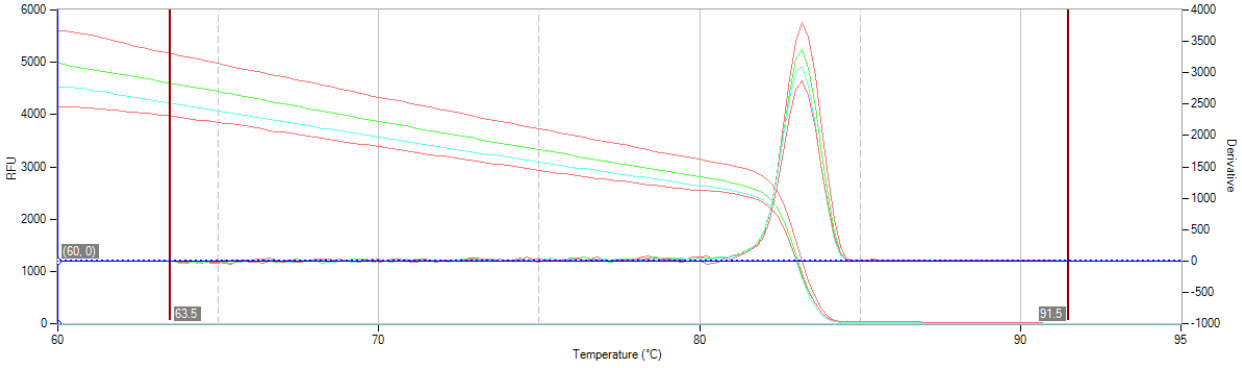

Example of a melting curve obtained from this study